ARMY RESEARCH LABORATORY

Investigation of Bulk-Loaded Liquid Propellant Gun Concepts

by Robert L. Talley, John Owczarczak,
and Matthew Geise

ARL-CR-335 September 1997

prepared by

Veritay Technology, Inc.
4845 Millersport Highway
P.O. Box 305
East Amherst, NY 14051-0305

under contract

DAAA15-93-C-0031

Army Research Laboratory
Aberdeen Proving Ground, MD 21005-5066

ARL-CR-335 **September 1997**

Investigation of Bulk-Loaded Liquid Propellant Gun Concepts

Robert L. Talley, John Owczarczak, Matthew Geise
Veritay Technology, Inc.

prepared by

Veritay Technology, Inc.
4845 Millersport Highway
P.O. Box 305
East Amherst, NY 14051-0305

under contract

DAAA15-93-C-0031

Abstract

The approach of using chamber geometry (in the forms of stepped-wall and multichambers) in conjunction with using a repeatable igniter was investigated as a means for controlling the interior ballistic variability in 20-mm and 30-mm bulk-loaded liquid propellant guns (BLPGs). Full-scale, gun firing tests were conducted using the liquid monopropellant XM46 to experimentally develop a database for assessing the utility of these mechanical control concepts.

The 30-mm gun test data indicate that a useful degree of control of both the pressure-time trace shape and the projectile muzzle velocity may be achieved by using either a stepped-wall or a multichamber geometry, and that a useful degree of ballistic repeatability can often be achieved, even in a nonoptimized test gun.

The 30-mm gun test data also indicate that the igniter needs to be tailored to the size and geometry of the input stage of the main liquid propellent chamber to achieve near-optimal ballistic repeatability.

TABLE OF CONTENTS

		Page
	LIST OF FIGURES	v
	LIST OF TABLES	ix
1.	INTRODUCTION	1
2.	BACKGROUND OF BALLISTIC PROCESS CONTROL NEEDS	3
3.	EXPERIMENTAL SETUP	6
3.1	20-mm Gun Test Fixture	6
3.1.1	Pyrotechnic Igniter	6
3.1.2	Chamber Inserts	9
3.1.3	20-mm Projectiles	9
3.1.4	Pressure Transducer Locations	13
3.2	30-mm Gun Test Fixture	13
3.2.1	Pyrotechnic Igniter	13
3.2.2	Chamber Inserts	14
3.2.2.1	Original Stepped-Wall Geometries	14
3.2.2.2	Modified Stepped-Wall Geometries	20
3.2.2.3	Multichamber	20
3.2.2.4	Multichamber Drilling Jig	24
3.2.3	30-mm Projectiles	28
3.2.4	Gun Test Fixture	28
3.2.5	Transducer Locations	31
3.3	Booster Propellant	31
3.4	Temperature Control	32
3.5	Liquid Propellant	33
3.6	Testing Procedures	33
3.6.1	Safety	33
3.6.2	Loading	34
3.7	Data Acquisition	35
3.7.1	Initial Parameters	35
3.7.2	Pressure Data	35
3.7.3	Velocity Data	36
3.7.4	Interferometer	38
3.8	Inverse Interior Ballistic Code	39
3.9	Database	39
4.	TEST FIRING RESULTS	39

		Page
4.1	Stepped-Wall Chamber Configuration	39
4.1.1	Ignition of XM46	39
4.1.1.1	20-mm Gun Tests	40
4.1.1.2	30-mm Gun Tests (Tests 70-108)	42
4.1.2	Projectile Mass Scaling	47
4.1.3	Control With Scaling	47
4.1.4	Plastic vs. Steel Chambers	50
4.1.4.1	20-mm Gun Tests	50
4.1.4.2	30-mm Gun Tests	51
4.1.5	Reproducibility Tests	61
4.1.5.1	20-mm Reproducibility Series	61
4.1.5.2	30-mm Reproducibility Series	62
4.1.6	Stepped-Wall, Rear Couple	67
4.1.6.1	First-Stage Diameter Changes	67
4.1.6.2	First-Stage Length Changes	72
4.1.7	Velocity Scaling	72
4.2	Multi chamber Configuration	74
4.2.1	Front Coupling	76
4.2.1.1	Tapering	76
4.2.1.2	Second-Stage Diameter	77
4.2.1.3	Third-Stage Diameter	79
4.2.2	Number of Tubes	79
4.2.3	Rear Coupling	81
4.2.3.1	Diameter Changes	81
4.2.3.2	Length Changes	85
4.2.4	Extension of Concepts	85
5.	SPURIOUS TEST RESULTS, SOURCES, AND CORRECTIONS	88
5.1	Pressure Sealing of Insert Chambers	88
5.2	Reducing Spurious Pressure Pulses	90
6.	CONCLUSIONS	94
7.	REFERENCES	97
	APPENDIX: RESULTS OF THE 20-mm AND 30-mm TEST FIRINGS	99
	DISTRIBUTION LIST	107
	REPORT DOCUMENTATION PAGE	113

LIST OF FIGURES

Figure		Page
1.	Single-shot 20-mm test gun fixture	7
2.	Pyrotechnic igniter (booster) housing designs	8
3.	Steel and plastic 20-mm chamber insert geometries (H and I are acrylic)	10
4.	Steel 20-mm test chamber insert geometries	11
5.	20-mm and 30-mm test projectiles	12
6.	30-mm plastic chamber insert geometries	15
7.	Plastic and steel 30-mm chamber insert sections	17
8.	Chamber insert with modular first-stage for 30-mm gun tests	18
9.	Chamber insert with interchangeable first-stage for 30-mm gun tests	19
10.	Cut-away view of steel stepped-wall chamber insert and modified 30-mm steel projectile	21
11.	Chamber inserts modified with Delrin for 30-mm gun tests	22
12.	Cut-away view of multichamber insert and modified GAU-8 projectile for 30-mm gun tests	23
13.	1-3-3, 1-4-4, 1-6-6, and 1-3-9 multichamber inserts for 30-mm gun tests	25
14.	Extended multichamber insert design for 30-mm gun tests	26
15.	Drilling jig for the production of the 1-3-3, 1-4-4, 1-6-6, and 1-3-9 multichamber configurations	27
16.	Original 30-mm gun test fixture	29
17.	Modified 30-mm gun test fixture	30
18.	Example of information taken from chamber 1 P-t traces	37
19.	Effect of decreasing the booster load density by increasing the booster mass	41

Figure		Page
20.	Effect of increasing the booster load density while decreasing both the booster mass and booster housing volume	43
21.	Booster pressures obtained when Unique and HC33 are used as the booster propellant	45
22.	Effects of increasing the HC33 booster mass and a comparison to a Unique booster test	46
23.	(a) Pressure-time trace variations with projectile mass and (b) displacement of projectiles with different masses measured with 15-GHz interferometer	48
24.	Controlling LP combustion with geometrical changes in the chamber	49
25.	Tests 62, 66, 67, and 81: effect of sequentially replacing plastic chamber sections with steel	52
26.	Effect of changing the amount of plastic in the first stage and the amount of booster in the booster housing cavity	54
27.	Booster mass as a function of the plastic wall thickness in the first stage of a 30-mm stepped-wall chamber	56
28.	Examples of controlled and uncontrolled ignition in the BLPG tests	57
29.	Pressure traces for tests 111, 113, 114, and 115 using an all-steel stepped-wall chamber	59
30.	Effects of using a black and white Delrin insert in the first-stage section	60
31.	Chamber pressures generated during six 20-mm reproducibility tests using identical initial test parameters	62
32.	(a) Chamber pressures and (b) projectile displacements with time for five 30-mm reproducibility tests with identical initial test parameters	64
33.	(a) Chamber pressures and (b) projectile displacements with time for one reproducibility test and two inconsistent tests	66
34.	Effects of increased first-stage chamber diameters in 20-mm test firings	69

Figure | Page

35. Effects of increasing first-stage diameters on the generated chamber pressures in the 30-mm gun 71

36. Effects of an increasing first-stage length on the pressures generated in a 30-mm gun 73

37. Increased ballistic performance without pressure from an increasing fourth-stage diameter 75

38. Pressures generated in 30-mm multichamber tests without tapering (test 134) and with tapering (test 135) 77

39. Chamber 2 pressures generated in 1-3-3 multichamber tests with an increased second-stage diameter 78

40. Chamber 2 pressures generated in 1-3-3 multichamber tests with an increased third-stage diameter 80

41. Chamber 1 pressure-time traces for the 1-3-3, 1-4-4, 1-6-6, and 1-3-9 multichamber tests 82

42. Position 1 chamber pressures generated during the test with the 20/24/30 plastic stepped-wall chamber insert 83

43. Chamber pressures (position 1) generated when the first-stage diameter of the 1-3-3 multichamber is increased 84

44. Effects of changing the first-stage length in the 1-3-3 multichamber configuration (chamber pressure position 2) 86

45. The effects of length changes in the second stage of the 1-1-19 multichamber design (chamber pressure position 2) 87

46. 30-mm single-shot gun fixture used in early tests 89

47. Base of unmodified 30-mm projectile and modified configuration to reduce spurious high-pressure pulses arising from this region 92

A-1. Initial parameters - 20-mm test firings 101

A-2. Results - 20-mm stepped-wall test firings 102

Figure		Page
A-3.	Initial parameters - 30-mm stepped-wall test firings	103
A-4.	Results - 30-mm stepped-wall test firings	104
A-5.	Initial parameters - 30-mm stepped-wall test firings	105
A-6.	Results - 30-mm stepped-wall test firings	106

LIST OF TABLES

Table		Page
1.	Type of Propellant and Amount of Herkote Deterrent in Each	32
2.	Partial Table of Physical and Chemical Data of Hercules Unique Canister Powder	32
3.	Initial Parameters and Results for Ignition Tests Using 20-mm H- and I-type Chambers	70

INTENTIONALLY LEFT BLANK.

1. INTRODUCTION

The objectives of the Phase II Small Business Innovative Research (SBIR) Program reported here involved examining the influence of the mechanical concept of chamber geometry as an approach (in conjunction with a repeatable igniter) for controlling interior ballistic variability and the overall shape of pressure-time (P-t) curves in medium-caliber (20 mm and 30 mm) bulk-loaded liquid propellant guns (BLPG).

The performance variabilities observed in past BLPG investigations and an understanding of the responsible processes up to the late 1980s has been admirably reviewed [1]. These variabilities have included frequent overpressures and occasional gun system failures. The basic problem arises because the combustion process within a BLPG depends on hydrodynamic instabilities developed during liquid propellant (LP) ignition and combustion evolution, rather than on a predetermined solid propellant grain geometry to define the burning surfaces.

The instabilities themselves may arise from a number of sources, including variations in igniter output, initial ullage, shot-start pressure, fluid motion to form a combustion gas cavity within the body of LP in the gun chamber in response to LP combustion and projectile motion, fluid turbulence and breakup resulting from liquid motion relative to the chamber walls, and liquid surface breakup arising from a velocity mismatch at the liquid-gas interface [2]. Typically, the characteristics of these instabilities vary in response to the prior sequence of events, and small disturbances that arise early in the BLPG combustion cycle can become amplified in absence of burn rate limiting characteristics.

While significant attention has been given to techniques of developing and emphasizing the need for repeatable ignition in BLPGs [3], features associated with combustion evolution, although certainly recognized early [1, 2, 3], appear to have received somewhat less attention.

The concept of using different geometries in igniters and in the igniter region of BLPGs to help couple the igniter output to the main LP charge was introduced as early as 1974 [4, 5]. The concept of utilizing a stepped-wall geometry in the BLPG combustion chamber itself as a potential means of exerting boundary control on combustion evolution during part of the interior ballistic cycle originated during diagnostic-type BLPG investigations conducted at Veritay in 1990 [6, 7]. This approach was further explored and tested during subsequent experimental investigations [8, 9, 10, 11].

An alternate multichamber concept for geometry control of combustion within the main chambers of a BLPG was also investigated experimentally at Veritay [12, 13, 14]. One multichamber concept explored at Veritay exhibited some similarities to the approach advanced by Puckett [15], but did not utilize the open plenum configuration at either end of the chamber tubes.

In addition to the BLPG testing and analysis conducted at Veritay, the data generated during this effort were used in independent, as well as cooperative, analyses by the U.S. Army Research Laboratory (ARL) [3, 16, 17].

The achievement of control over the ignition and combustion processes of bulk-loaded LP in a closed, vented chamber under high-pressure conditions is an important technological goal from the standpoint of obtaining satisfactory uniformity in ballistic performance and overall safety in gun operation. Further, these combustion control issues are important for successful, dual-use civilian applications of the bulk-loaded LP propulsion technology base, including items such as explosively driven airbag restraint apparatus; oil and gas-well stimulation via ballistically tailored, pulse-shaping soil displacement; propellant-driven concrete anchors for the construction industry; mining and tunneling applications; explosive bonding; welding and cladding of dissimilar metals; pulse-power generators for high-power microwave sources; resonant charging of capacitors; and possible use in fusion research.

Potential military applications include direct-fire bulk-loaded guns in medium-caliber and small-arms sizes, and bulk-type ignition systems for large guns. The BLPG system is itself a particularly attractive candidate for small- and medium-caliber weapons because the gun hardware can be simple. It can likely be implemented for use over a range of muzzle velocities to achieve selected degrees of controlled lethality because the use of a LP in such guns offers potential advantages in vulnerability, logistics, and cost over comparable weapons that use solid propellants.

2. BACKGROUND OF BALLISTIC PROCESS CONTROL NEEDS

In the past, a typical BLPG system was frequently viewed as consisting of a near-bore diameter cylindrical combustion chamber, an igniter at the breech end, and a projectile seated at the forward end of the chamber just inside the barrel. This classical BLPG system arrangement has essentially been adapted directly from a solid propellant gun configuration and, indeed, features the utmost in mechanical simplicity. However, this layout offers few means in BLPG systems to control and stabilize the ignition and combustion processes or the fluid dynamics and combustion instabilities that often develop during combustion evolution.

The general nature of ignition and combustion of liquid gun propellants is briefly summarized in the following paragraphs to indicate some of the problems encountered and to enable a better understanding of the significance of some unique features of process control needs and concepts.

Generally, liquid or gel propellants may contain solid components, but all such propellants have a liquid as the continuous phase. Since most of the combustion occurs in the droplet or vapor phase, the igniter must vaporize a small amount of propellant and then heat the vapor to a temperature at which exothermic reactions occur.

Several problems must be overcome or addressed to achieve successful initiation and combustion of LP in a bulk-loaded configuration, including the following.

- Ignition and combustion gas cannot flow throughout the charge since the LP permeability is essentially zero; instead, the gas is confined.

- Gas evolving from the igniter or from combustion of the LP can create both radial and axial pressure waves and strong combustion interactions at liquid-gas interfaces.

- The ignition gas kernel must be sufficiently large and energetic to avoid being quenched by expansion cooling caused by projectile motion.

- The ignition-combustion burning surface is not well defined geometrically; rather it is characterized initially by the growth and geometry of the bubble of ignition and combustion gases or Taylor cavity [1, 2]. Once the projectile motion becomes significant, the gas cavity is expected to push through the LP to the projectile base, and gas driven Helmholtz instabilities are expected to appear on the LP at the liquid-gas interface [1, 2]. These instabilities may grow and cause some of the liquid to break up and form droplets; thereby, enhancing the burn surface area and the overall rate of LP combustion.

- Generally, combustion processes in an LP can be more repeatable if the process can be made to occur in a manner that maintains both hydrodynamic and combustion symmetry with respect to the boundaries of the containment vessel. Typically, such symmetry goals can often apply to turbulent flow conditions also.

- The igniter output and early combustion must increase the chamber pressure to a level where reaction kinetics are rapid and self-sustaining, or a controlled progressive combustion occurs, and the ullage is compressed to form a more rigid liquid charge, even with projectile motion.

- The amount of LP and the rate at which the LP is ignited is critical for control of peak pressure in the chamber.

- Sufficiently large pockets of gas (air or LP vapor), referred to as ullage, can cause unwanted local ignition by adiabatic compression heating during the early time-pressure rise.

- Additional pockets, or localized regions of LP vapor caused by cavitation of LP during flow past sharp corners in the chamber, can cause local, secondary ignition by adiabatic compression heating of these regions if they are subjected to even moderately large pressure pulses within the chamber.

- High-pressure pulses within a chamber can be generated by reflective enhancement of lower pressure pulses from concave curved surfaces and sometimes from flat surfaces.

These various features indicate that the igniter must be tailored to the LP charge to some extent. Both overignition or underignition can cause excessive pressures to occur in bulk-loaded LP chambers. Pressure waves in the LP that impinge on liquid-gas-free surfaces may cause spallation and droplet formation (with an increase in burn surface area) and cause increased overall combustion rates and possible overpressures. Therefore, igniter and chamber designs should be configured to minimize pressure wave effects, while providing the sustained output required to achieve positive ignition without excessive time delay.

Since the initial gas cavity within the LP-filled main gun chamber is generated by the igniter, overall combustion reproducibility depends to some extent on the inherent reproducibility of the ignition system itself, the way this initial cavity develops, and the tendency for combustion within this cavity to stabilize early during its development and growth within the chamber.

Early, the projectile remains nearly stationary as the igniter creates a burning gas bubble within the liquid phase to achieve adequate pressure and gas volume to support initial projectile motion while maintaining combustion. By the time the projectile velocity has become significant (i.e., about 200 m/s), an appreciable fraction of the high-pressure portion of the ballistic cycle is over; only a few percent of the propellant has burned, and the gas pressure tends to be somewhat unstable because of the relatively large rate of change of volume and the low, compressive nature of the liquid. This early portion of the ballistic cycle is typically characterized by the occurrence of a high-pressure pulse and can be strongly influenced by the igniter.

Once the projectile has achieved significant velocity and displacement, the mode of combustion appears to change into one dominated by burning of droplets stripped from the liquid layer next to the chamber wall [2]. While all the mechanisms are not well understood, it is believed that this mode may begin when the initial gas cavity penetrates the liquid to the projectile base as a result of projectile motion. The rate of burn surface generation and global combustion appears to increase for a period, corresponding to increases in the projectile velocity. The corresponding pressure then decreases as the projectile continues to move down the barrel. Combustion during this period is often well-behaved if the ignition and combustion progressivity are in a suitable range, but it can present problems of developing high pressures unless some control over combustion progressivity is exercised. The achievement of reproducible P-t behavior in this later portion of the ballistic cycle may be much more difficult, yet this may not be critical since a sizeable portion of the pressure influence on projectile velocity has occurred relatively early in the projectile travel down the barrel.

3. EXPERIMENTAL SETUP

3.1 <u>20-mm Gun Test Fixture</u>. Early firing tests in this program were conducted using the single-shot 20-mm test gun fixture (Figure 1). This gun test fixture was developed under previous programs [8, 9] and consisted of different components that could be assembled into the gun fixture in a modular fashion; it was supported by a large, steel beam to control the gun recoil. A 20-mm rifled Mann barrel with a heavy-wall steel chamber housing made up the main gun assembly, and the separate modular parts were included during the setup of each test. The chamber was designed with an oversized cavity to accommodate chamber inserts approximately 44.37 mm in diameter and 97.2 mm long that could be individually configured to achieve different interior chamber geometries. Each chamber insert was held in place by a threaded breech assembly. Pressure transducers were inserted into the heavy-wall chamber housing that included through-ports aligned with openings in the chamber insert. The breech assembly consisted of a booster housing with a percussion primer and a pyrotechnic igniter, firing pin, and appropriate o-ring seals. Ignition was achieved by remotely activating an air solenoid attached to the firing pin assembly; this caused the firing pin to strike the primer. This gun assembly was used throughout the 20-mm testing without any modifications. Additional important parts associated with the use of this gun test fixture included a standard 20-mm projectile, velocity measuring equipment (conducting breakstrips), and data acquisition devices.

3.1.1 Pyrotechnic Igniter. In the 20-mm firing tests, two different pyrotechnic igniter (booster) designs, B17-600 and B17-006, (Figure 2) were used to ignite the LP. A third booster housing design, B17-111, is also shown in Figure 2 for convenience, but was used only in 30-mm gun firing

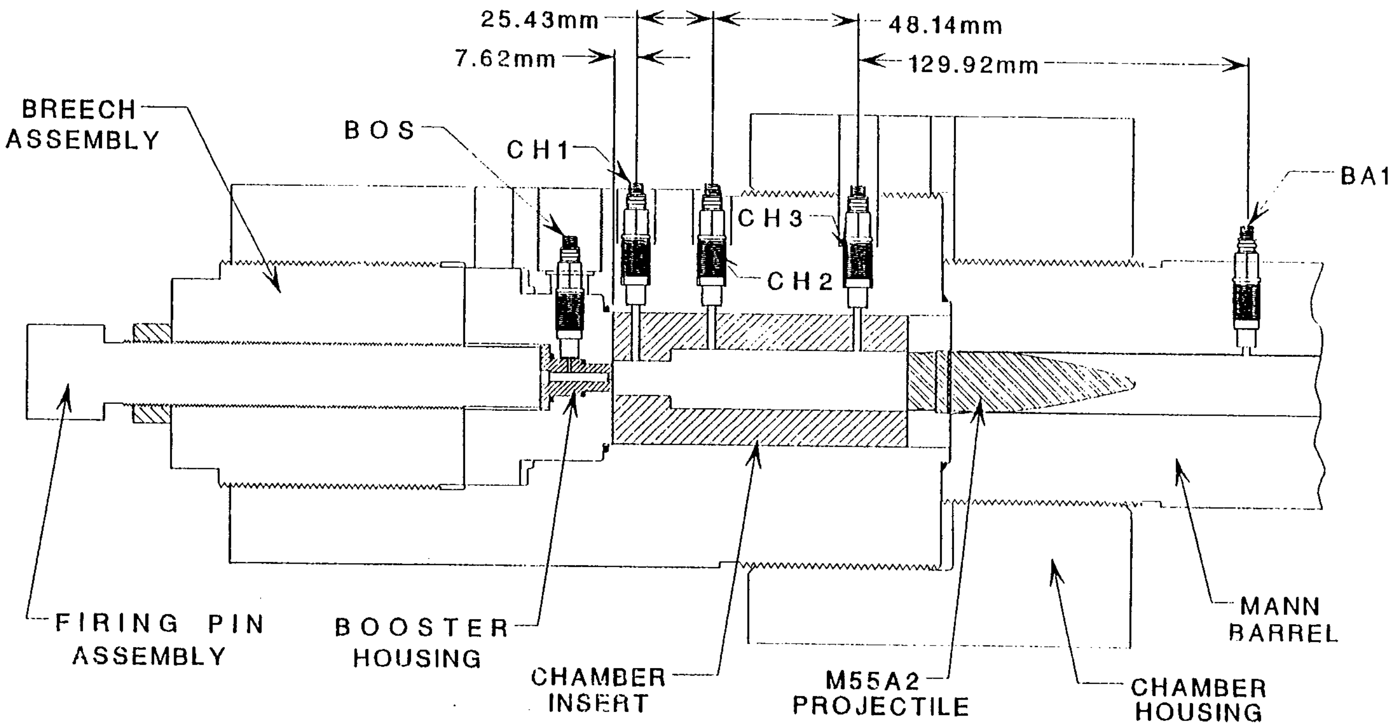

Transducers

Type	Mount	Longitudinal Position	Orientation (From Breech)
BOS	BOOSTER PRESSURE	---	---
CH1	RECESS MOUNT CHAMBER PRESSURE POSITION 1	7.62 mm FROM BREECH FACE	0° (TOP)
CH2	RECESS MOUNT CHAMBER PRESSURE POSITION 2	33.05 mm FROM BREECH FACE	45° CLOCKWISE
CH3	RECESS MOUNT CHAMBER PRESSURE POSITION 3	81.19 mm FROM BREECH FACE	0°
BA1	STANDARD MOUNT BARREL PRESSURE POSITION 1	211.11 mm FROM BREECH FACE	0°
BA2	STANDARD MOUNT BARREL PRESSURE POSITION 2	541.31 mm FROM BREECH FACE, NOT SHOWN	0°
MUZ	STANDARD MOUNT BARREL PRESSURE AT MUZZLE	1436.66 mm FROM BREECH FACE, NOT SHOWN	0°

Figure 1. Single-shot 20-mm test gun fixture

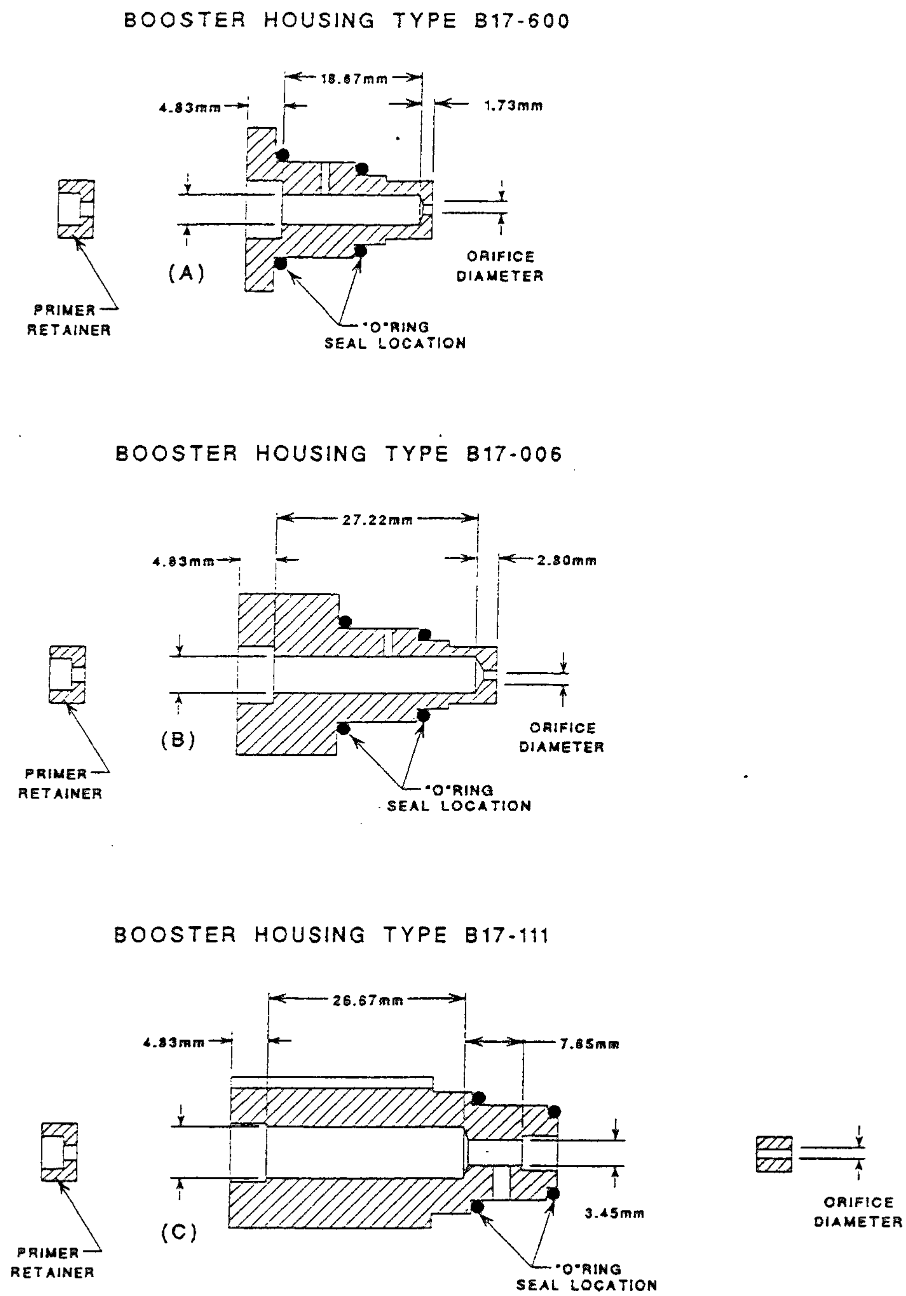

Figure 2. Pyrotechnic igniter (booster) housing designs.

tests. Use of this particular housing is discussed later (section 3.2.1). These igniter designs (booster housings) were inserted into the breech assembly. Both of these booster housings were machined with an interior cavity to accept pyrotechnic-igniter (booster) propellants. This interior cavity had a relatively large diameter that was varied from 3.73 mm to 5.61 mm and transitioned into a smaller orifice diameter of approximately 1.32 mm. The orifice allowed for the hot gases generated from the burning propellant to build up to a relatively high-pressure level and then escape into the LP-filled main chamber. Each of the booster housings was loaded with the booster propellant and then sealed with a primer retainer and a CCI-400 primer. A pressure port was located perpendicular to the main booster cavity, which lined up with a pressure transducer port with the aid of a locating pin. Two Viton-rubber o-rings, fitted on two steps on the exterior of the booster housing, prevented gas leakage and permitted accurate measurement of the booster pressure.

3.1.2 Chamber Inserts. Chamber inserts were utilized in the 20-mm work so that each test could be loaded and fired on an individual basis. In the initial 20-mm tests, two plastic chamber designs were used to investigate the ignition of the XM46. These are the H and I geometries in Figure 3 (the remainder of the chamber inserts in Figure 3 were made of steel). Two plastic inserts (the same as the one designated type B17-A in Figure 4), each with a straight cylindrical geometry, were also test fired before the remainder of the steel insert geometries shown in Figure 3 and in Figure 4 (including type B17-A) were tested.

The interiors of the steel chamber inserts used in these later 20-mm firings were initially single, open cylinders with constant diameters. From these given first-stage single diameters, steps to successively larger diameter cylindrical sections were added to produce each stepped-wall design. To investigate the effects on the combustion evolution and duration, different numbers of steps with different diameters were used in the bulk-loaded LP tests. The steel chambers used in this testing are shown in Figures 3 and 4.

3.1.3 20-mm Projectiles. The projectiles used in this effort were standard M55A2TP 20-mm projectiles (Figure 5). These were used without modifications since interferometer velocity measurements were not made. In the projectile mass scale testing, the M55A2TP projectiles were

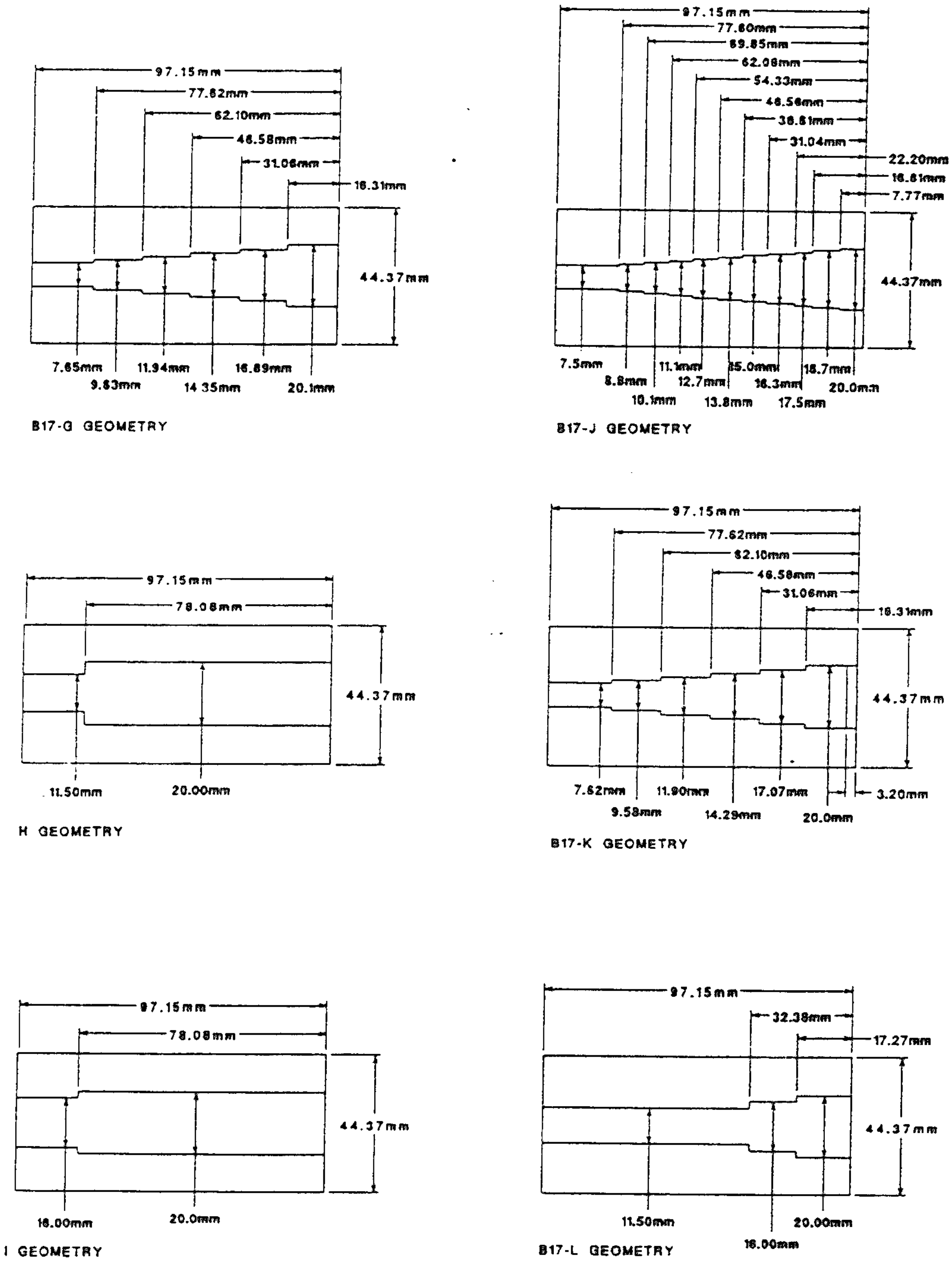

Figure 3. Steel and plastic 20-mm chamber insert geometries (H and I are acrylic).

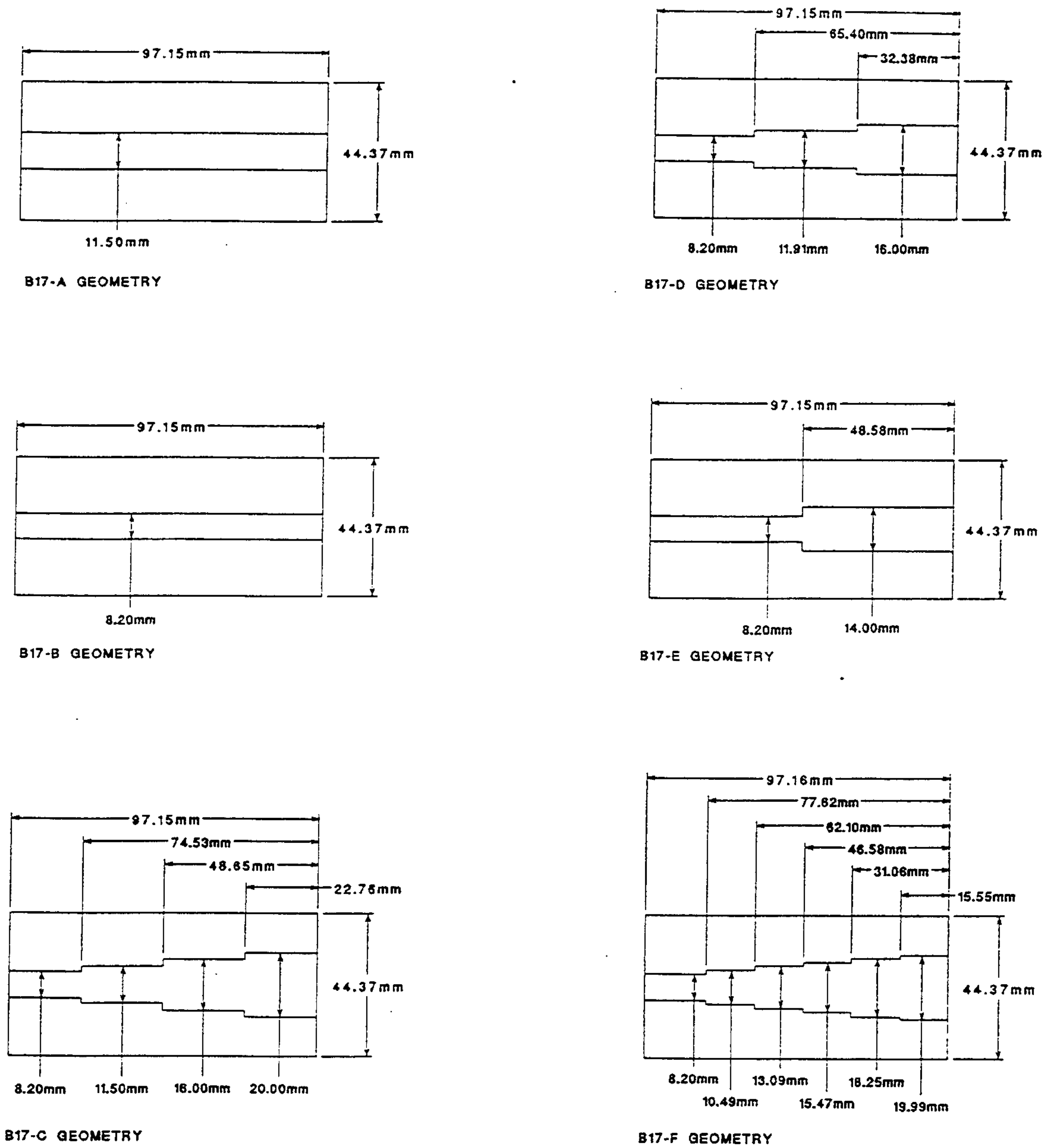

Figure 4. Steel 20-mm test chamber insert geometries.

20mm PROJECTILES

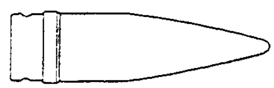

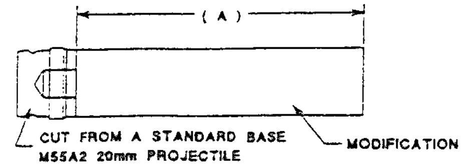

MODIFICATION #	"A" DIMENSION(mm)	MASS(g)
B17-502	10.16	67
B17-503	23.37	100
B17-504	66.04	200
B17-505	85.60	250
B17-506	106.22	300
B17-507	126.82	350
B17-508	138.13	378

30mm PROJECTILES

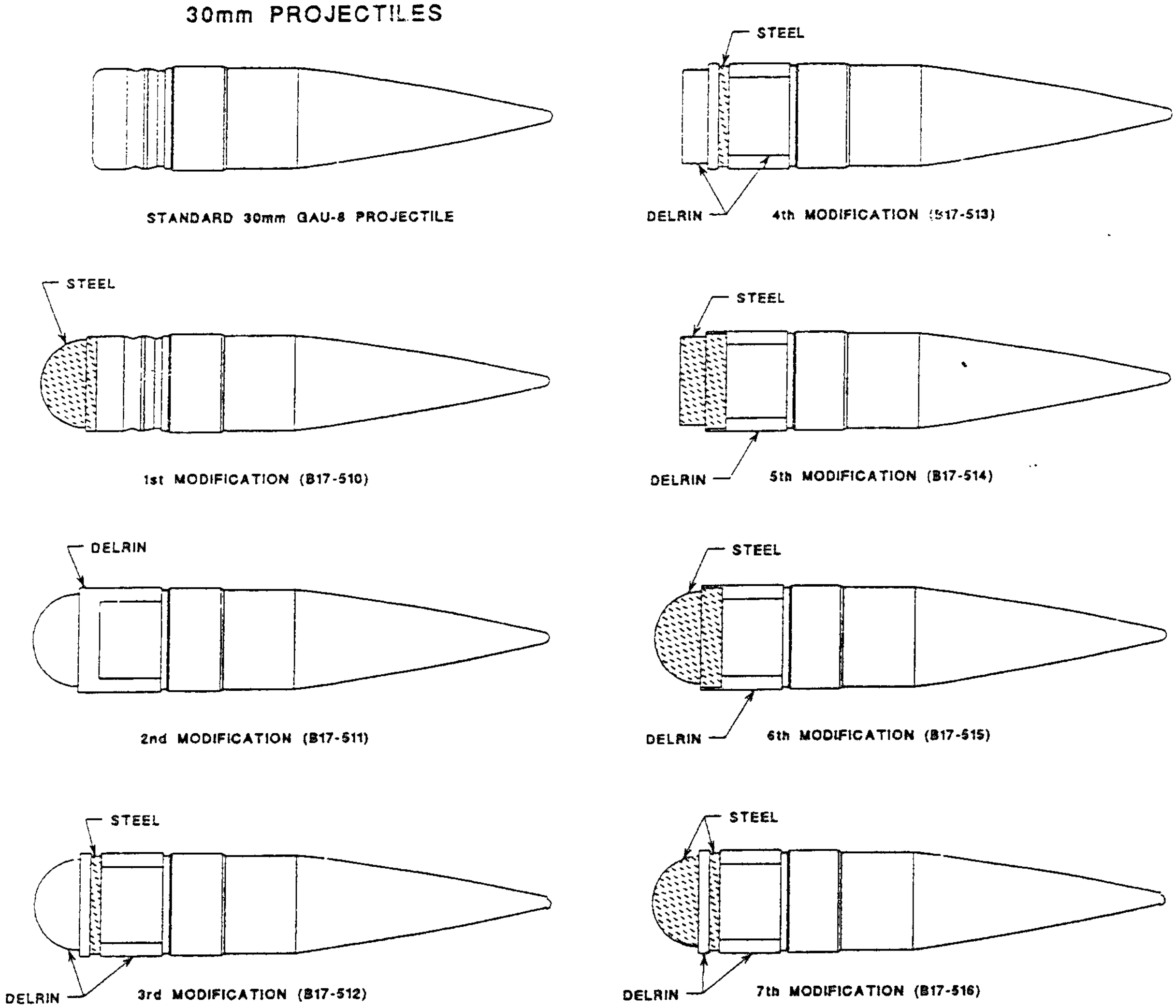

Figure 5. <u>20-mm and 30-mm test projectiles</u>.

modified by removing the section in front of the rotating band and replacing it with a length of steel rod welded to the projectile base. The length of these rods was dependent on the projectile mass desired and varied from 10.16 mm to 138.13 mm to achieve projectile masses from 67 g to 376 g (Figure 5).

3.1.4 Pressure Transducer Locations. Seven pressure transducers were used during the testing of the 20-mm bulk-loaded LP test gun. The distances of all of the transducers from the breech face of the 20-mm gun along with the distances from each other are given in Figure 1. One transducer was located in the breech assembly, three were located in the chamber section, and three were located in the barrel. The transducer located in the breech (BOS) was used to measure the pressure generated within the booster housing. The three chamber pressure transducers (CH1, CH2, and CH3) were located in line to record the pressures generated in the chamber during the test. These pressures in the main chamber were obtained through long ports 2.26 mm in diameter that led to the main chamber cavity. The barrel transducers (BA1, BA2, and MUZ) were recess-mounted and were important in determining the pressures that originated in the barrel and created delayed pressures in the chamber. The muzzle pressure was important to determine the amount of muzzle blast from the combustion event.

3.2 <u>30-mm Gun Test Fixture</u>.

3.2.1 Pyrotechnic Igniter. The booster housing used in the 30-mm firings of this effort was configured to accommodate different pyrotechnic igniter propellants and could be easily modified to test different booster housing interior volumes. The propellants used as the booster were contained within a cavity that consisted of a large cylindrical section, together with a smaller cylindrical section toward the chamber. A schematic of the booster housing B17-111 used is shown in Figure 2. For a series of tests, the larger section diameter was changed while the smaller region remained constant. A through-hole penetrated the smaller region at a 90° angle and was lined up with a pressure port by the use of a guide pin during insertion of the booster housing into the test gun fixture. A plug with an orifice diameter from 1.4 mm to 1.7 mm was pressed into the front end of the booster housing, and this orifice allowed the booster gases to exit into the chamber cavity. Since the orifice diameter could become larger through erosion by high-temperature, high-velocity gases during the tests, the orifice plug was removed and replaced before every bulk-loaded LP test.

To permit alterations to be made to the interior of the booster housing, a removable primer retainer was included in the design. The diameter of the housing interior was varied simply by removing the primer retainer and drilling the housing to a larger diameter, or by pressing a sleeve into the housing to decrease the diameter.

3.2.2 Chamber Inserts. Some, but not all, of the insert chambers used directly in the 30-mm gun fixture testing were stepped-wall cylindrical-type combustion chambers (Figure 6). In general, the chamber designation, such as "AAA GEOMETRY," is used in this report mainly to indicate the interior geometry of each chamber. The materials from which each tested chamber was constructed (such as plastic, steel, or percentages of each of these materials) are indicated explicitly as part of the initial parameters for test firing data summarized in the Appendix.

In each case for the insert chambers shown in Figure 6, the interior geometry was formed by a sequence of cylindrical sections joined end-to-end and located along a common axis. By properly configuring the diameter and length of each section of the chamber-wall geometry, the postulated progressivity and stability of combustion within the chamber was controlled more effectively. The magnitude, and to some extent, the shape, of the P-t combustion behavior within such a step chamber could be adjusted by changing the chamber geometry to achieve low-, medium-, or high-muzzle velocity ballistic performances.

3.2.2.1 Original Stepped-Wall Geometries. As a result of previous 20-mm stepped-wall chamber test work [7, 8, 9], the early firing tests conducted here used a single-shot 30-mm test gun fixture fitted with different individual types of chamber inserts of plastic, steel, or a combination of both. These 30-mm chamber inserts were surrounded by a heat-treated 17-4 PH steel insert sleeve* that provided added strength and reduced the overall compressibility of the chamber inserts used in the tests. These chamber inserts included the following.

*This steel insert sleeve component is illustrated in Figure 16.

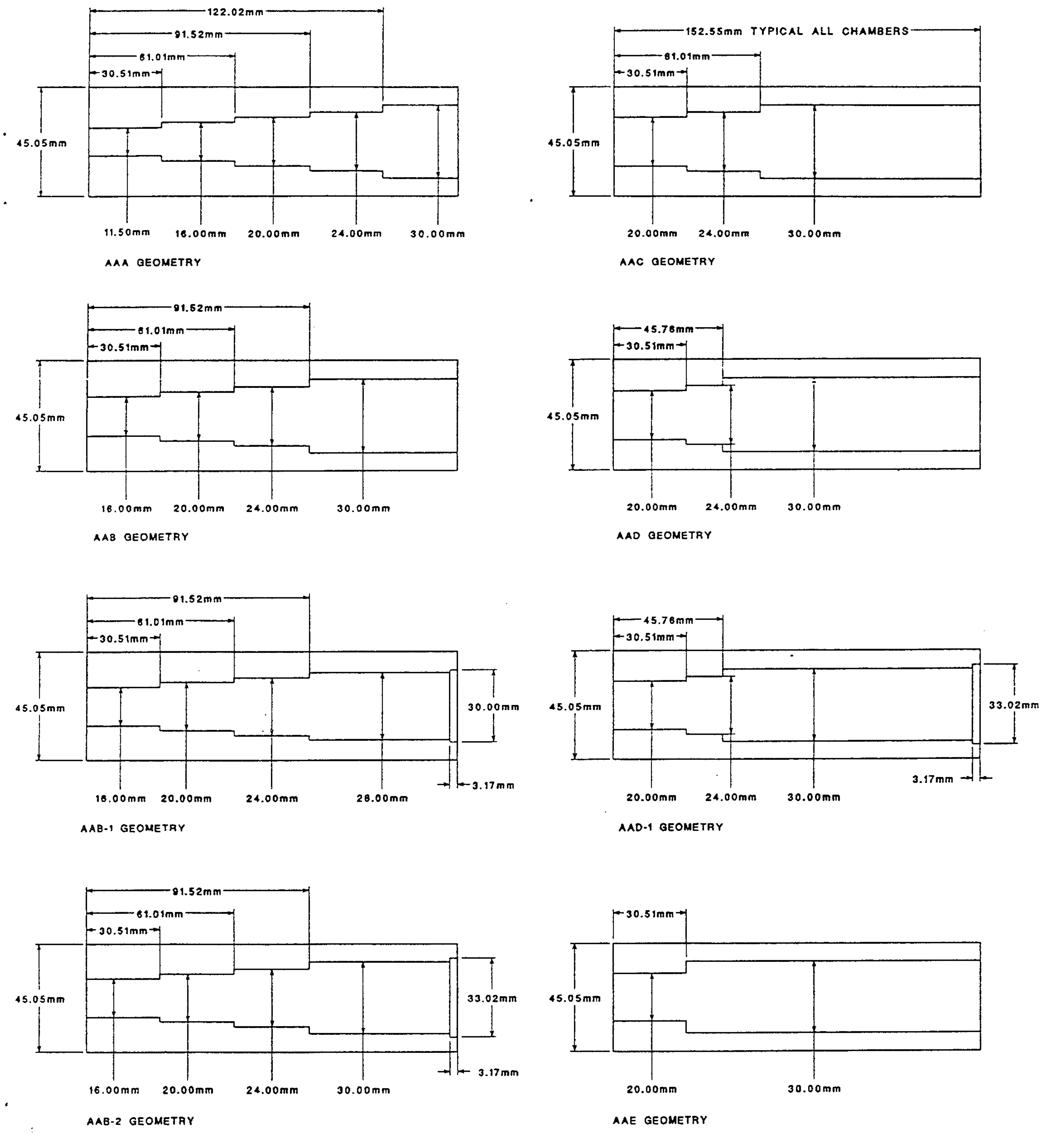

Figure 6. 30-mm plastic chamber insert geometries.

- The individual acrylic-plastic chamber inserts with the interior geometries corresponding to those indicated in Figure 6.

- The combinations of separate rear-plastic and front-steel insert sections of different lengths (to vary the proportion of steel used) (shown in Figure 7).

- The combination of a long, front, stepped-wall steel insert and three candidate, short, rear, first- stage insert sections with different amounts of plastic and steel (to be used individually with the long insert to further increase the proportion of steel used at the initiator end of the chamber) (shown in Figure 8).

Later, the 30-mm test gun fixture was modified to enable the pressure transducers to be positioned closer to the combustion event in the insert cavity and thereby shorten the length between the cavity and face of each pressure transducer. This modification enabled a flush-mounted pressure transducer to be introduced with zero setback in addition to the standard mount (recessed mount) with a 2.29 mm (0.090 in) setback; this was partially to improve the frequency response of the pressure measurements. It further reduced spurious pressure pulses, which may have originated as a result of the coupling between the transducer and the combustion event.

This modification also resulted in the elimination of the surrounding steel insert sleeve noted previously. Instead, a one-piece, heat-treated 17-4 PH steel insert chamber with a larger outside diameter, improved high-pressure seals on each end, and a partially fixed, stepped-wall geometry arrangement was used.* This steel insert chamber (Figure 9) also included a short, first-stage insert section of plastic and steel at the initiator end of the long steel chamber. Three first-stage insert sections tested are also shown in Figure 9. Their use permitted further examination of the suspected tendency of plastic in this initiation region to help reduce the magnitude of pressure oscillations or pulses that have sometimes been observed as part of the overall P-t traces generated in BLPG tests.

*This modified steel insert sleeve component is illustrated in Figure 17.

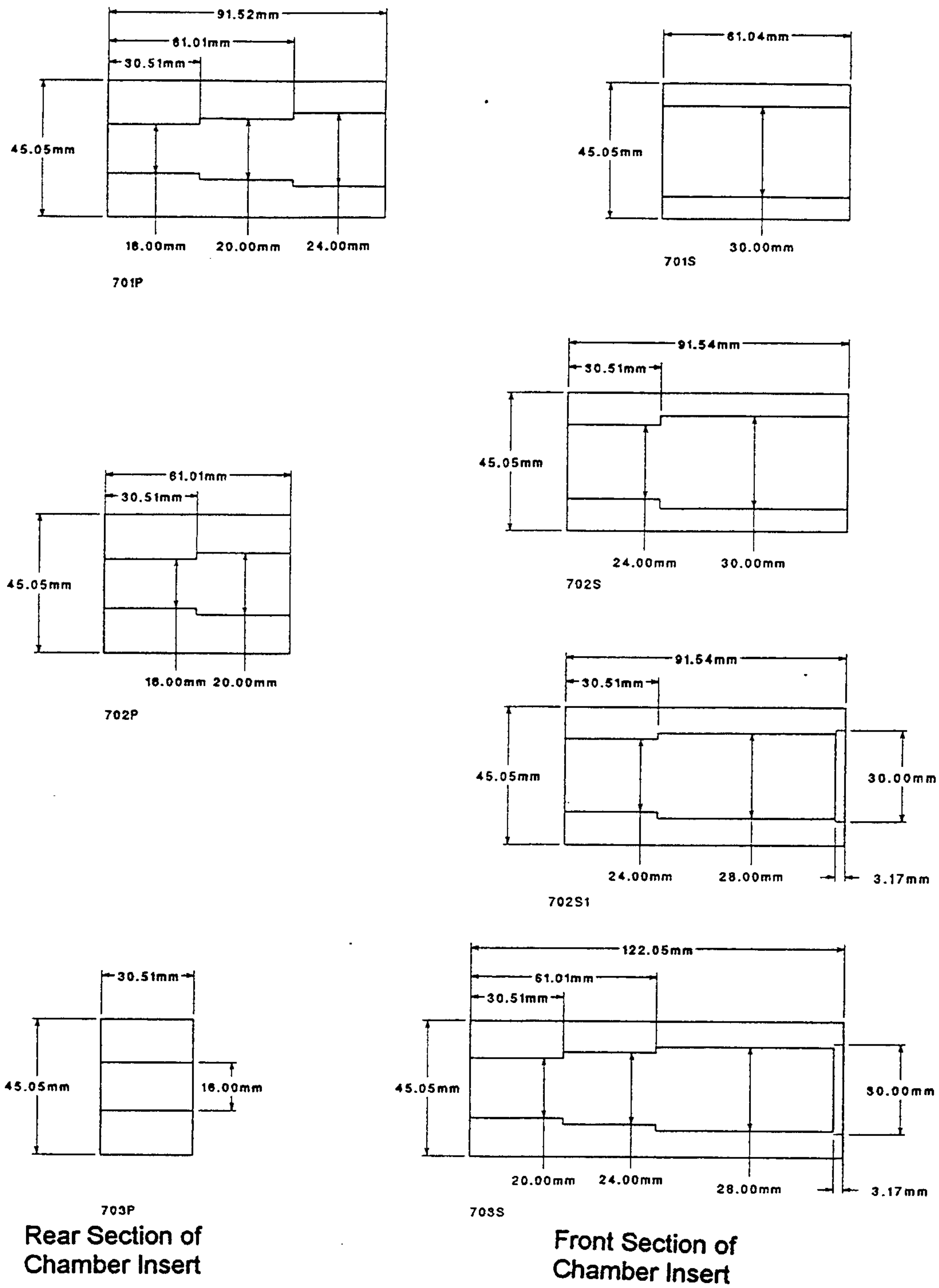

Figure 7. Plastic and steel 30-mm chamber insert sections.

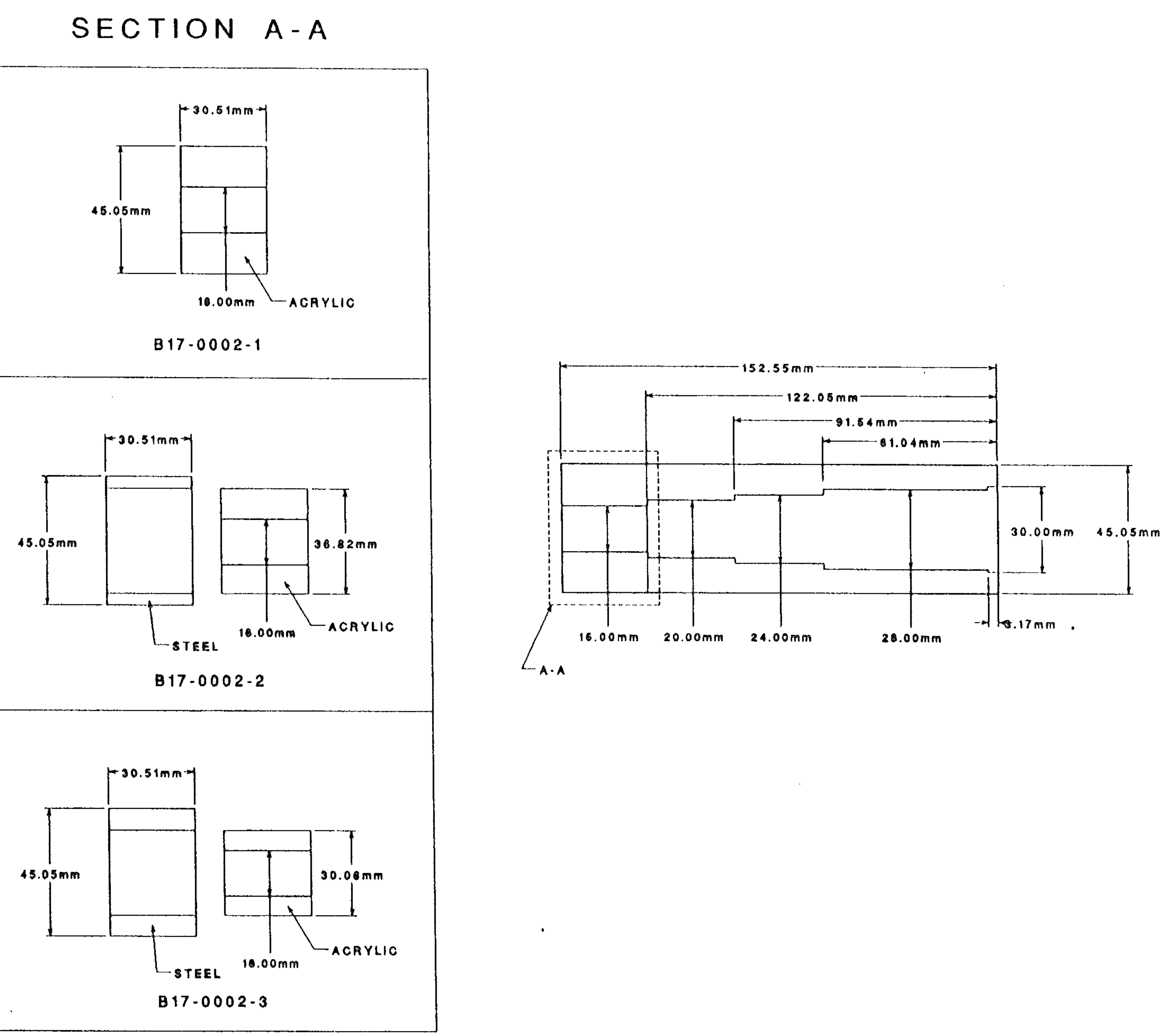

Figure 8. Chamber insert with modular first-stage for 30-mm gun tests.

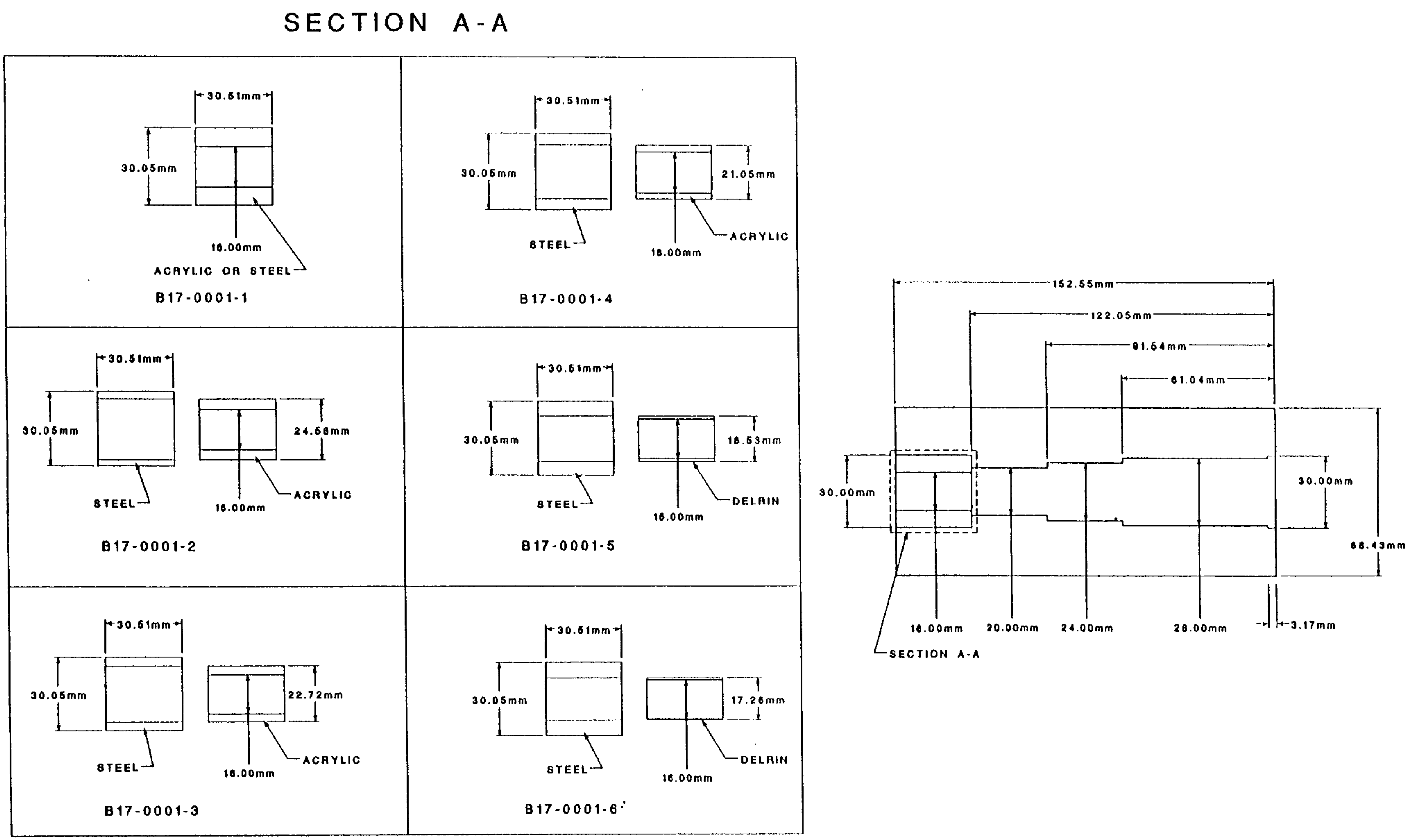

Figure 9. Chamber insert with interchangeable first-stage for 30-mm gun tests

3.2.2.2 Modified Stepped-Wall Geometries. The design of the 30-mm stepped-wall chamber inserts were changed slightly after test 115 to accept the 30-mm projectiles shown in Figure 5 with modified bases of either steel or Delrin to serve as hemispherical wave deflectors or wave absorbers. The Delrin was larger than the chamber diameter, so there was approximately a 0.05-mm pressed fit when the projectile was seated in the front of the chamber insert. This created a strong seal that allowed the LP to be poured into the rear end of the chamber without seepage.

The first stage of each of these modified stepped-wall insert chambers was 16-mm inside diameter, when fitted with a Delrin insert sleeve with wall thickness of 1.27 mm (0.050 in).

A perspective, cut-away view of a 30-mm steel stepped-wall chamber insert together with a modified GAU-8 30-mm inert projectile is shown in Figure 10. Schematics of the modified chamber inserts used in the modified 30-mm gun test fixture are shown in Figure 11.

3.2.2.3 Multichamber. The second type of 30-mm plastic chamber insert investigated was the multichamber configuration (Figure 12). The principal geometry of the multichamber inserts consisted of a single, cylindrical first- stage section followed by a second section containing 1,3, 4, or 6 cylindrical tubes, and a third section containing 3, 4, 6, 9, or 19 cylindrical tubes. An important part of this design, derived through experience and testing, is the transition region from the last-stage tubes to the bore diameter.

In the first multichamber test, it was observed that the pressures in the chambers increased significantly following initial ignition and early pressure development. This significant pressure increase was attributed to more vigorous combustion in the turbulent region just downstream from the termination of the tubes. This turbulence was likely caused by LP flow past the abrupt steps at the ends of the holes formed by the cross-sectional area of material between the tubes themselves. This turbulent region downstream from this central core region was essentially eliminated by tapering the front ends of the tubes with respect to the central axis of the chamber to eliminate the large, central step changes. In addition, a transition ring was added at the front of this region where

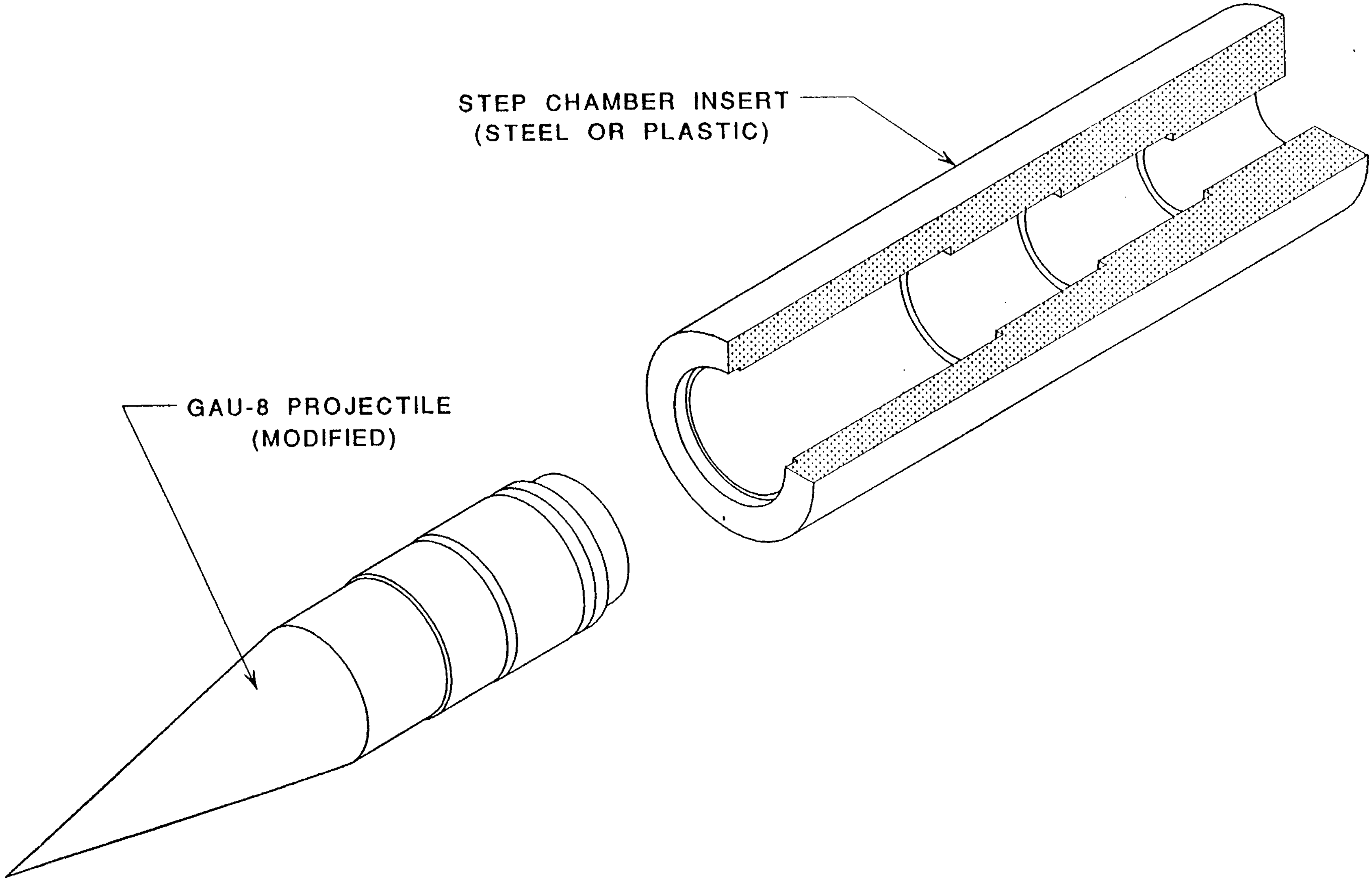

Figure 10. Cut-away view of steel stepped-wall chamber insert and modified 30-mm steel projectile.

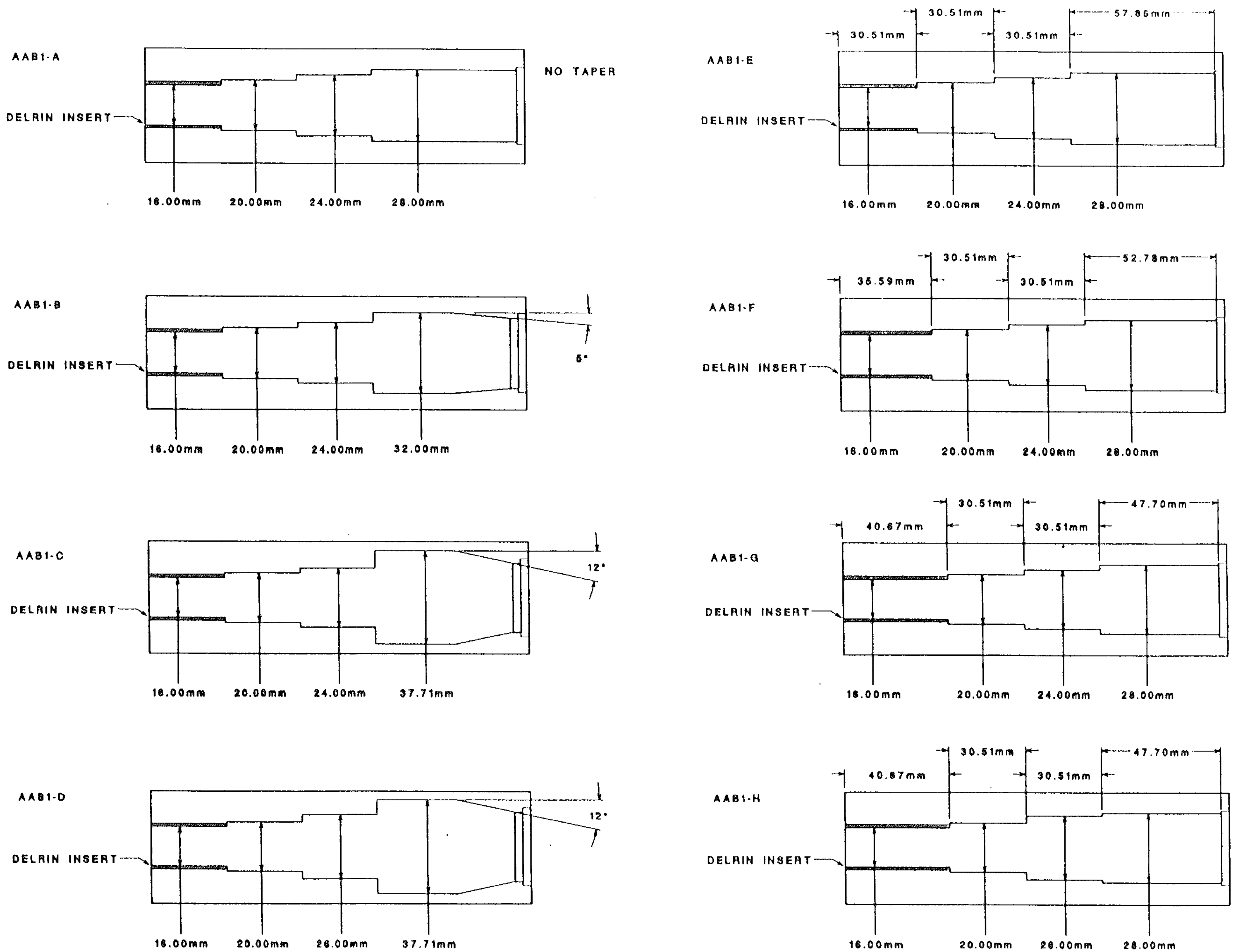

Figure 11. Chamber inserts modified with Delrin for 30-mm gun tests.

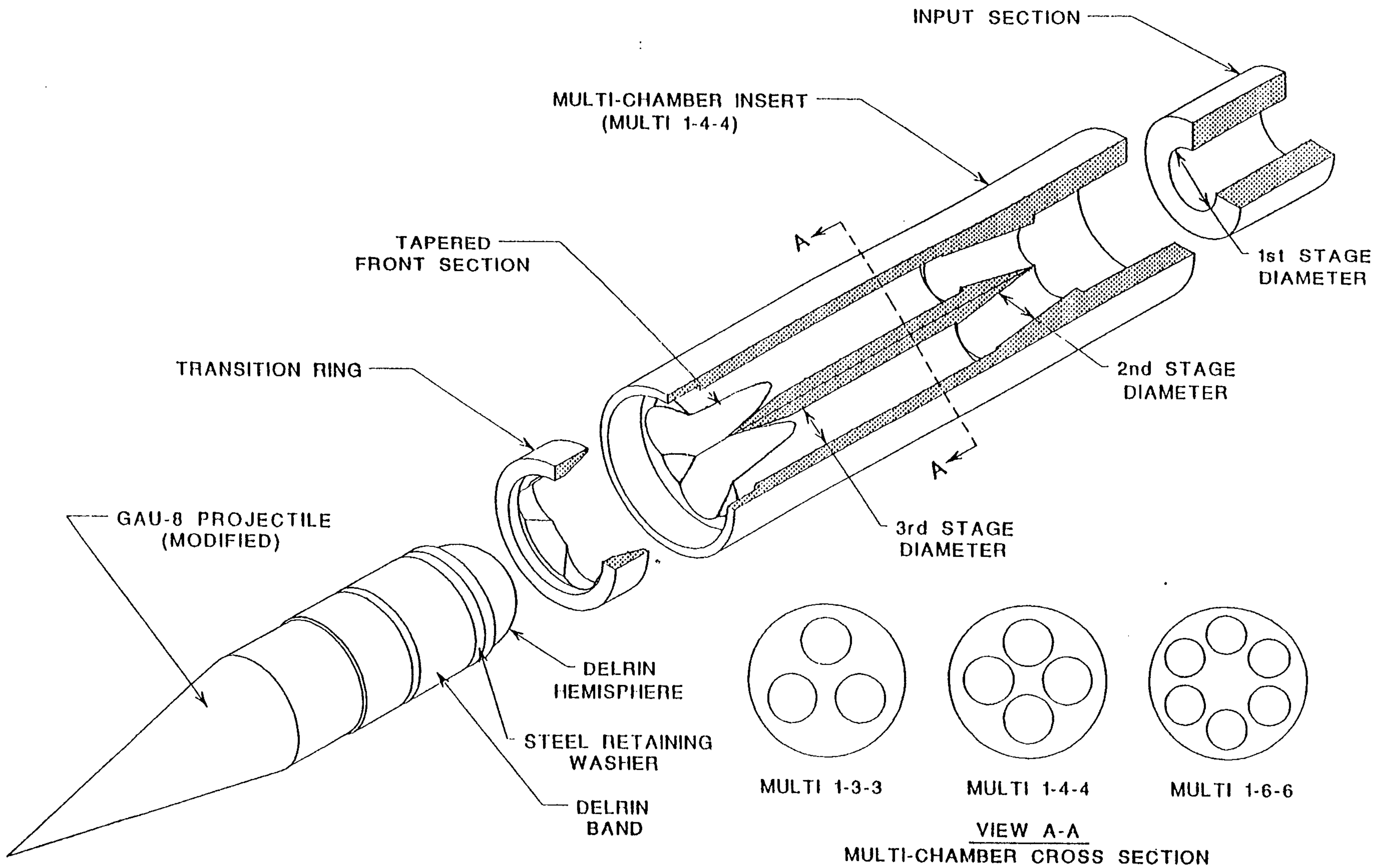

Figure 12. Cut-away view of multichamber insert and modified GAU-8 projectile for 30-mm gun tests.

the tubes joined, since the outer diameters of the tubes were larger than the gun-bore diameter. This ring formed a single, chamber-chambrage region that directed excess LP and combustion gas into the barrel without causing further turbulence from sharp corners. A three-dimensional, cross-sectional view of the multichamber with a modified GAU-8 30-mm inert projectile is presented in Figure 12.

The multichamber configurations in the proceeding sections were designated by the number of chamber tubes present in each of the chamber sections, as noted in Figure 13. Thus, a multichamber, designated 1-3-3, consisted of a single-cylinder input section, a three-chamber (or tube) transition region, and a three-tube third section. Correspondingly, the designation 1-1-19 refers to a single-cylinder input section, a single, large-diameter, plenum transition section, and a 19-tube multichamber region (Figure 14). Since the cross-sectional area of each section of the stepped-wall chamber inserts has been identified as an important feature of the chamber performance, an equivalent single diameter in millimeters of the combined cross-sectional area of tubes in each region may be identified. For instance, some of the multichamber configurations used had equivalent chamber diameters of 20 mm, 24 mm, and 29 mm.

3.2.2.4 Multichamber Drilling Jig. To fabricate the multichamber configurations, and especially the tapered front section of the chambers, drilling jigs were machined and utilized to increase the efficiency and accuracy of the fabrication and, hence, the testing. The straight tubes in the front section of the chamber insert were located and drilled first, then a pin (alignment insert) in the drilling jig (Figure 15) was used to locate the holes and drill the angled holes that intersected the straight tubes. This jig was used with minor modifications for the 1-3-3, 1-4-4, 1-6-6, and 1-3-9 configurations. To create the tapered section between the straight holes, a 45° angle was machined at the front end starting at the outer edge and cutting into the chamber. The drilling jig was used again to hold the insert at an angle, and a drill was used to remove material from between the straight holes. The tapering in the transition ring holding in the projectile was accomplished by using a simple drilling jig and an angled drill mount.

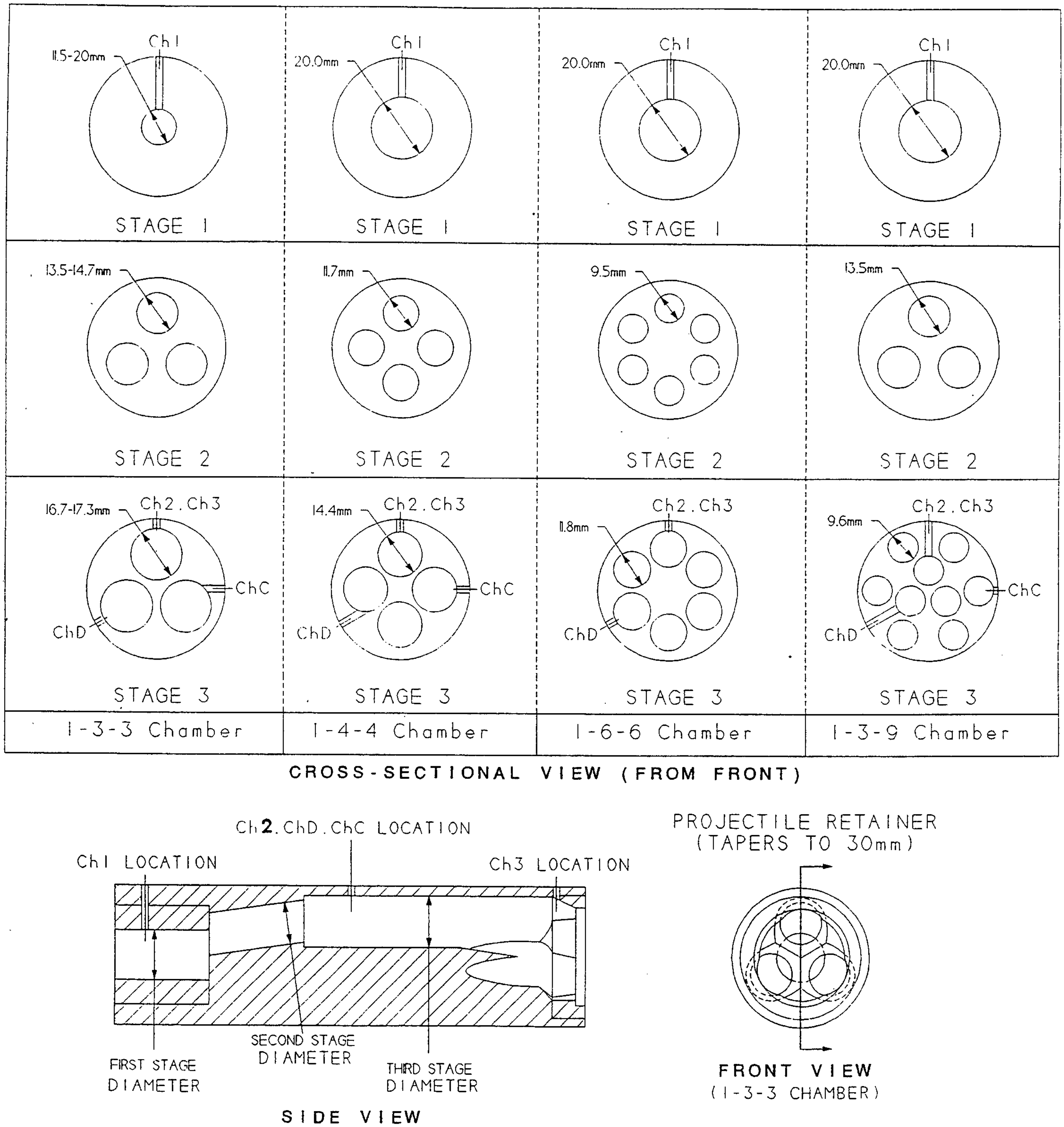

Figure 13. 1-3-3, 1-4-4, 1-6-6, and 1-3-9 multichamber inserts for 30-mm gun tests.

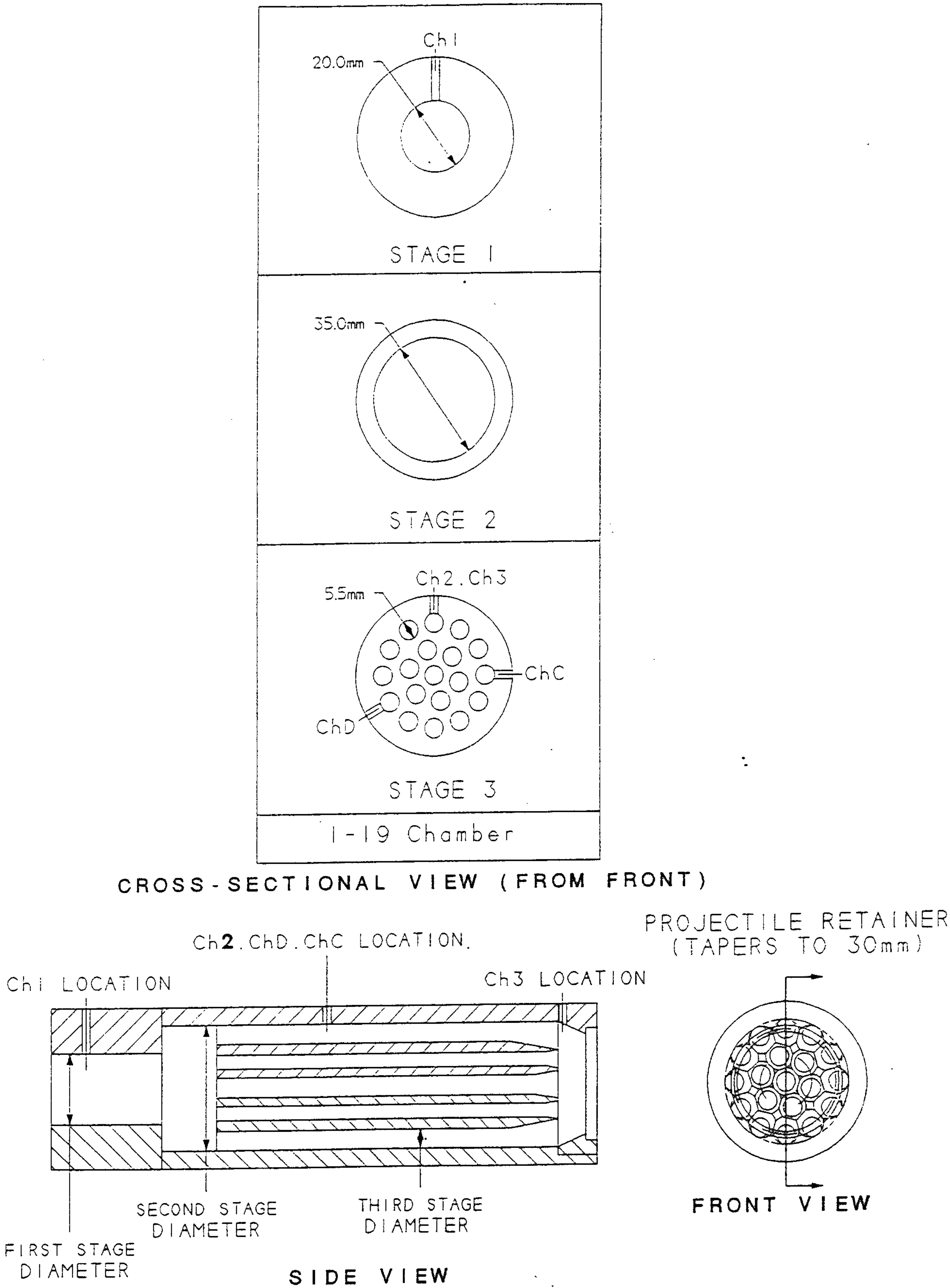

Figure 14. Extended multichamber insert design for 30-mm gun tests.

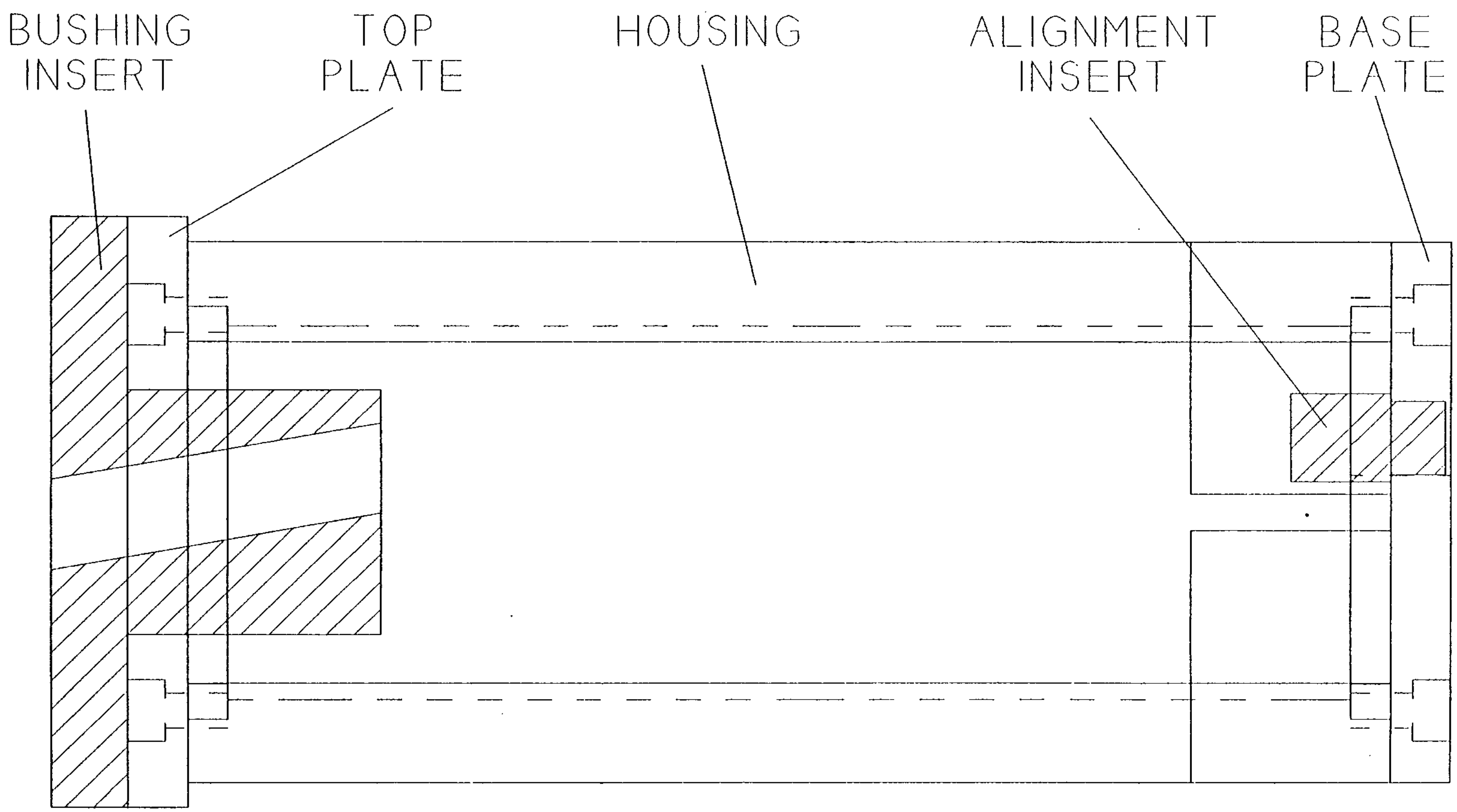

Figure 15. <u>Drilling jig for the production of the 1-3-3, 1-4-4, 1-6-6, and 1-3-9 multichamber configurations</u>.

3.2.3 30-mm Projectiles. The original projectile used was a GAU-8 30-mm projectile whose wind screen was removed from the nose before firing. This exposed the flat nose of the projectile body and enhanced the reflection of signals from the 15-GHz microwave interferometer. It was further modified with steel and/or Delrin at different times during the testing to aid in the loading procedure or to investigate the effects of the changes. Following test 115, the rear end of the GAU-8 projectile was machined to accept various steel or Delrin modifications. These modifications were either in the form of a hemisphere or a flat surface on the rear of the projectile. Schematics of the projectile modifications used in all of the 30-mm tests are shown in Figure 5.

3.2.4 Gun Test Fixture. The gun test fixture used in the 30-mm phase of testing consisted of a rifled Mann barrel screwed into a steel chamber and attached to a rigid steel beam. The chamber attachment was designed to accept various chamber lengths. In this testing, the chamber insert was approximately 153 mm long and 45 mm in diameter and could hold various amounts of LP depending on the interior geometry of the chamber insert. The chamber insert was placed into the chamber and secured by a breech assembly screwed into the rear end of the chamber. The booster housing was inserted and secured into the breech assembly by the firing pin, and a high-pressure transducer was inserted near the booster through a long channel to measure the pressures generated by the booster. The original gun assembly used in this effort is shown in Figure 16 with a partial barrel to indicate the details of the chamber assembly.

After about 55 tests with the original 30-mm gun test fixture, modifications were made that reduced spurious test results associated with the pressure ports and the modular form of the fixture. This modified gun test fixture is shown in Figure 17 and explained in more detail. Clearance holes were drilled into the chamber to allow insertion of the high-pressure transducers directly into the chamber insert through the main chamber. Also, grooves were machined in both the barrel- and breech-end faces to accept o-rings upon assembly of the chamber insert. A Veritay-owned Mann barrel was machined and used in the interim because the original low-strength barrel had expanded. Although this gun design could also be used for tests without the o-rings, grooves were cut into both chamber faces and aligned with the breech and barrel grooves. When the gun test fixture was assembled, the o-rings filled 90% of the void created from the grooves and acted as high-pressure seals to contain LP and LP combustion gas during test firings.

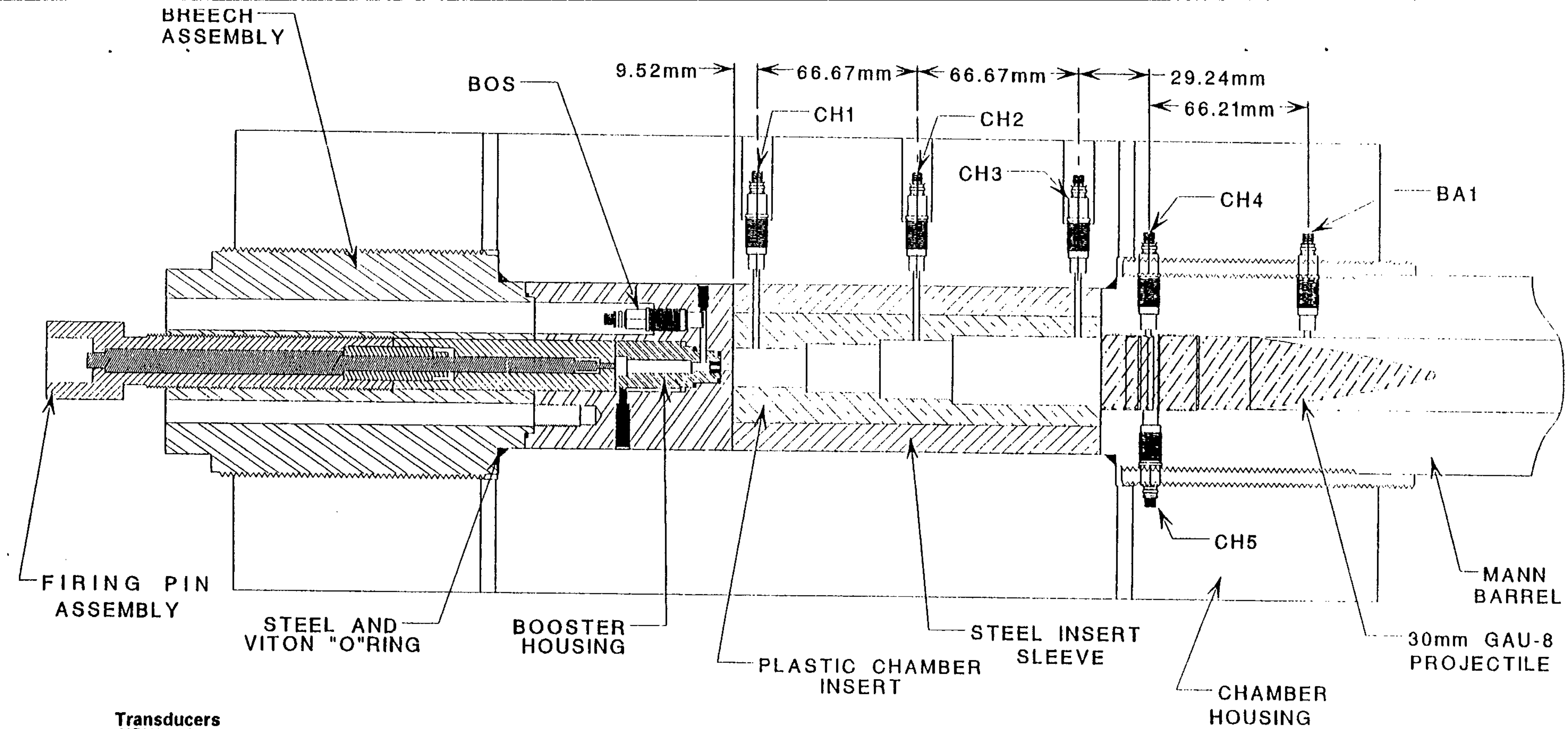

Transducers

Type	Mount	Longitudinal Position	Orientation (From Breech)
BOS	BOOSTER PRESSURE	---	—
CH1	RECESS MOUNT CHAMBER PRESSURE POSITION 1	9.52 mm FROM BREECH FACE	0° (TOP)
CH2	RECESS MOUNT CHAMBER PRESSURE POSITION 2	76.19 mm FROM BREECH FACE	0°
CH3	RECESS MOUNT CHAMBER PRESSURE POSITION 3	142.86 mm FROM BREECH FACE	0°
CH4	STANDARD MOUNT CHAMBER PRESSURE POSITION 4	172.10 mm FROM BREECH FACE	90°
CH5	FLUSH MOUNT CHAMBER PRESSURE POSITION 5	172.10 mm FROM BREECH FACE	0°
BA1	STANDARD MOUNT BARREL PRESSURE POSITION 1	240.10 mm FROM BREECH FACE	0°
BA2	STANDARD MOUNT BARREL PRESSURE POSITION 2	1256.10 mm FROM BREECH FACE, NOT SHOWN	0°
MUZ	STANDARD MOUNT BARREL PRESSURE AT MUZZLE	2119.70 mm FROM BREECH FACE, NOT SHOWN	0°

Figure 16. Original 30-mm gun test fixture.

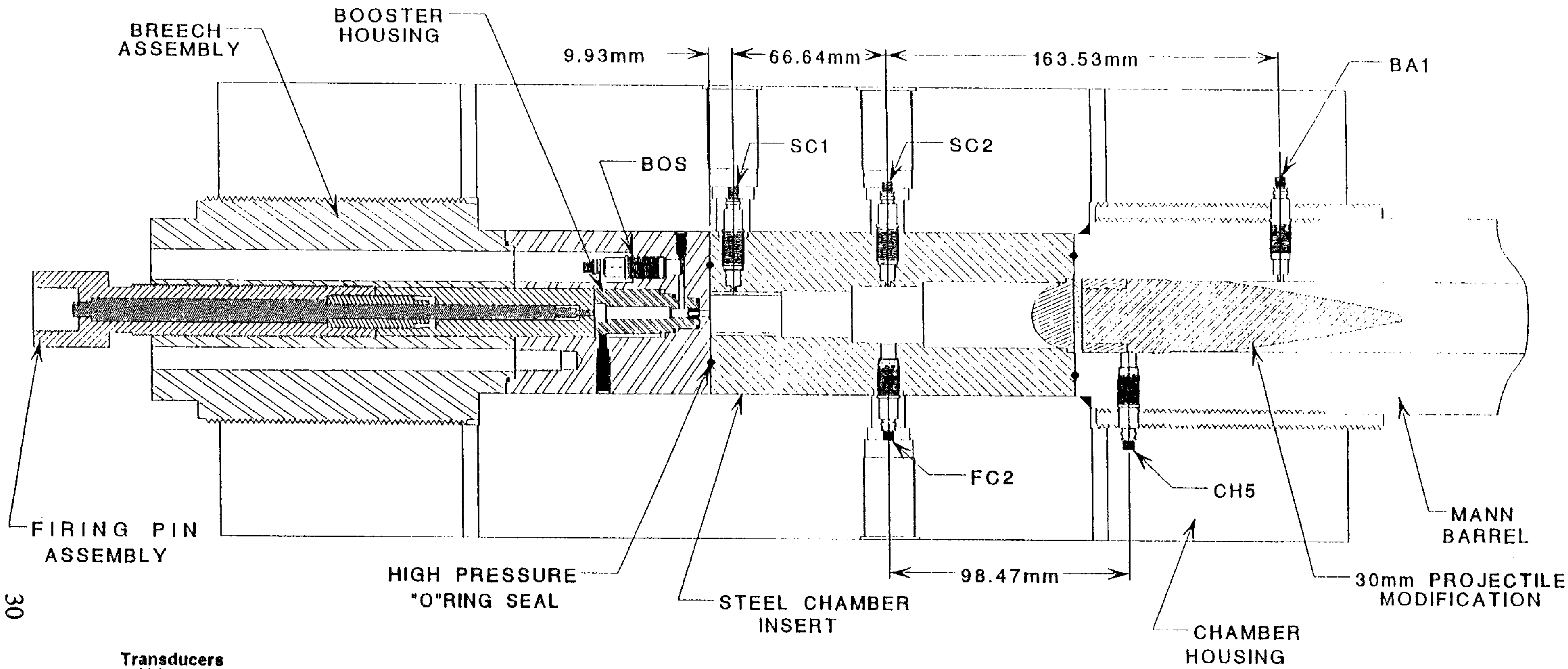

Transducers

Type	Mount	Longitudinal Position	Orientation (From Breech)
BOS	BOOSTER PRESSURE	—	—
SC1	STANDARD MOUNT CHAMBER PRESSURE POSITION 1	9.93 mm FROM BREECH FACE	0°(TOP)
SC2	STANDARD MOUNT CHAMBER PRESSURE POSITION 2	76.57 mm FROM BREECH FACE	0°
FC2	FLUSH MOUNT CHAMBER PRESSURE POSITION 2	76.57 mm FROM BREECH FACE, SHOWN 90 OFF RADIALLY	270° CLOCKWISE
CH5	FLUSH MOUNT CHAMBER PRESSURE POSITION 5	175.04 mm FROM BREECH FACE	0°
BA1	STANDARD MOUNT BARREL PRESSURE POSITION 1	240.10 mm FROM BREECH FACE	0°
BA2	STANDARD MOUNT BARREL PRESSURE POSITION 2	1256.10 mm FROM BREECH FACE, NOT SHOWN	0°
MUZ	STANDARD MOUNT BARREL PRESSURE AT MUZZLE	2119.70 mm FROM BREECH FACE, NOT SHOWN	0°

Figure 17. Modified 30-mm gun test fixture.

3.2.5 Transducer Locations. Nine transducers were used during tests 57–115 of the original 30-mm BLPG (Figure 16). One was located in the breech assembly, three in the chamber, two at the base of the projectile, and three in the barrel. Three-letter acronyms were used to distinguish each transducer location and data received from the transducer ports. The transducer located in the breech (BOS) was used to measure the pressure generated from the booster housing, and the three-chamber recessed transducers (CH1, CH2, and CH3) were located in line to record the pressures generated in the chamber during the test. Three transducers were used for easier identification of the origin of pressure pulses within the chamber. The two transducers at the base of the projectile (CH4 and CH5) were added after test 102 to investigate pressure pulses occurring as the projectile began to move. The barrel transducers (BA1, BA2, and MUZ) were important in determining the pressures that originated in the barrel and in determining the amount of muzzle blast from the combustion event. The distances of the chamber and barrel transducers from the face of the breech are shown in Figure 16.

The modified 30-mm gun test fixture (Figure 17) utilized eight transducers during testing. As with the original gun, a booster transducer was located in the breech assembly (BOS) and three were in the barrel (BA1, BA2, and MUZ). Note that two transducers in the chamber were standard-mounted and one was flush-mounted in the modified gun. The transducers were placed directly in the chamber insert instead of utilizing a long pressure port leading to the chamber transducers, as in the original gun fixture. The standard-mount transducers (SC1 and SC2) were in line and in the same axial positions as the CH1 and CH2 transducers in the original gun, and the CH3 transducer was blocked off in this test fixture. The flush-mount transducer (FC2) was in the same axial location as the SC2 transducer, but was rotated 270° about the chamber axis. The transducer in the CH5 position in the original gun was used in the modified design, but CH4 was not used because of its tendency to sense water-hammer-type pressure effects using a standard-mount transducer.

3.3 <u>Booster Propellant</u>. Early in this effort, a combination of different booster propellants, including Hercules Unique, HC25, and HC33, was examined to select a candidate(s) to be used in the booster housing configuration of the 30-mm gun test fixture. Small-scale booster-only tests (section 4.1.1.2) were completed with Hercules Unique, HC25, and HC33 booster propellants in a previous effort [18]. These HC propellants were deterred from 0 to 4% with Herkote to change the burn rate of the booster. The propellants used in the test are shown in Table 1. From the booster tests, only the HC33-BS664 propellant was chosen as a candidate for the full gun tests. The Hercules Unique canister powder was used for 158 out of the 163 full-scale tests. The properties of the canister powder Unique are given in Table 2.

Table 1. Type of Propellant and Amount of Herkote Deterrent in Each

Booster Type	Deterrent %
HC33-BS664	0
HC25-BS661	2.07
HC25-BS662	2.57
HC25-BS663	3.95

Table 2. Partial Table of Physical and Chemical Data of Hercules Unique Canister Powder [19]

Property	Unique
Impetus (J/g)	1099
Heat explosion at 25° C (cal/g)	1088
Tv (K)	3379
Moles of Gas per Gram (mol/g)	0.0391
Specific Heat at Constant Volume (cal/g-°C)	0.3417

3.4 Temperature Control. A temperature-control system was employed throughout testing to maintain the LP and gun fixture at an ambient temperature (23° C). This temperature control was needed to ensure that the LP stored in unheated, outside magazines and the gun fixture in the test range were both brought to a reproducible temperature for tests. The system was composed of two immersion-type heaters; one heater was used to control the temperature of the gun fixture and the other to control the temperature of the LP. The gun fixture heater was immersed in a ethylene glycol/water bath and plumbed via 9.52-mm (3/8 in) rubber hose to the fixture where it coupled to 9.52-mm (3/8 in) flexible copper tubing tightly coiled around the diameter of the gun chamber. The coil and fixture were insulated with a clear, plastic wrap.

The LP conditioning system consisted of a similar heater/water bath/tubing configuration as that for the gun. This section, however, terminated at a 20.3-cm (8 in) high by 15.4-cm (6 in) diameter thin-walled steel can with a removable lid. The copper tubing was coiled near the inside wall of the can. The can was insulated on the exterior by a layer of foam rubber. The LP to be conditioned was poured into a glass or polyethylene container and placed inside the conditioning can until the desired temperature was reached.

3.5 Liquid Propellant. The LP used in this effort was XM46 liquid monopropellant with a density of 1.43 g/cm^3. Before each test firing, the LP was conditioned in the temperature-control system and the temperature was measured with a thermometer. All pretest temperatures were between 23 and 25° C.

3.6 Testing Procedures. Because of the hazardous nature of the XM46, it was very important in this testing that the LP was loaded in a consistent and safe manner. Standard operating procedures containing safety and procedural information were written, approved by the cognizant Defense Logistics Agency (DLA) explosives safety inspector, and followed throughout testing.

3.6.1 Safety. Testing with the BLPG was potentially hazardous if the LP was not handled properly. A standard operating procedure (SOP) was prepared and used during the LP work to establish a safe operating procedure and assign responsibilities for the loading and firing of percussion-primed, medium-caliber LP test weapons with projectile diameters between approximately 15 mm and 40 mm. This SOP describes the scope, applicability, responsibility, personnel limits, hazardous material limits, general safety requirements, and personal-protective equipment requirements for these medium-caliber LP test guns. The sequence of operations to safely load and fire the 20-mm and 30-mm LP guns was provided to the testing personnel by means of a checklist. This checklist was revised in an iterative fashion as the hardware was modified or changed so that the sequence followed was the safest and most efficient possible. Also, a misfire procedure was contained in the SOP and was supplied in the testing room to aid in tests that did not fire.

3.6.2 Loading. The loading procedure for the 20-mm work and in early 30-mm work utilized tape and silicone grease to seal the chamber insert without allowing for propellant seepage. Packing tape was placed over the forward end of the chamber insert, and silicone grease was used to fill the 2.3-mm transducer ports to create a nonleaking cavity in the chamber. A piece of clear tape was used to cover the LP after it was poured into the chamber, and a syringe was used to fill the chamber to the top. Additional silicone grease covered the hole created from the syringe.

Following the loading procedure, the projectile was inserted into the gun and was followed by the LP-filled chamber insert. With the chamber insert in place and the pressure ports lined up, the breech assembly (consisting of the breech, booster housing, and firing pin) was screwed into place and tightened. The breech utilized a steel and Viton o-ring at the base of the breech, which when tightened, created a seal between the breech and the rear face of the chamber.

After test 115, the procedure for loading the LP into the chamber insert was varied slightly to reduce possible spurious results associated with the original loading procedure. The Delrin modification on the rear of the 30-mm projectile was pressed into the forward end of the chamber insert after tape was placed over the inside of the insert holes created for the pressure transducers. The transducer side of each taped insert hole was coated with a thin layer of silicone grease before insertion of each pressure transducer. The possibility exists that a very small amount of air was trapped in each hole upon insertion of a transducer. The LP was then poured into the cavity formed from the projectile and chamber. Once the propellant filled the cavity nearly to the top, a piece of clear cellophane tape was placed over the hole to seal the chamber. A syringe was used to inject LP into the chamber and fill it to the top; a second piece of tape sealed the pinhole made by the syringe. The breech end of the chamber was machined with a 0.015-mm deep step in order to account for the thickness of the two pieces of tape. When the tape was cut around this step, the tape and the end of the chamber were flush with each other. The use of two pieces of tape instead of one piece of tape and a coating of silicone grease, as in previous work, seemed to lower the variation of the igniter caused by the silicone grease, altering the generation of booster gas.

The order in which the booster housing and firing pin were assembled into the breech was changed in the later 30-mm work from that used in the 20-mm and the early 30-mm work. Previously, the firing pin, booster housing, and booster transducer were assembled into the breech before the breech was screwed into the main chamber. Because the o-ring between the breech and the chamber insert in the modified design could trap air on assembly, the breech was screwed into the main chamber before the booster and firing pin were assembled. This may have reduced the variation arising from the setup.

3.7 Data Acquisition. Data sheets and pressure data were produced for each test. Initial hardware parameters, velocity data, and pertinent pressure and time information were contained on the data sheets.

3.7.1 Initial Parameters. Important booster or chamber parameters were measured and/or calculated before each bulk-loaded LP test. The temperature and mass of the XM46 propellant and the mass of the projectile were measured. The dimensions measured in the booster housing were the length (*l*) and diameter (*D*) of the main volume of the cavity. From these measurements and the booster mass (*m*), the booster load density could be calculated by the following equation:

$$\rho_{load} = \frac{4 \bullet m}{l \pi D^2}. \quad (1)$$

All of the measured and calculated initial parameters are included in the database in the Appendix. Because many modifications were performed on the chamber inserts, the interior diameters and lengths of each stage section were measured and compared to the design drawing before each test.

3.7.2 Pressure Data. Data for the bulk-loaded LP tests were acquired with a LeCroy data acquisition system. Up to ten channels were used for pressure measurements with data being acquired at a rate of 1 point every 2 μs. Originally, data was taken every 5 μs with a small window. Later the window was increased to 64 ms, and the time per point was decreased to 2 μs. Time zero was considered to be the time at which the firing pin impacted the primer, and 64 ms of data was acquired after that point. Normally, the entire combustion event occurred within 4 ms, but if there was a long ignition delay, it was possible for the event to occur after 4 ms. The 64-ms data acquisition window was used for all tests in attempt to make certain that the data were recorded for each test.

The pressures obtained as a function of time during each LP test varied slightly depending on the design of the gun and the pressures desired. For all tests, the booster pressure (BOS) and three barrel pressures were obtained. At least three chamber pressures were obtained from the tests using the 20-mm, 30-mm, and modified 30-mm guns, but the three transducers were in different axial and radial positions depending on the design.

Important points on each of the pressure curves were recorded on the data sheets for later comparisons. Normally, the maximum pressure in each curve was acquired along with the time that it occurred. Since the pressure in the first-stage chamber section was identified as important in the ignition and combustion of the LP, two more characteristics were obtained from the CH1 pressure trace. Time for the pressure to reach 70 MPa was obtained and was known as the ignition delay. The pressure rise rate P-dot was established as the pressure change per unit time from 70 MPa to the maximum in the CH1 curve. An example of these values is shown in Figure 18.

3.7.3 Velocity Data. Velocity data was obtained by measuring the time required for the projectile to penetrate paper breakstrips positioned known distances apart. Three separate times were obtained: from the first to second breakstrip, V_{1-2}; from the second to third breakstrip, V_{2-3}; and from the first to the third break strip, V_{1-3}. Three separate velocities were obtained so that if the projectile did not pass through one of the breakstrips, at least one velocity could be recorded. The average velocity (V_{1-3}) of the projectile was included in the database for each test.

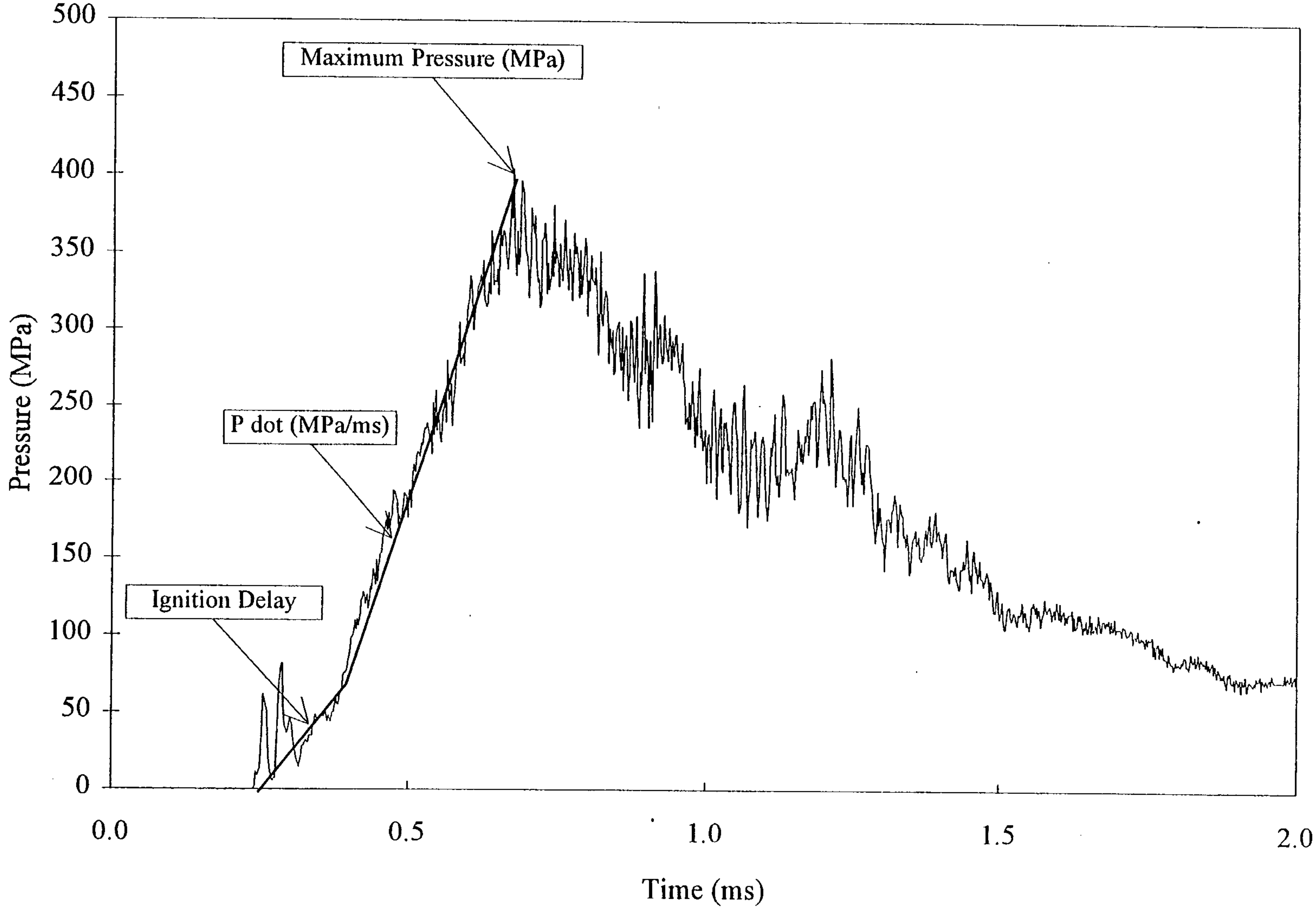

Figure 18. Example of information taken from chamber 1 P-t traces.

3.7.4 Interferometer. A microwave interferometer was positioned on a rigid steel shelf approximately 91.4 cm alongside the gun fixture and 122 cm behind the muzzle. The high-frequency beam was aimed at an aluminum piepan reflector, which was located about 68.6 cm beyond the muzzle. Interferometer orientation was adjusted using a field-strength meter (FSM) so that the maximum signal strength occurred at the point where the beam converged with the projectile path and the reflector. The reflector was mounted on an adjustable steel support that required reorientation before each test, due to the effect of the muzzle blast on the support. To make certain the beam was traveling down the barrel and striking the projectile squarely, the signal strength at the initial projectile position was maximized using the FSM.

The response of the interferometer as a result of the projectile movement was recorded on the LeCroy system at an acquisition rate of 1 point every 2 μs. From this curve, the time at which the sinusoidal curve began was acquired along with the time at each peak (or every-other peak) along the curve. The wave displacements are different for waves traveling through a known gun bore diameter and through air. Therefore, the peak time values along the interferometer curve were not used when the curve became unstable, or at the time beyond when the peak of the return signal corresponded to arrival of the projectile at the muzzle. The instantaneous velocity of the projectile moving in the barrel is found from each complete wavelength and the measured time corresponding to a single wavelength. The interferometer was measured as having an initial frequency of 14.987 GHz; the displacement was 1.086438 cm for each complete wavelength.

For a given interferometer frequency, barrel diameter, and projectile starting and ending time, the time between each peak of the sinusoidal interferometer output was obtained with custom written software. From this waveform data, the displacement was obtained as a function of time. When waveforms were clipped, however, the software manipulation was less effective, and the wave forms were solved manually.

After test 115, the displacement vs. time data obtained from the raw interferometer tests were incorporated into spreadsheet software and converted into initial-acceleration, initial-velocity, and muzzle-velocity data. This was accomplished by fitting a section of the data with a polynomial equation at a specific displacement, solving the derivative or second derivative of the equation, and obtaining the inverse of the solved equation to obtain velocities in m/s and accelerations in m/s^2. The initial accelerations and velocities for each test were calculated at 1 cm, and the muzzle velocity was calculated at 2.056 m of displacement (the length from the initial projectile placement to the muzzle transducer). Although many of these muzzle velocities were within 1 or 2%, some differed up to 6% from the velocities obtained by the breakstrip technique.

3.8 Inverse Interior Ballistic Code. In this effort, work was done briefly using an inverse, interior ballistic code in conjunction with the bulk LP testing. This code would have aided in the understanding of the pressure development in the gun system from specific parametric changes. Although time was spent including and varying physical parameters from an existing interior ballistic code developed at Veritay, this effort did not address in detail enough physical phenomena to accurately and reliably predict the test results.

Since the inverse, interior ballistic code was not developed past this stage, other software was written to increase the productivity and efficiency of the testing. Data reduction software converted and graphed selected pressure data to be used in reports and data analysis. Also, data for the displacement of the projectile with time were extracted from interferometer waveforms through software manipulation. All of the data were supplied to ARL on disk and on hardcopy.

3.9 Database. A database of many measured and calculated values associated with LP gun firing tests is included in the Appendix. These values were compiled so that a coupling between the starting parameters and the test responses could be made easily and efficiently. Many of the values listed in the database have not been analyzed, but are included for future analysis.

4. TEST FIRING RESULTS

4.1 Stepped-Wall Chamber Configuration.

4.1.1 Ignition of XM46. The ignition of XM46 was investigated in the 20-mm test firings and in later 30-mm tests by varying different parameters within the pyrotechnic igniter. Two booster housings with different designs and internal volumes were used in the 20-mm test firings without varying the volume of either of the housings. These housings were filled with different amounts of Hercules Unique canister powder or the orifice diameter was increased or decreased to investigate the effect on the test results. In the 30-mm gun firings, the booster load density (booster mass/booster housing volume) was used as a guide for the performance of the booster. The booster load density was varied in some of the tests by changing the booster mass, the volume of the booster housing cavity, or both at the same time. The effects of the different load densities (because of changes in mass and/or volume) on the ignition of XM46 is discussed later.

4.1.1.1 20-mm Gun Tests. In early ignition tests utilizing the H- and I-type chamber geometries and different projectile masses, the booster mass and the orifice diameter of the booster were varied.

The effects of a changing booster mass on the booster performance and, therefore, the chamber pressures, were investigated by decreasing the amount of the booster in the pyrotechnic igniter. In this 20-mm testing, the dimensions of the booster housing (Figure 2, B17-006) and the chamber (Figure 3, geometry A) remained constant. The booster load was decreased from 335 mg in test 40, to 300 mg in 41, to 240 mg in test 44, in a cavity volume of 0.574 cm^3. The booster densities for the three tests were 0.584 g/cm^3, 0.523 g/cm^3, and 0.418 g/cm^3, respectively. Decreasing the booster load densities generally decreased both the rise rate and peak pressures of the booster response (Figure 19). For the same combustion-chamber diameter, decreasing the booster loads appeared to cause larger initial pressure pulses as well as an increased duration of ignition pressure. The low-amplitude pressure pulses in test 40, as compared to tests 41 and 44, are probably the direct result of using a plastic chamber insert in test 40, vs. a steel chamber insert in tests 41 and 44.

The orifice diameter of the booster housing for the 20-mm tests was varied in an attempt to optimize the igniter's performance. Although the effects of changes in orifice diameter were not well-understood, the testing showed that the orifice diameter was also an important parameter to consider when attempting to ignite XM46. Since liquid combustion occurs in the vapor phase, the igniter must vaporize a small amount of LP and heat the vapor to a temperature at which exothermic

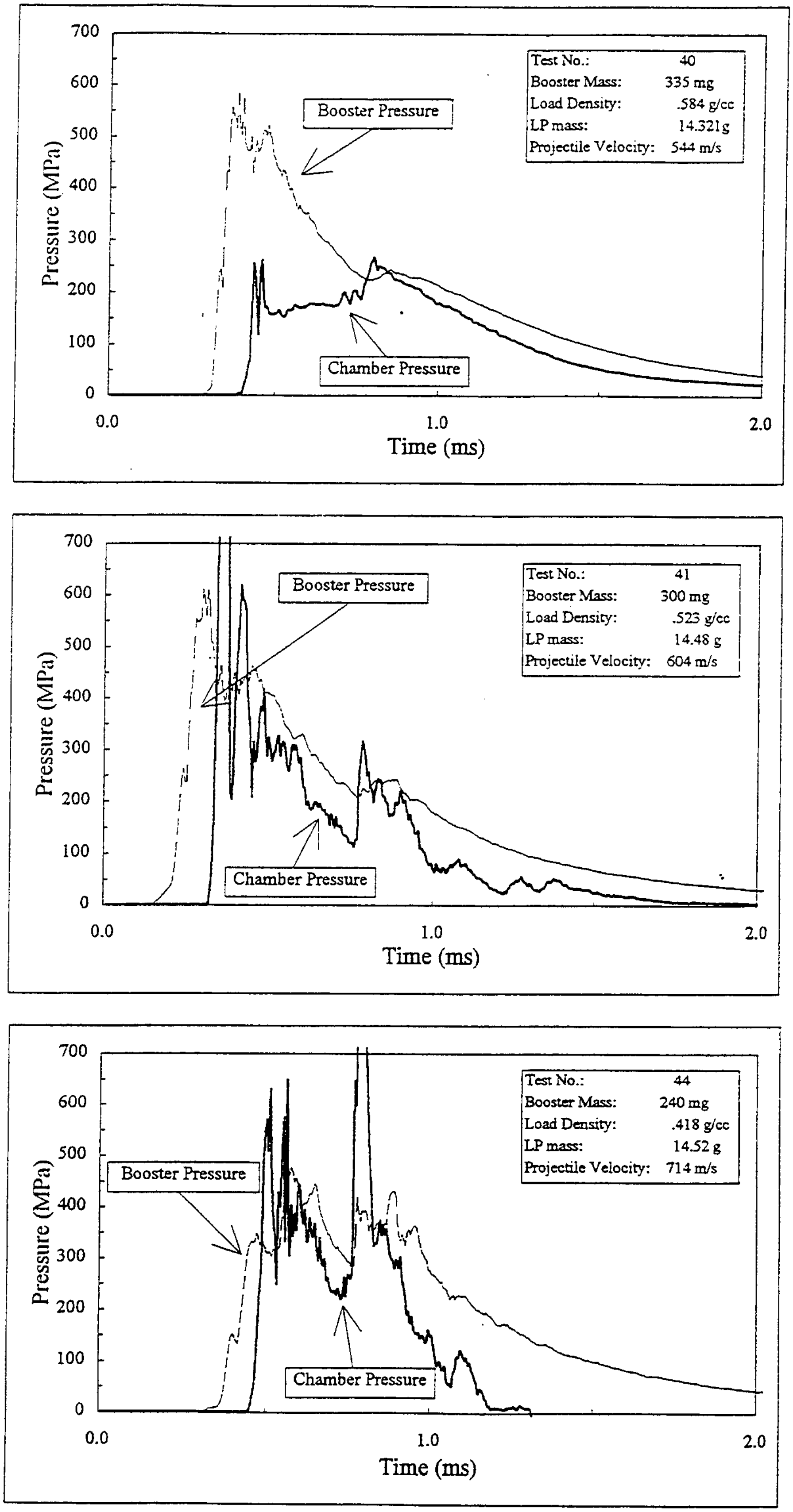

Figure 19. Effect of decreasing the booster load density by increasing the booster mass.

reactions occur. Since the booster orifice diameter controls the mass flow rate out of the booster cavity, the rate in which the LP is vaporized and heated is directly related to the diameter of the orifice.

To begin testing in the 30-mm gun, a booster load was estimated from the 20-mm test results. A simple ratio method was used that related the booster mass per LP volume in good 20-mm tests to the booster mass and LP volume to be used in 30-mm tests. Along with this, the booster load density was kept between 0.4 g/cm^3 and 0.5 g/cm^3, the same booster load density range found to produce good results in the 20-mm firings. In the initial tests in the 30-mm gun, this ratio method produced a good estimation for obtaining adequate and safe chamber pressures to start the 30-mm tests.

4.1.1.2 30-mm Gun Tests (Tests 70–108). In tests 70–108, the booster parameters were varied in the process of reducing the amount of plastic in the first stage of the chamber insert. The diameter of the main section of the booster housing (Figure 2, B17-111) or the mass of propellant within the cavity was increased or decreased to obtain desirable booster load densities. From these tests, the booster housing parameters, important in the ignition and ultimately the combustion of the XM46, were investigated. Also, the type of the booster propellant used in the gun test fixture was investigated.

In tests 87–89, the mass of the booster and the volume of the booster housing were reduced simultaneously. Although these parameters were reduced, the booster load densities actually increased. Test 87 did not ignite adequately, and combustion did not occur in the chamber (Figure 20). In test 88, combustion occurred, but a long and uneven ignition delay suggested that the combustion was not stable. The largest load density and smallest mass of the three tests had the most favorable results. In this case, the ignition delay in the chamber pressure was slightly shorter and the pressure rise was consistent. The peak pressures in this test were approximately 400 MPa, which were considered to be at a favorable level.

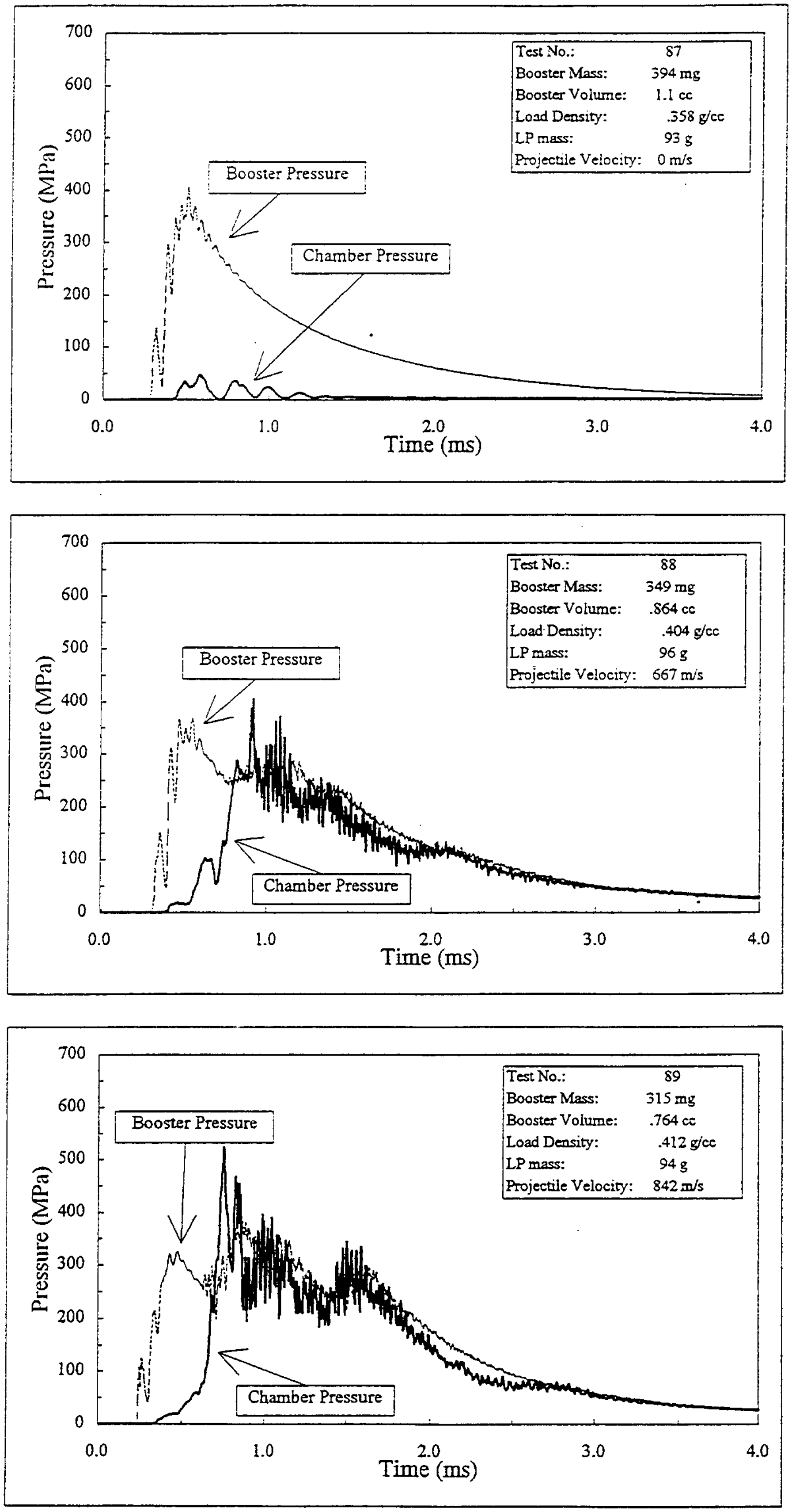

Figure 20. Effect of increasing the booster load density while decreasing both the booster mass and booster housing volume.

The booster propellant used in all but five of the 30-mm gun test firings was Hercules Unique. The five tests, numbers 70–74 inclusive, which did not use the Unique, used Hercules HC33-BS664 gun propellant.

Prior to testing an alternate booster propellant in the full-up 30-mm gun test fixture, the performance of different solid propellants, examined under a previous effort [18], was examined and compared to the Hercules Unique booster propellant used throughout most of the 20-mm and 30-mm test firings. Hercules gun propellant type HC33-BS664 was chosen to be tested in the full-up gun fixture. The HC33-BS664 propellant was chosen primarily because of its slower burn rate. The slower burn rate booster propellant was expected to reduce the pressure noise spikes found in the gun chamber during the early stages of ignition.

In tests 70–74 inclusive, Hercules HC33-BS664 gun propellant was used as the booster propellant. To obtain nearly the same peak pressure in the booster cavity that was obtained during tests that used Hercules Unique, a greater mass of HC33-BS664 propellant was needed. Figure 21 shows the P-t traces for 0.420 g of Hercules Unique and 0.894 g of Hercules HC33-BS664 when fired in a booster chamber with a 1.32-mm diameter exit orifice. Both propellant loads were initiated by a CCI-400 small-rifle primer. Since the peak pressure obtained when using the HC33-BS664 propellant in the booster-only test was slightly higher than the booster test that used Unique, a lower (0.751 g) amount was used in the first gun test firing (test 70), which used HC33-BS664 booster propellant.

Furthering the investigation involving HC33-BS664 booster propellant, the type AAB-1 plastic chamber insert (Figure 6) using a 16-mm first-stage diameter, a 20-mm second-stage diameter, a 24-mm third-stage diameter, and a 30-mm fourth-stage diameter was used in tests 72 and 74. The amount of HC33-BS664 propellant used in test 74 was 891 mg, while in test 72, 905 mg were used. The peak pressures and ignition delays in the main chamber P-t traces decreased (Figure 22) as the booster load increased. When Unique was used (Figure 22, test 75), the ignition delay was short and combustion control appeared better.

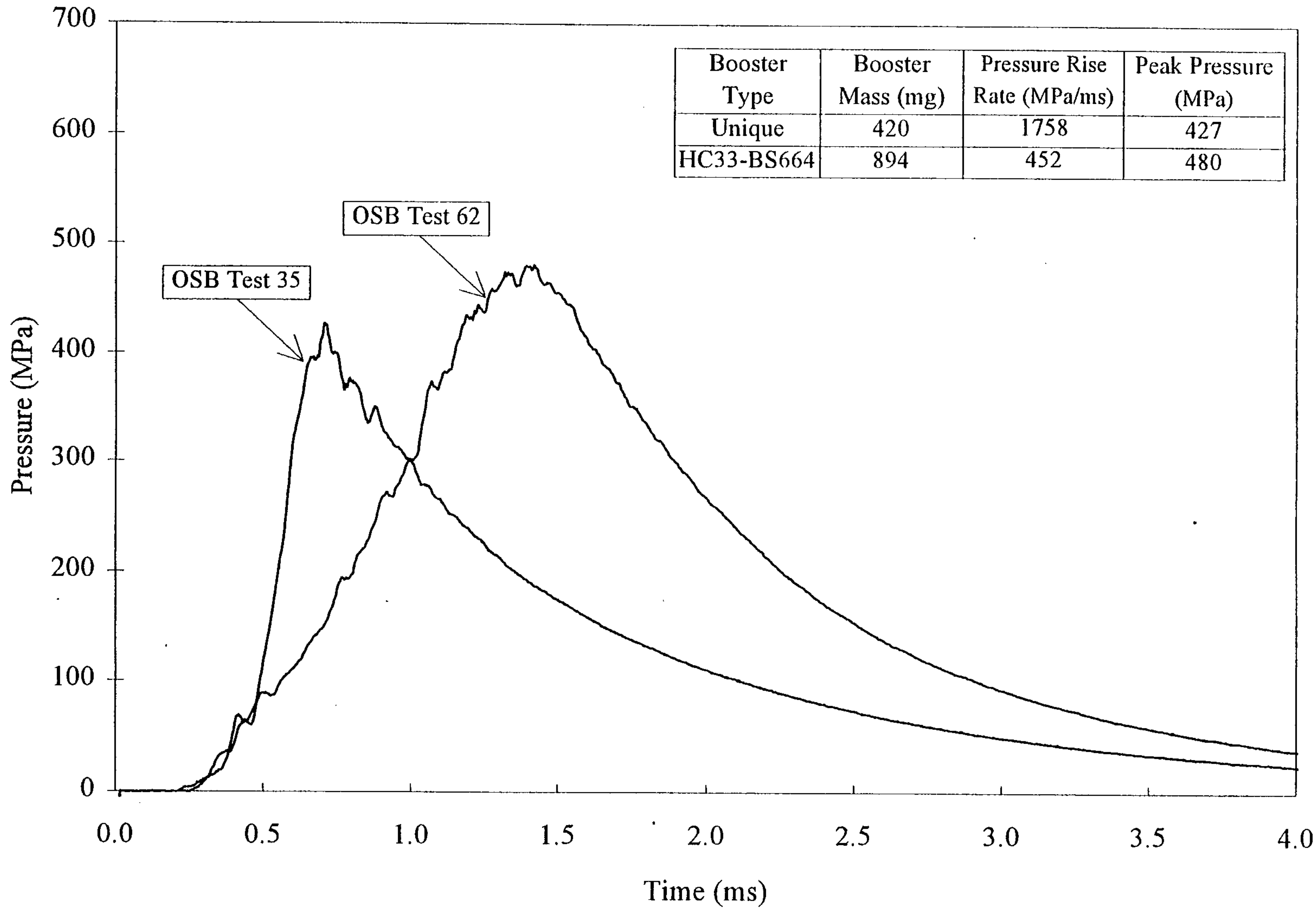

Booster Type	Booster Mass (mg)	Pressure Rise Rate (MPa/ms)	Peak Pressure (MPa)
Unique	420	1758	427
HC33-BS664	894	452	480

Figure 21. Booster pressures obtained when Unique and HC33 are used as the booster propellant.

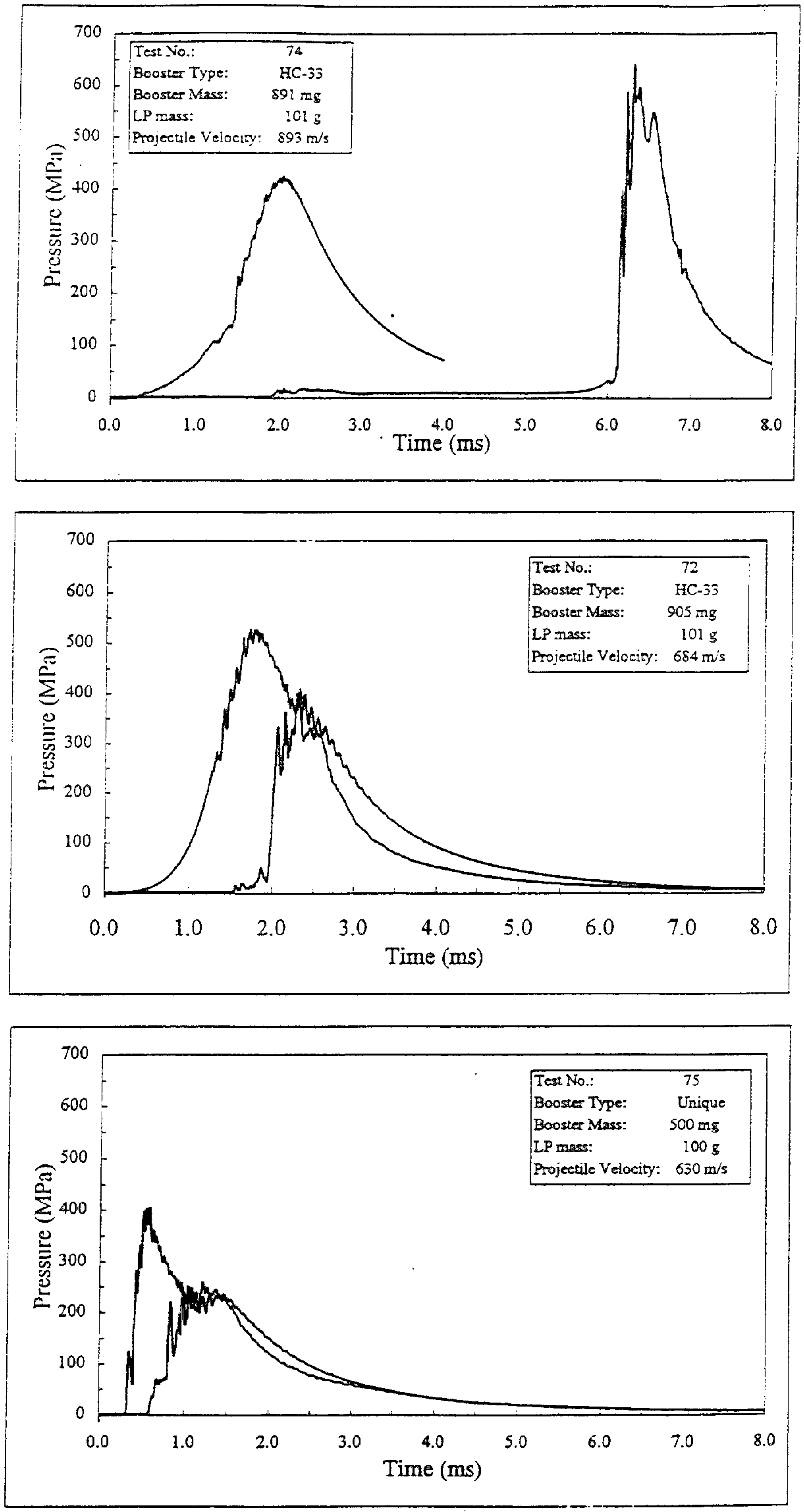

Figure 22. Effects of increasing the HC33 booster mass and a comparison to a Unique booster test.

A key observation from these tests using the HC33-BS664 propellant as the booster was that a long ignition delay is evident in all the tests. If the delay is long enough, as in test 74, the combustion control suffers. As a result, efforts to use the HC33-BS664 propellant as a booster load were not pursued further under this program; rather subsequent testing was conducted using Unique as the primary type of booster propellant load.

4.1.2 Projectile Mass Scaling. To explore the effects of different projectile masses on the ignition and combustion of XM46, a group of projectiles with increasing masses were designed, fabricated, and tested in the 20-mm bulk- loaded gun. These tests were safely fired in a series (tests 27, 18, 28, 36, and 38) in which the projectile masses were changed incrementally over the range from 67 to 376 g. The fronts of the M55A2TP projectiles were extended with solid steel rods to obtain the desired masses (Figure 5). Figure 23 shows the effect on the P-t traces using projectiles of different masses, while keeping the remaining test parameters essentially constant. It is interesting to note from this figure that although the projectile mass was varied by a factor of 5.6, the peak chamber pressure did not increase significantly, but actually created a more flat-topped curve with the heavier projectiles. The displacements of the projectiles determined from measurements made with a 15-GHz interferometer (Figure 23) are consistent with the postulated acceleration and velocity-dependent combustion mechanisms discussed earlier; the larger masses accelerate more slowly and produce lower final velocities. The heaviest of the 20-mm projectiles was approximately the same mass as the standard 30-mm projectile (379 g). This fact was encouraging because it suggested that the 30-mm projectile could be used with a similar type of chamber.

4.1.3 Control With Scaling. After a series of ignition and mass scaling tests was completed in plastic chambers, steel chambers were tested in the 20-mm gun fixture. The initial design was a straight tube of constant diameter that created secondary pressure spikes within the chamber (Figure 24). This straight tube could hold only 7.6 g of LP and the projectile velocities were low. This secondary pressure was thought to be a result of incomplete burning of LP in the chamber and, as a result, some unburned LP was pushed forward out of the chamber and was ultimately ignited and burned in the barrel. By adding expanded regions in front of the single cylindrical section, the secondary spikes were reduced, though not eliminated, while the LP volume and projectile velocities

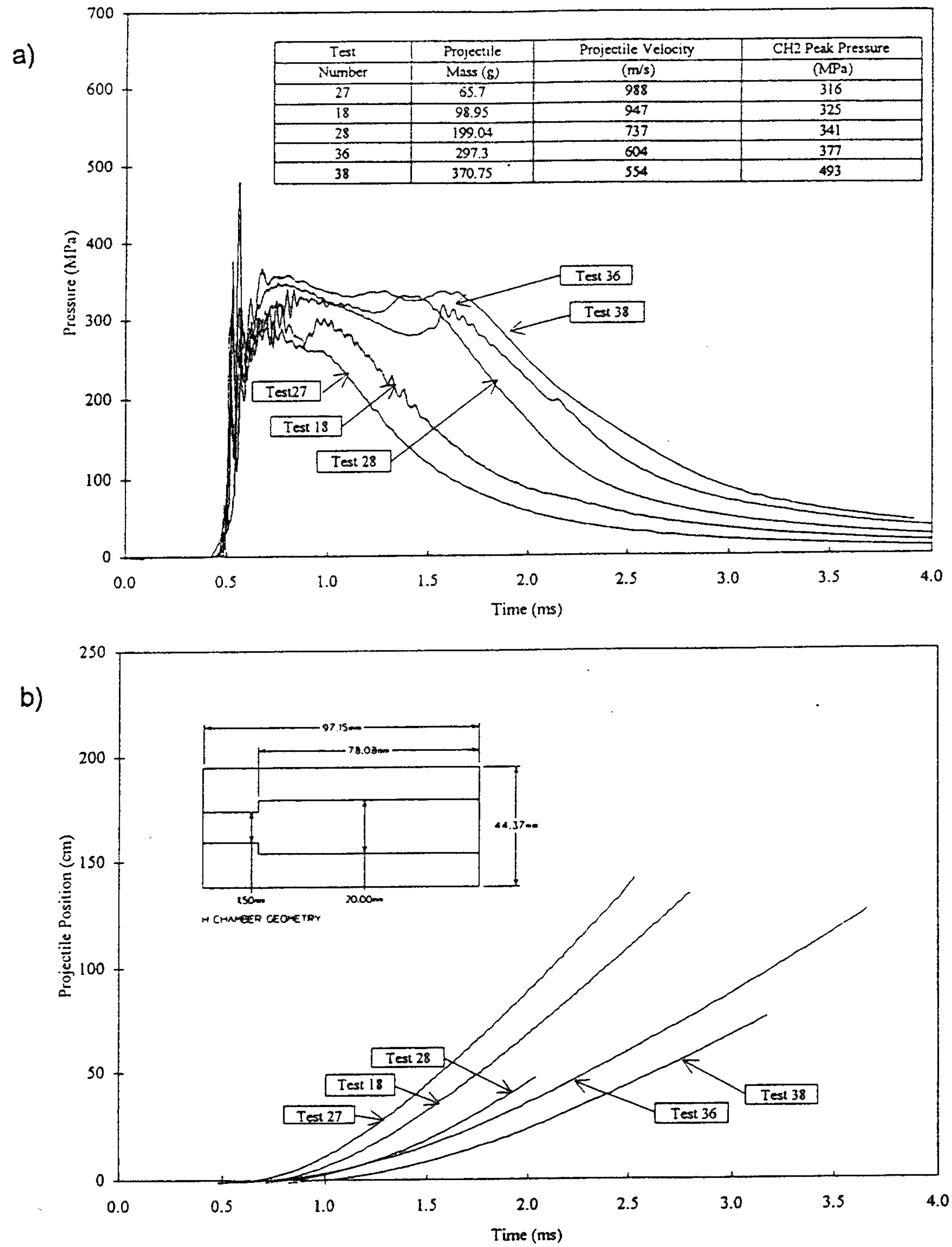

Test Number	Projectile Mass (g)	Projectile Velocity (m/s)	CH2 Peak Pressure (MPa)
27	65.7	988	316
18	98.95	947	325
28	199.04	737	341
36	297.3	604	377
38	370.75	554	493

Figure 23. (a) Pressure-time trace variations with projectile mass and (b) displacement of projectiles with different masses measured with 15-GHz interferometer.

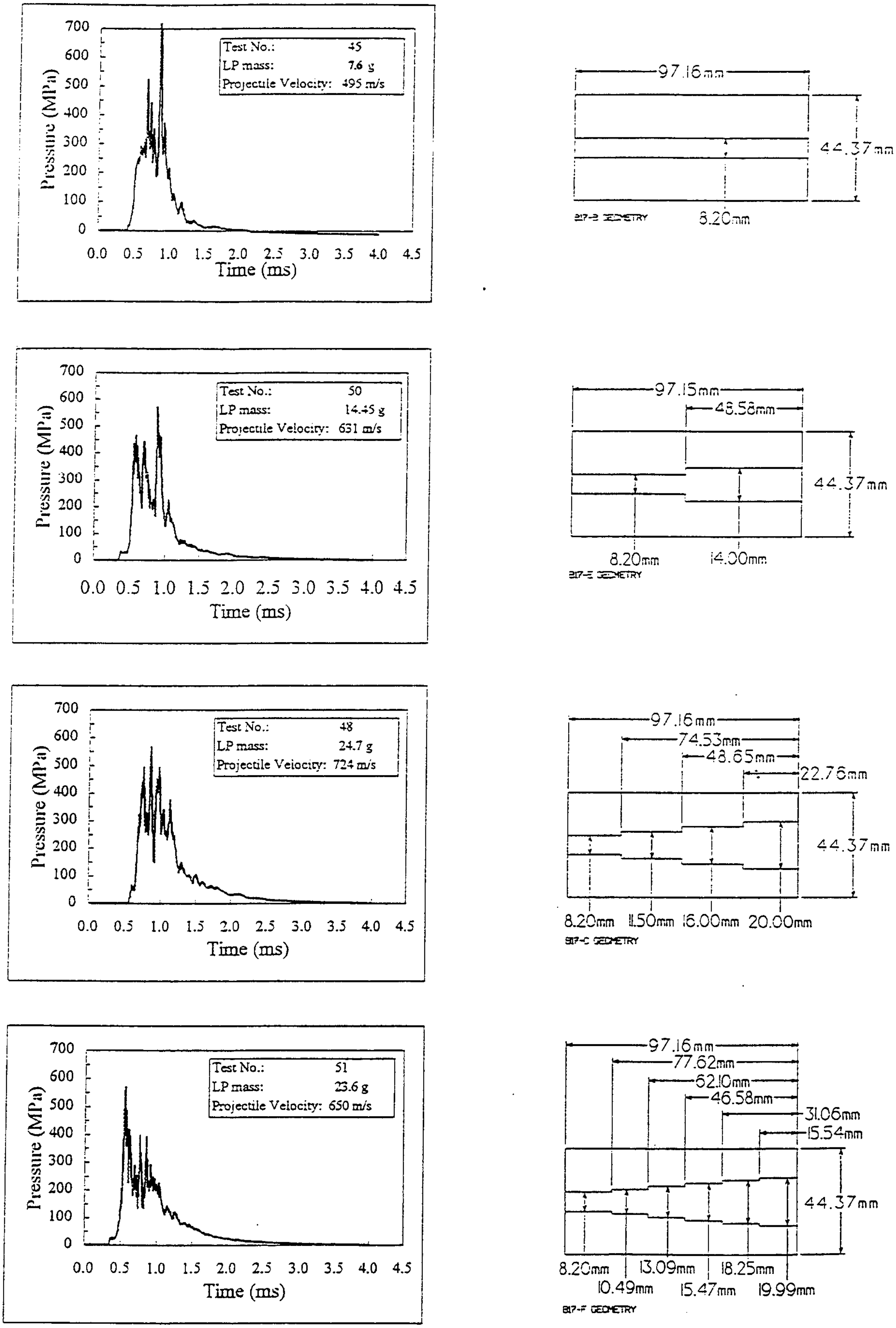

Figure 24. Controlling LP combustion with geometrical changes in the chamber.

were increased. As more steps with increasingly larger diameters were added to the chamber design, the secondary pressure spikes were further reduced (Figure 24). Along with these decreases, the mass of LP increased from 7.6 g in the single chamber to 24.7 g in the three-step four-sectioned chamber (Figure 3, B17-C geometry). The chamber design with five steps and six cylindrical sections was intended to provide the most combustion control of the chambers used. Through this type of analysis, it appears that the ignition and combustion of LP may be controlled somewhat by adding steps of increasing diameter to the initial cylindrical section. This control of the ignition and combustion may prove to be beneficial when a high-projectile velocity is desired without producing extremely high pressures.

4.1.4 Plastic vs. Steel Chambers. The plastic chamber inserts used in the 20-mm gun test fixture and in the 30-mm gun investigations afforded a quick, inexpensive means of varying the chamber geometry during explorations of stepped-wall and multichamber configurations. It was always recognized, however, that the plastic insert would eventually need to be replaced with a steel chamber configuration. In 20-mm testing, plastic chambers were used for early ignition tests, then all-steel chambers were used after test 39. In these later tests, the interior dimensions of the steel chamber were varied in attempt to optimize the combustion within the chamber and had limited success. One of the objectives pursued in the later 30-mm gun tests (tests 65–115, section 4.1.4.2) was the systematic reduction of the plastic chamber inserts to obtain a controlled combustion in an all-steel chamber configuration. These tests were based on the procedure of firing a sequence of tests in which portions of an all-plastic chamber were replaced by identical steel portions.

4.1.4.1 20-mm Gun tests. Plastic chambers in the 20-mm gun tests were replaced with complete steel chambers to begin exploring the effects of different step changes on the control of combustion. This rapid change from all plastic to all steel created large pressure pulses and, at times, uncontrollable combustion. Therefore, different stepped-wall chamber geometries were investigated in an attempt to optimize the combustion within the chamber. The preliminary results obtained indicated that it was unlikely for complete combustion control to be explored safely using steel stepped chambers alone. This approach was not pursued further in the 20-mm gun tests. The conversion from plastic to steel was readdressed later in the 30-mm gun tests and approached in a different manner. The amount of plastic in the chamber was reduced slowly to incrementally optimize the initial parameters, and to minimize the poorly controlled combustion in nonoptimal steel chamber inserts used in tests.

4.1.4.2 30-mm Gun tests. A series of test firings in the 30-mm gun fixture was completed in which the plastic in the chamber was sequentially replaced section by section with steel in a cumulative fashion until a significant fraction of the total amount was replaced. In tests 62, 66, 67, and 81, plastic insert sections were replaced with steel sections starting with the steel replacement at the projectile end of the chamber. Figure 25 shows the behavior of P-t traces in the second chamber stage (CH2) obtained in these tests. Test 62 used the all-plastic AAB chamber (Figure 6). Test 66 used the 701s and 701p chambers, test 67 used the 702s and 702p chambers, and test 81 used the 703s and 703p chambers. These steel and plastic chambers (designated as "s" and "p" at the end of the chamber number) are shown in Figure 7. The plastic and steel chambers in tests 66 and 67 were combined to create the AAB chamber geometry, and the chambers in test 81 combined to create the AAB-1 geometry. Both the AAB and AAB-1 chamber geometries are shown in Figure 6. The AAB geometry consisted of a 16-mm first-stage diameter, a 20-mm second-stage diameter, a 24-mm third-stage diameter, and a 30-mm fourth-stage diameter. In the AAB-1 chamber geometry, which is very similar to the AAB chamber, the first three stages had the same diameters, but the fourth-stage diameter of the AAB-1 was 28 mm with a small 30-mm step at the end of the insert. This small 30-mm step was added to all chambers after test 72 in an attempt to reduce spurious test results associated with the loading procedure. The reduced fourth-stage diameter and the small step at the projectile end of the chamber, however, were not considered to adversely affect the generated chamber pressures in test 81, as compared to tests 62, 66, and 67. The series of these four tests (Figure 25) used the same booster load (500 mg) and booster load density (0.455 g/cm^3). The end result of this stage of testing was a chamber configuration that was all steel, except for a plastic first-chamber section.

The P-t traces for the sequence of tests shown in Figure 25 tend to exhibit similar pressure magnitudes and shapes, even though some minor differences in the short-duration pressure pulses

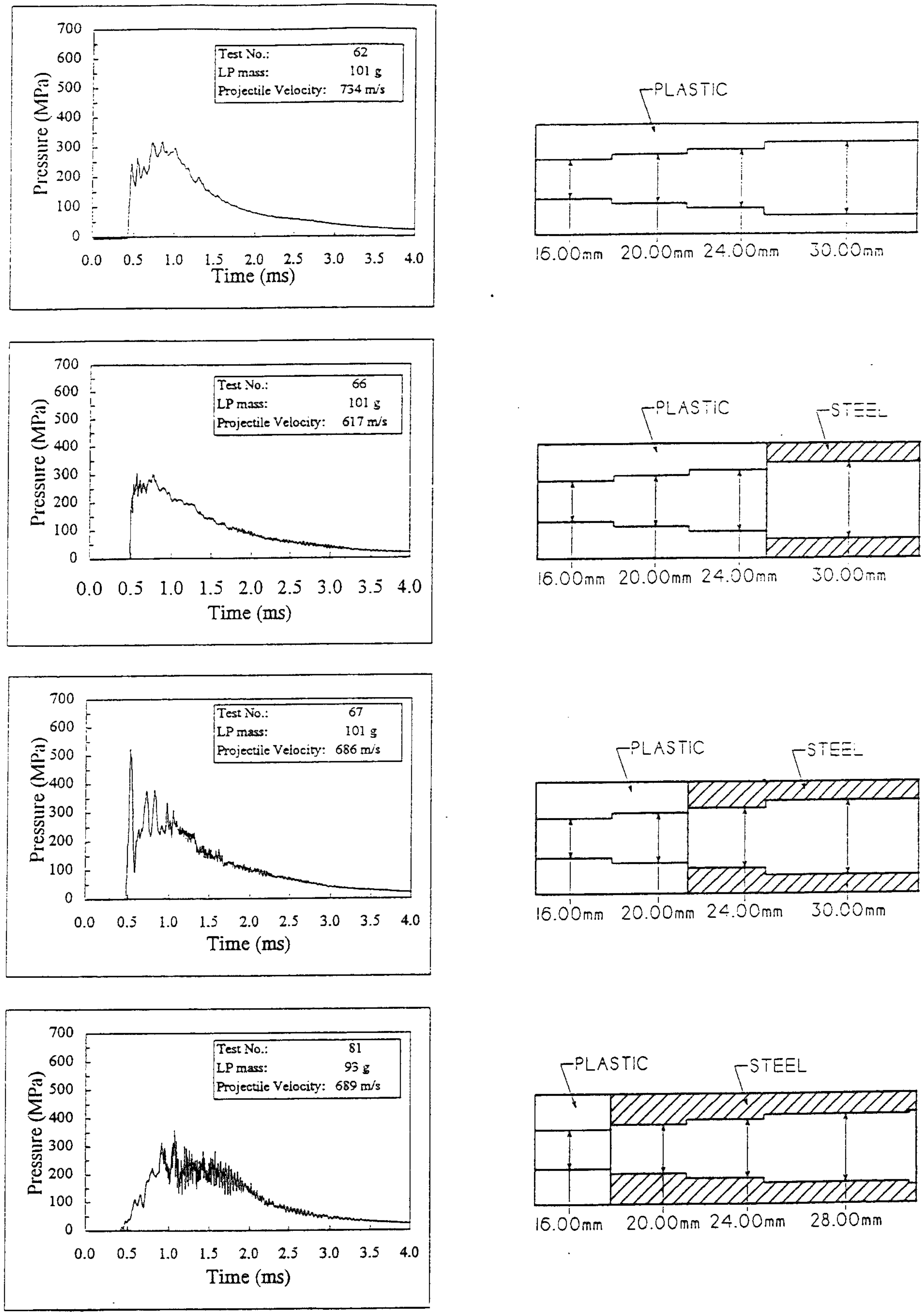

Figure 25. Tests 62, 66, 67, and 81: effect of sequentially replacing plastic chamber sections with steel.

are apparent. It will be observed, however, that an increased number and size of pressure pulses appear as noise in the trace (chamber pressure in position 2) for the chamber insert with the greatest amount of steel.

Since it was suspected in the 20-mm test firings that steel near the igniter end caused major pressure pulses to occur during the ballistic cycle, the plastic in the first-stage chamber section in this phase of 30-mm test firings was reduced carefully. Steel cylinders with increasing thicknesses were used outside the plastic inserts to systematically reduce the volume of plastic inserts without changing the interior diameter of the first-stage section. These replacements (Figure 8, chambers B17-0002-1 to B17-0002-3) were combined with chamber 703s (Figure 7) to achieve 3-step, four-stage chamber inserts with a 16-mm first-stage diameter, 20-mm second-stage diameter, 24-mm third-stage diameter, and a 28-mm fourth-stage diameter. The small 30-mm step at the forward end of the chamber insert was filled with a plastic disc during loading and was not considered to affect the generated pressures. Since the P-t behavior in the first-stage section of each chamber tested was of main interest here, the results obtained using the first-stage transducer CH1 are shown for these tests. The P-t traces shown previously in Figure 25 were obtained using transducer CH2 and may be slightly different.

Test 83 reduced the plastic in the first-stage section and used the same mass of booster powder (500 mg) in the pyrotechnic initiator as in test 81. This proved to increase the pressures in the first stage significantly (Figure 26). It was speculated that the decreasing compression of the plastic and the LP in the chamber as a result of a decreasing plastic needed to be accompanied by a "softer" ignition. This could be accomplished by decreasing the booster load. To test this hypothesis, test 84 was conducted with the same chamber geometry as test 83, but the booster load was reduced by 10% from 500 mg to 450 mg. The resulting P-t trace in test 84 showed a reduction in combustion delay (i.e., the time from the first appearance of pressure to the time at 70 MPa) and in the peak pressure created in chamber 2. This combustion delay, being shorter, produced a pressure trace similar in appearance to test 81, which had a larger volume of plastic in the first stage and a larger booster load. The series of these three tests is shown in Figure 26.

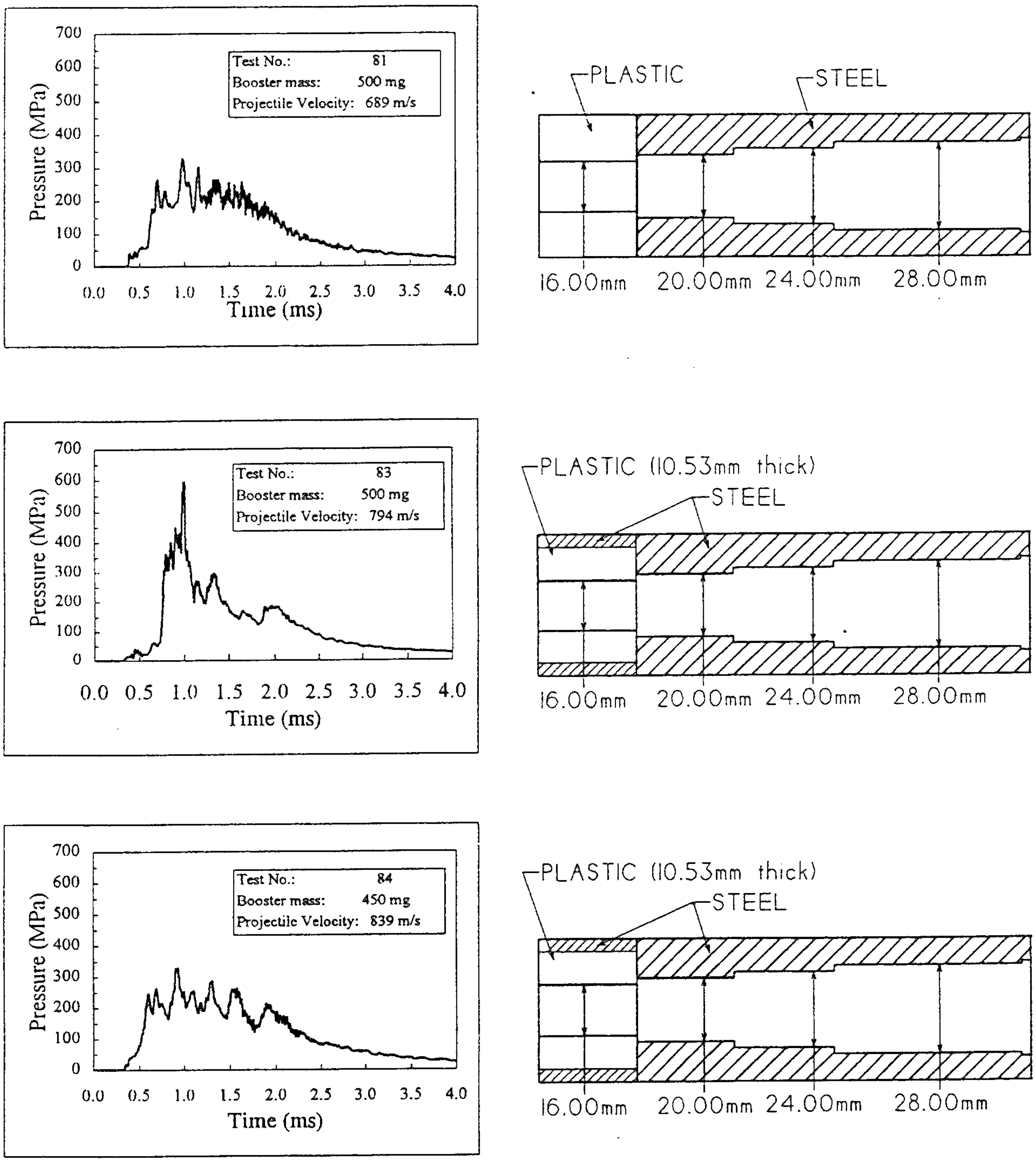

Figure 26. Effect of changing the amount of plastic in the first stage and the amount of booster in the booster housing cavity.

During tests 84–86, some unexplained pressure pulses were observed that were attributed to the modular form of the fixture hardware. As a result, the hardware design was modified by reducing the number of parts in the chamber, and a one-piece steel chamber was fabricated, which could accept various inserts. The plastic/steel insert combinations are shown in Figure 9 with the one-piece steel chamber design. This hardware modification was used in tests 87–115 to reduce the volume of plastic in the first-stage section of the chamber along with reducing possible test artifacts associated with the modular design.

As the wall thickness of the acrylic was reduced below 2.5 mm, the acrylic fractured and possibly affected the combustion results. The acrylic plastic was replaced by the more ductile Delrin. A thickness of 2.5 mm of white Delrin was used in the first stage of the chamber for the remaining tests.

In tests 85–115, the booster mass was reduced as the volume of plastic was decreased in the first stage to obtain P-t traces that were similar to the P-t trace in test 81. As testing continued, it was found that the load density of the booster (booster mass/booster housing volume) was also important in estimating the correct booster configuration for continued plastic reductions. As the plastic thickness approached all steel, the relation of booster mass-to-plastic wall thickness was used to more closely predict the booster configuration for more tests. The correspondence of booster mass-to-plastic wall thickness required to achieve approximately the same P-t performance in the first-chamber section is shown in Figure 27.

Combustion delay time was used as an operational correlation parameter for the data obtained as a result of reducing the amount of plastic in the combustion chamber, from an all-plastic stepped-wall chamber to a mostly steel stepped-wall chamber. A combustion delay time of less than 200 μs produced a controlled ignition of the LP. The term "controlled ignition" refers to the early, self-sustained chamber combustion evolution in which the pressure increases fast enough to not result in a pressure spike. Figure 8 provides an example of a controlled (test 88) and a less controlled (test 86) ignition. When a longer ignition delay occurs, a pressure spike appears near the beginning of combustion, and this spike subsequently produces uncontrolled pressure waves that affect the remaining chamber combustion evolution.

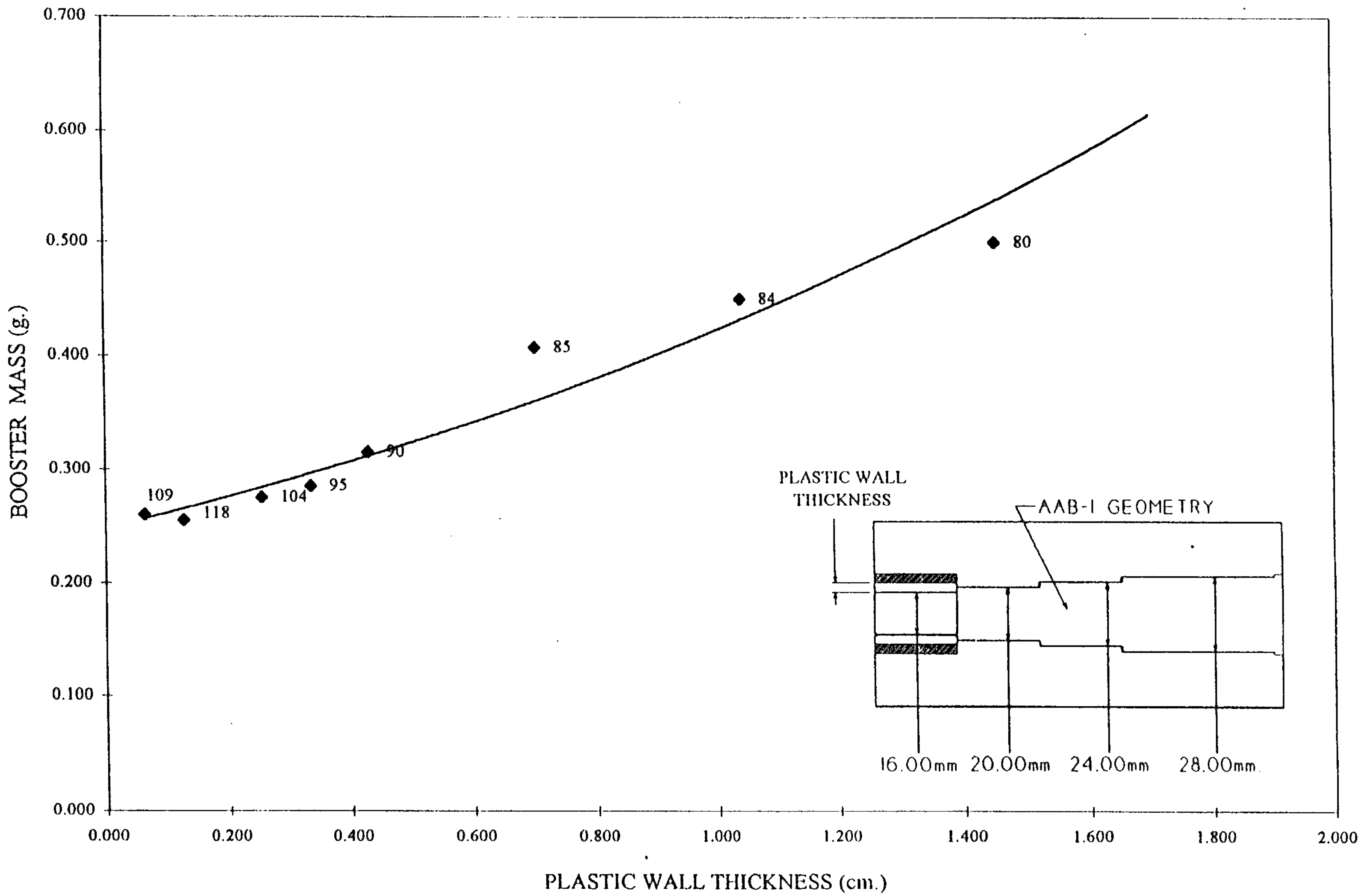

Figure 27. Booster mass as a function of the plastic wall thickness in the first stage of a 30-mm stepped-wall chamber.

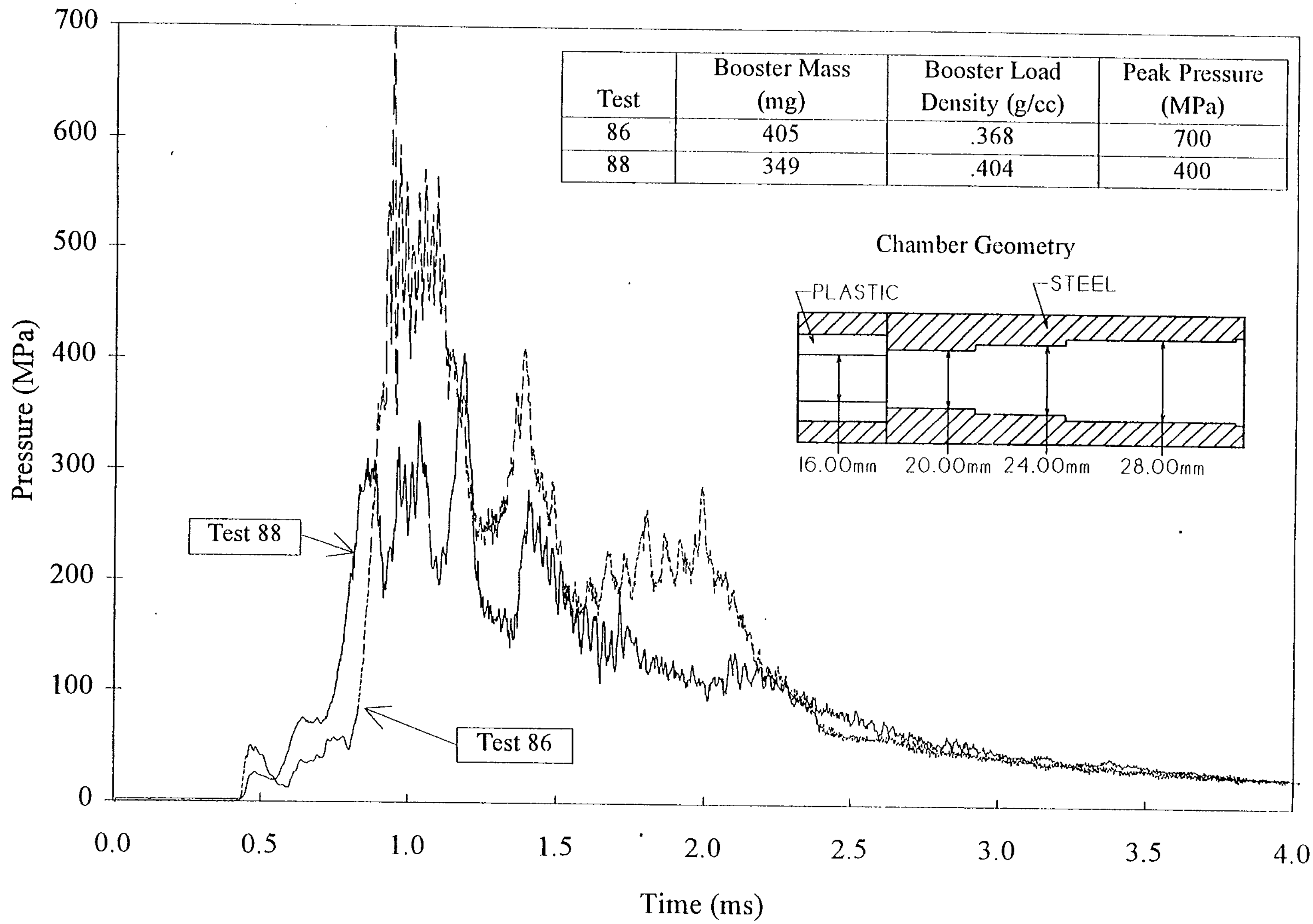

Figure 28. Examples of controlled and uncontrolled ignition in the BLPG tests.

Tests 111, 113, 114, and 115 were completed with no plastic in the first-stage section. The initial results of the all-steel chamber configuration testing were encouraging, but later results were almost catastrophic. The P-t peaks in tests 111 and 113 occurred within the first 4 ms of the event, but for test 114, it occurred at 48 ms, and for test 115, it occurred outside the 64-ms data acquisition window. These results were puzzling at the time, so a first-stage Delrin sleeve with a thickness of 1.27 mm was used from that time on. Later, it was speculated that, since the first-stage section of the steel chamber may not have been thoroughly cleaned (or polished) before each test in this series, there could have been an increasing amount of off-colored char-buildup in the first stage from test 111 to test 115. The worsening pressure traces from test 111 to 115 are shown in Figure 29. This suggested that radiation might play a significant role in the ignition of the LP.

To test this hypothesis, test 132 was run to study the effect of chamber reflectivity on ignition. This was accomplished by replacing half of the white Delrin with black Delrin. These two halves were 1.27 mm thick, and the white Delrin section was closest to the igniter end of the chamber. White Delrin was replaced with black Delrin to produce a test condition in which the radiant energy of the booster ignition would be partially absorbed. This slight change in the white Delrin proved to be very detrimental to the ignition of the LP. After the booster pressure reached its usual peak of approximately 450 MPa (Figure 30), there was no noticeable pressure increase in the chamber or barrel until after the 64-ms window had been reached. Since the velocity of the projectile in this test was similar to that in other tests, it was assumed that the pressures were not drastically different in magnitude from the pressures found in test 81.

The tests reducing the plastic chambers to all steel were very important in obtaining chamber configurations suitable for potential use in actual gun applications. Results obtained here indicated that the peak chamber pressures in properly ignited test guns that yield "normal," one-humped, P-t traces were determined primarily by the geometrical size and shape of the first-stage section, the compressibility, and maybe by the reflectivity of the material in the first-chamber section. Using a properly sized plastic first-stage section, the remainder of the plastic chamber insert can be replaced mostly with an all-steel insert without altering the combustion performance. Further reduction of

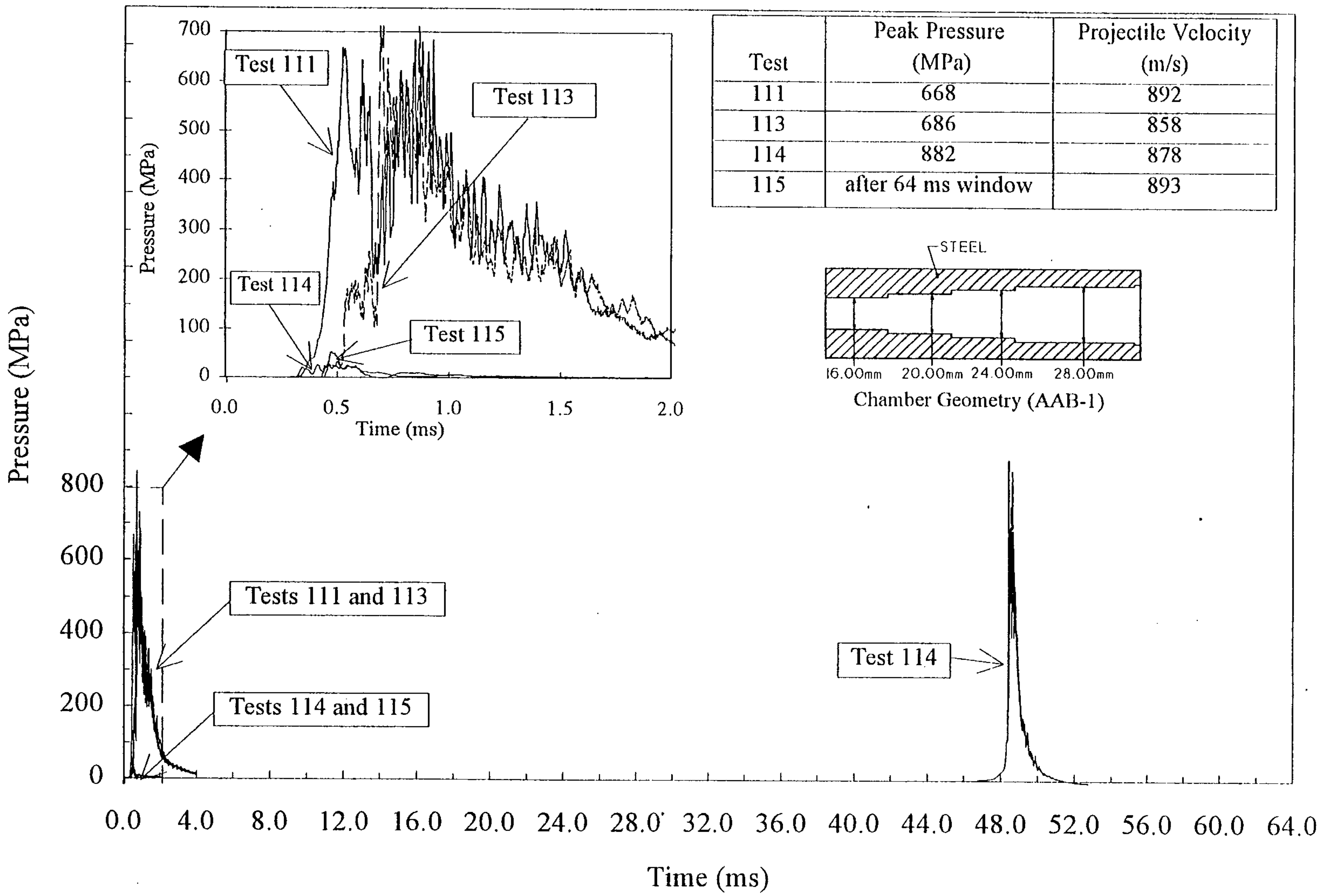

Test	Peak Pressure (MPa)	Projectile Velocity (m/s)
111	668	892
113	686	858
114	882	878
115	after 64 ms window	893

Figure 29. Pressure traces for tests 111, 113, 114, and 115 using an all-steel stepped-wall chamber.

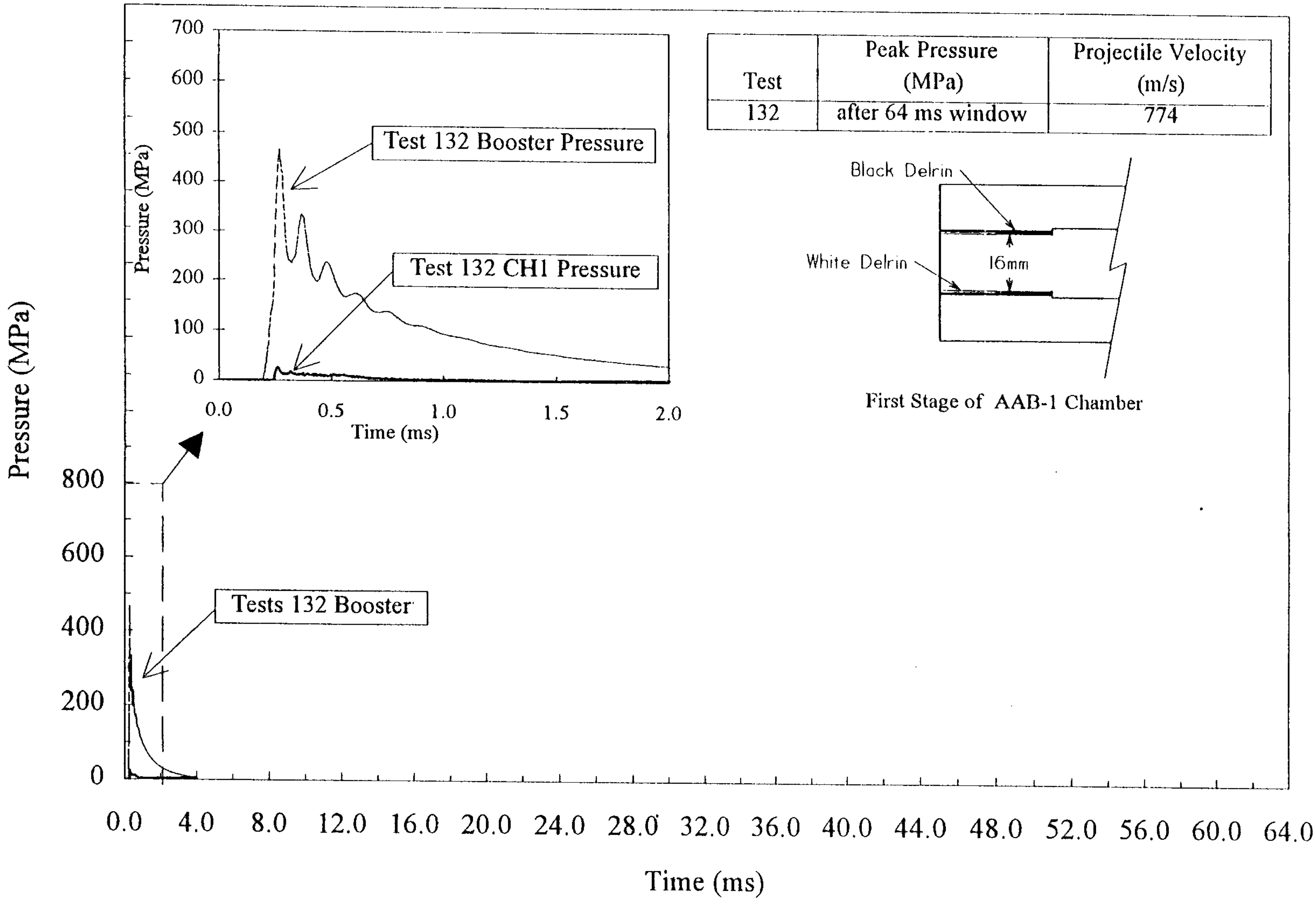

Test	Peak Pressure (MPa)	Projectile Velocity (m/s)
132	after 64 ms window	774

Figure 30. Effects of using a black and white Delrin insert in the first-stage section.

the plastic in the first-stage section of the chamber insert had little effect on combustion performance, provided the pyrotechnic initiator was properly sized. As the plastic in the first-stage section was reduced from a wall thickness of 1.27 to 0 cm, the initiator (booster) load Hercules Unique Canister Powder needed to be reduced while keeping the range of booster load densities between 0.40 g/cm^3 to 0.46 g/cm^3. The single black Delrin test result, when compared with other tests with white Delrin in the ignition region of the chamber, also suggested that the color of the Delrin may be more important as a consistently absorbing material rather than as a buffering material. This implies, as indicated in Figure 27, that the main features in transforming the combustion behavior observed in plastic chambers to those expected in all-steel chambers can be carried out completely and may depend primarily on parameters associated with ignition and combustion that occur within the first chamber section. This approach of transitioning from all-plastic to nearly all-steel chambers has not been carried out for the 20-mm BLPG case. It has been successfully applied to a similar 40-mm test gun in which the plastic first-stage section of steel combustion chamber was replaced with mostly steel [10, 11].

4.1.5 Reproducibility Tests.

4.1.5.1 20-mm Reproducibility Series. Early exploratory 20-mm gun firings conducted under this program included a set of reproducibility tests. Six tests (tests 11, 18, 19, 20, 21, and 22) were run to investigate the variability of the peak chamber pressures and the muzzle velocities using a simple one-step, two-section plastic chamber (Figure 4, chamber geometry H). The chamber consisted of a first-stage diameter of 11.5 mm and length of 19.5 mm, and a second-stage diameter of 20 mm and length of 78 mm. A CCI-400 primer initiated the 250 mg of Unique within the booster housing and that, in turn, ignited approximately 38 g of XM46 in the chamber to propel the 99-g M55A2TP projectile. The chamber geometry and ignition parameters were not optimized; therefore, reproducibility of this set is only considered to be fair. It is, however, indicative of a moderate degree of controlled combustion behavior. The P-t traces obtained from these tests are shown in Figure 31. These P-t traces were very similar in shape, the peak pressures were at an acceptable level of approximately 330 MPa, and adequate muzzle velocities averaging 888 m/s were

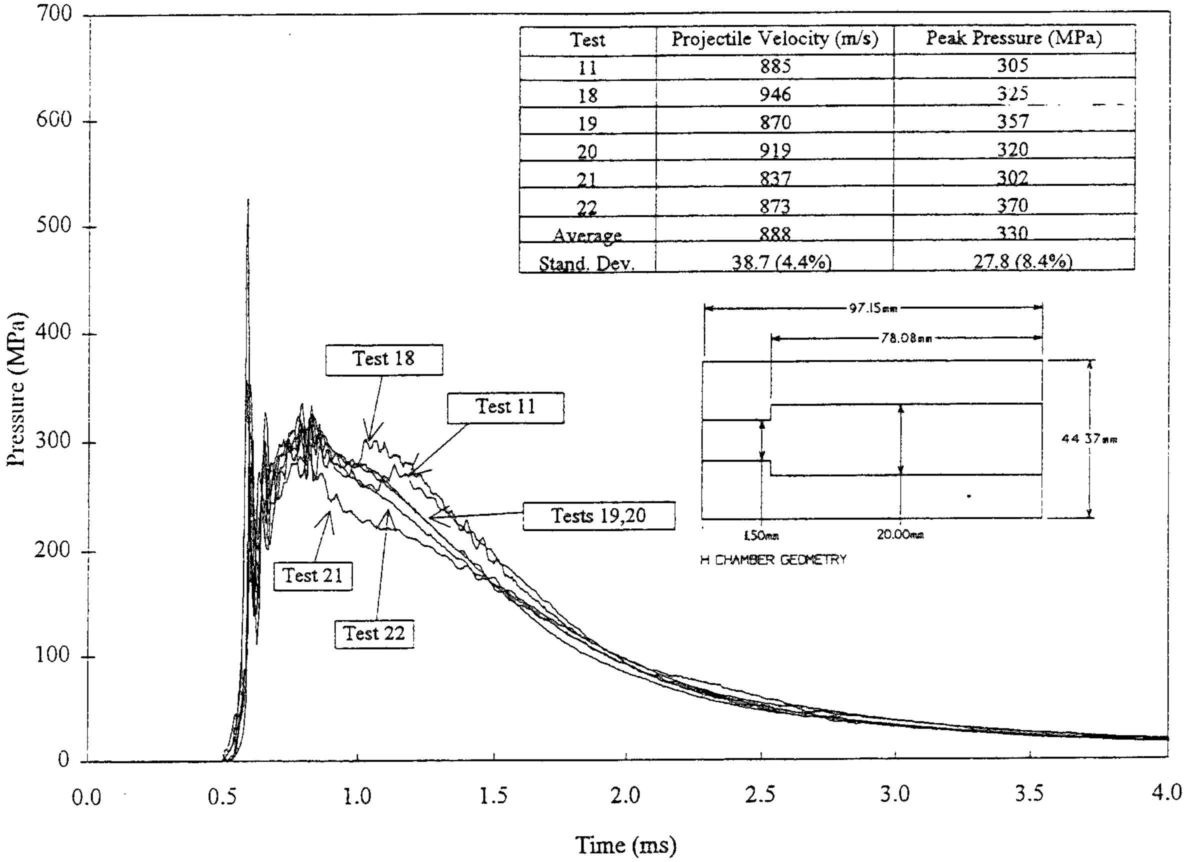

Test	Projectile Velocity (m/s)	Peak Pressure (MPa)
11	885	305
18	946	325
19	870	357
20	919	320
21	837	302
22	873	370
Average	888	330
Stand. Dev.	38.7 (4.4%)	27.8 (8.4%)

Figure 31. Chamber pressures generated during six 20-mm reproducibility tests using identical initial test parameters.

obtained. The standard deviation in the peak pressures was ±8.4%, and for the projectile velocities, it was ±4.4%.

4.1.5.2 30-mm Reproducibility Series. A set of reproducibility tests was run that utilized the modified 30-mm gun test fixture described earlier in the experimental setup section of this report. The main features of this gun included

- high-pressure seals between the breech and chamber insert and between the chamber insert and barrel face to reduce gas leakage;

- clearance holes in the gun chamber to allow for pressure transducers to be inserted directly into the chamber insert;

- two standard-mount transducers and one flush-mount transducer in the chamber insert;

- a projectile modification with a Delrin rotating band, a steel washer, and a hemispherical attachment that pressed into the front end of the chamber; and

- a loading procedure reducing the amount of silicone grease.

A mostly steel, three-step chamber having section diameters of 16 mm, 20 mm, 24 mm, and 28 mm was used for this set of reproducibility tests. The first-stage steel section was lined with a 1.27-mm (0.050 in)-thick white Delrin tube with a final inside diameter of 16 mm, and the front three chambers were of steel. All of these tests used the same type of primer (CCI-400), an axial booster housing with a 0.562-cm^3 capacity containing 255 mg of Unique canister powder as the booster charge, a 1.32-mm booster orifice diameter, approximately 85 g of XM46 LP as the main charge, and a modified GAU-8 30-mm projectile (approximately 355 g) with a Delrin and steel base region modification. This particular chamber configuration was not optimized, but had well-behaved P-t results. The smoothed P-t traces for the five tests of this series are shown overlayed in Figure 32(a) along with the displacement of the projectiles with time in Figure 32(b). A 20-point moving average was used on these curves so that comparisons could be made more easily. Although the rapid pressure pulses were significantly reduced with the modifications, some noise was still present. The peak pressure variation indicated a mean value of 409 MPa with an unbiased standard deviation of 5.3%. It is interesting to note that test 153 was fired as a repeat test several months after the other tests in the series. Although there was a rapid increase in the chamber pressure during this test, the movement and final velocity of the projectile, as a result of this pressure, was very similar to the other tests. The difference in pressure development may have been a result of barrel growth

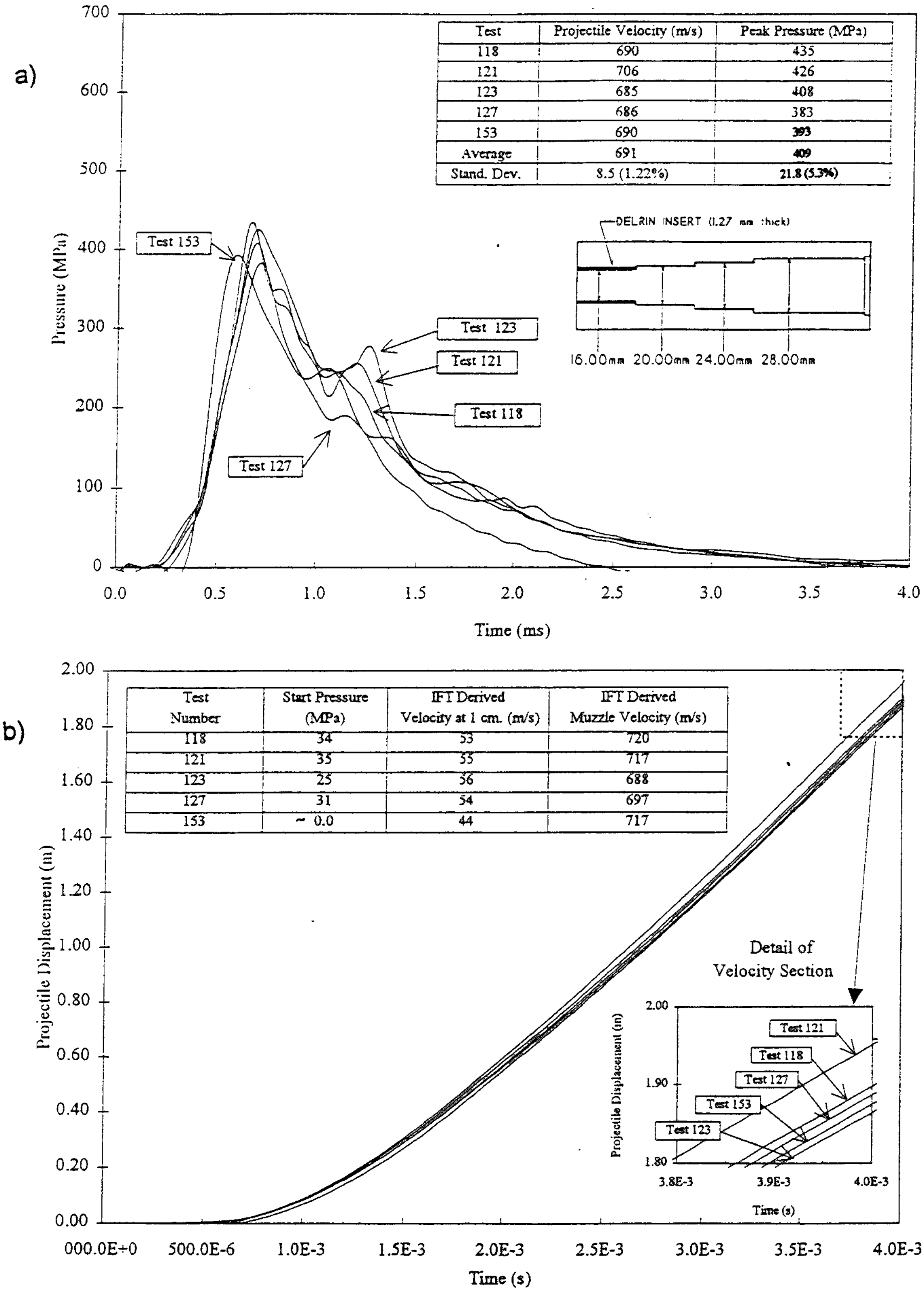

Test	Projectile Velocity (m/s)	Peak Pressure (MPa)
118	690	435
121	706	426
123	685	408
127	686	383
153	690	393
Average	691	409
Stand. Dev.	8.5 (1.22%)	21.8 (5.3%)

Test Number	Start Pressure (MPa)	IFT Derived Velocity at 1 cm. (m/s)	IFT Derived Muzzle Velocity (m/s)
118	34	53	720
121	35	55	717
123	25	56	688
127	31	54	697
153	~ 0.0	44	717

Figure 32. (a) Chamber pressures and (b) projectile displacements with time for five 30-mm reproducibility tests with identical initial test parameters.

from previous tests. The reproducibility in the projectile velocity is also considered to be good with an unbiased standard deviation of ±1.2% and about an average muzzle velocity of 691 m/s.

Muzzle-velocity values were obtained from timed intervals between each projectile passage through paper-breakstrip switches placed at known distances apart. The breakstrip velocities are in good agreement, and the microwave interferometer measurements made of projectile travel in the barrel during tests (Figure 32[b]) proved to have very similar projectile displacements with time down the barrel. The projectile velocity data obtained here using breakstrip switches are considered to be more accurate for the tests conducted here than the velocities obtained using the interferometer. The interferometer-derived velocities at 1 cm and at the muzzle of the barrel (2.06 m from the initial position of the projectile in the gun) tend to correlate (i.e., when the velocity at 1 cm was high, the muzzle velocity was low).

The 30-mm reproducibility tests were encouraging, but there were inconsistencies present during the tests. Two tests (tests 125 and 126) were completed in which the velocities were significantly different from the velocities for the reproducibility tests. The velocities obtained by the use of velocity screens after the projectile was out of the gun were about 85 m/s faster in tests 125 and 126, although the pressures in the chamber were very similar to those in the reproducibility series (Figure 33). In Figure 33, test 121 was selected to illustrate the reproducibility series because it had the highest velocity of the five. The displacement curves for the three tests (Figure 33) physically indicate why the velocities are higher. The projectiles were initially accelerated about the same in all three tests, but after about 1.75 ms, the projectiles from tests 125 and 126 continued to accelerate to the end of the barrel, while the projectile from the reproducibility test moved with a much lower acceleration rate. The velocities derived from the interferometer displacement curves also show that the projectile in test 125 was 137 m/s faster and in test 126 was 96 m/s faster than test 121.

The pressure at the first noticeable sign of projectile movement was recorded for each test. This pressure is known as the shot-start pressure. In tests 125 and 126, these shot-start pressures (Figure 33) were higher than those in the other reproducibility tests. This was initially considered to be the principal cause of the large velocity differences. On further inspection of the displacement

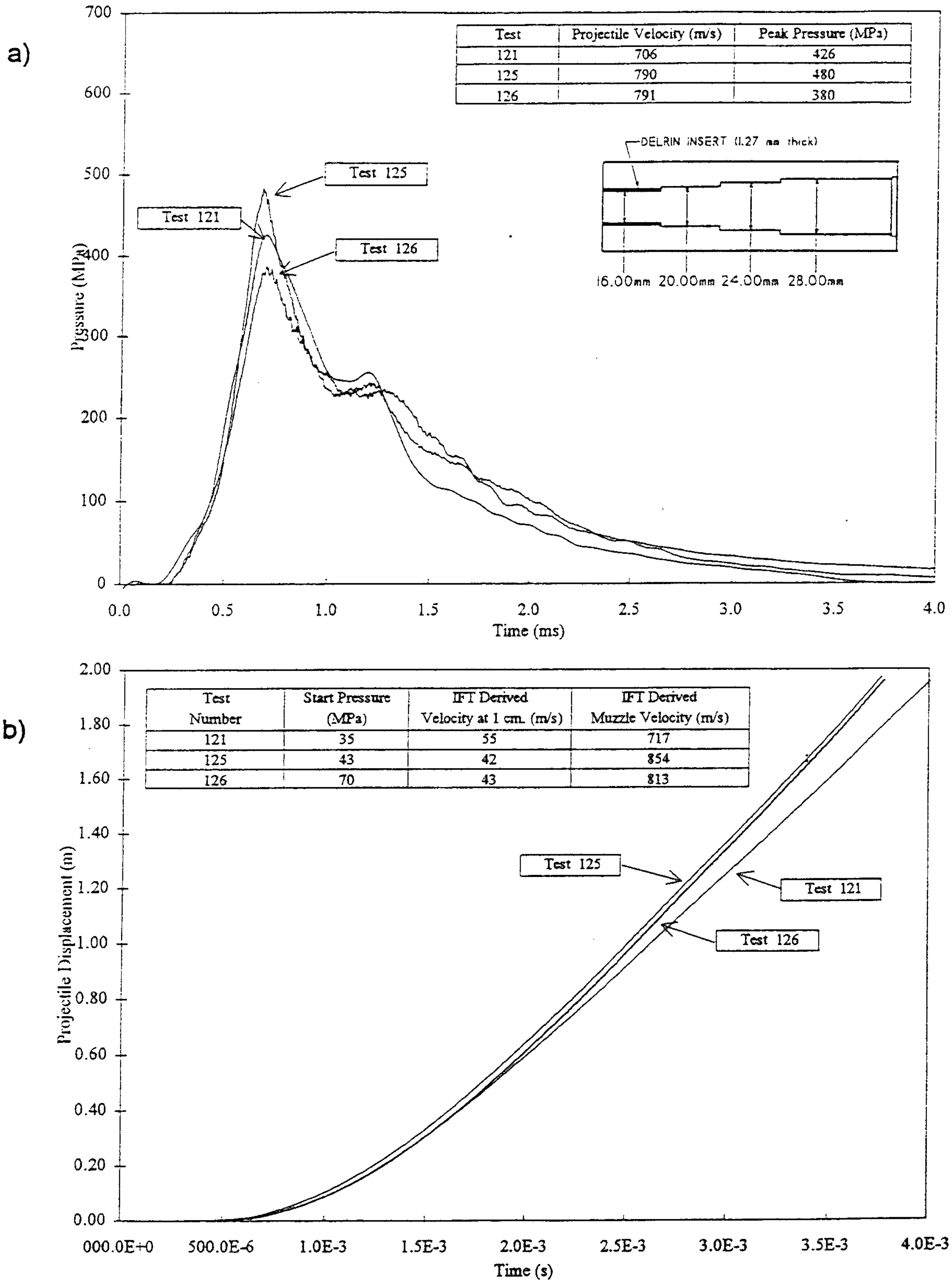

Figure 33. (a) Chamber pressures and (b) projectile displacements with time for one reproducibility test and two inconsistent tests.

data, it appears as though another unknown feature may have been present that affected the projectile displacements near the center and muzzle of the barrel. This is because the projectiles in these two tests continued to accelerate with noticeable pressure differences at CH1 (higher than that exhibited in test 121) in the later portions of their P-t curves.

4.1.6 Stepped-Wall, Rear Couple. This stepped-wall, rear couple examination had a three-fold objective in this program. The first was to determine if the moderate degree of combustion control observed in other work at Veritay [7, 8, 12] using the LP OTTO II could be maintained when the LP XM46 was used instead at both the 20-m and the 30-mm gun scale. The second was to determine whether the effects on overall peak chamber pressures arising from increasing the first-stage diameters and lengths would still be operative and provide useful geometrical means of influencing combustion control. The third was to use these findings early in this program to explore whether significant high-pressure combustion problems might arise in a 20-mm gun chamber if the projectile mass typically used in this gun increased in a step-by-step manner to a greater projectile mass often used in a 30-mm gun. The absence of such potential combustion problems would, thereby, enable straightforward scaling of the 20-mm gun to a 30-mm size. This third item of projectile mass scaling was briefly discussed earlier (section 4.1.2) and is noted briefly here in conjunction with combustion control explorations.

4.1.6.1 First-Stage Diameter Changes. The effects on peak pressures from increasing first-stage chamber diameters were explored early in the 20-mm and 30-mm gun tests in this effort. In these situations, the first stage in the chamber was the cylindrical section closest to the igniter (rear of the chamber).

In the 20-mm tests, the H- and I-type plastic chamber geometries were used to investigate the effects of increasing the first-stage diameter on the combustion pressures. The H-type chamber insert consisted of a first-stage diameter of 11.5 mm (19 mm long) and a second-stage diameter of 20 mm (78 mm long). The only difference in the I-type chamber insert was that the first-stage diameter was increased from 11.5 mm to 16 mm (Figure 4). All other dimensions were identical. Tests 27 (H-type) and 25 (I-type) used a 335-mg booster mass in a 0.69-cm^3 booster housing cavity, a booster orifice diameter of 1.7 mm, an LP mass from 40 g to 42 g, and a projectile mass of 66 g. Similarly, tests 33 and 24 used a 420-mg booster mass in a 0.69-cm^3 booster housing cavity, an orifice diameter of 1.32 mm, and a projectile mass of 199 g. In both of these situations, the pressure rise rates in the chambers increased approximately the same, but the peak pressures were higher with the larger first- stage diameters (Figure 34). Generally, changes from chamber type H to I (diameters from 11.5 mm to 16 mm) changed the peak chamber pressures and velocities in the 20-mm gun (Table 3).

The peak chamber pressures (generally taken at location CH2) increased when a large booster orifice diameter of 1.7 mm was used, and decreased (except in one test of the largest projectile mass) when a small booster orifice diameter of 1.32 mm was used (Table 3). The projectile velocities, in turn, generally increased when the large booster orifice of 1.7 mm was used. When a small booster orifice of 1.32-mm diameter was used, the limited results were mixed. For the 66-g projectiles, the velocity remained nearly constant in one case and increased a small amount in two other cases; for the 99-g projectiles, a velocity decrease was observed; and for the 199-g projectiles, a small velocity increase was observed.

In the 30-mm test firings, the first-stage diameter was increased in plastic chamber inserts to investigate the effects on the pressure development. Unlike the H- and I-type chambers, the first-stage diameters in the 30-mm gun tests were increased by moving the second-stage diameter to the first stage and lengthening the last stage (the 30-mm diameter section). Therefore, the 11.5/16/20/24/30 chamber in test 60 turned into a 16/20/24/30 chamber in test 62, and into a 20/24/30 chamber in test 63. These were identified as the AAA, AAB, and AAC chambers in Figure 6 in the setup section of this report. The results of this series of tests (Figure 35) were similar to those found in the 20-mm test firings; the peak pressures increased as the first-stage diameter increased.

In test 64 (not shown in Figure 35), the second stage (24-mm section) was decreased from test 63 and added to the length of the 30-mm section. The results of test 64 showed that the peak pressure was higher than that in test 62 (first-stage diameter of 16 mm), but the duration of the high pressures

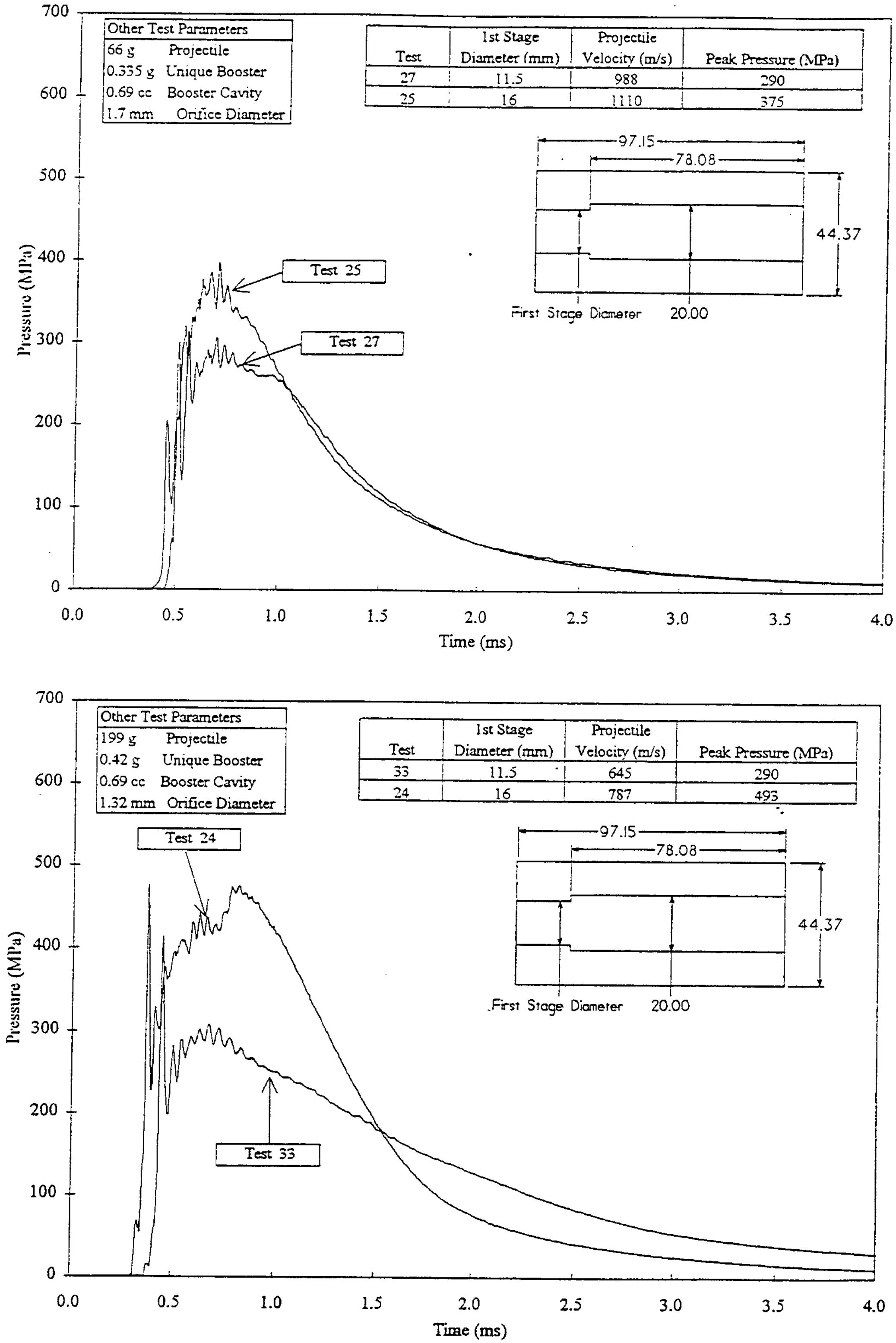

Figure 34. Effects of increased first-stage chamber diameters in 20-mm test firings.

Table 3. Initial Parameters and Results for Ignition Tests Using 20-mm H- and I-Type Chambers

Booster Load (mg)	Booster Volume (cm^3)	Booster Orifice Dia. (mm)	Projectile Mass (g)	Test Number H-Type	Peak Pressure (MPa)	Projectile Velocity (m/s)	Test Number I-Type	Peak Pressure (MPa)	Projectile Velocity (m/s)
335	0.69	1.32	99	9	651	1,056	31	364	888
335	0.69	1.7	99	11	304 CH1	885	8	491 CH1	1,037
335	0.69	1.32	66	15	468	947	12	405	1,001
335	0.69	1.32	198	16	575	761	13	428	770
335	0.69	1.7	66	27	316	988	25	397	1,110
335	0.69	1.7	198	28	341	737	26	489	773
420	0.69	1.32	66	29	546	992	23	366	989
420	0.69	1.32	198	33	445	645	24	493	787

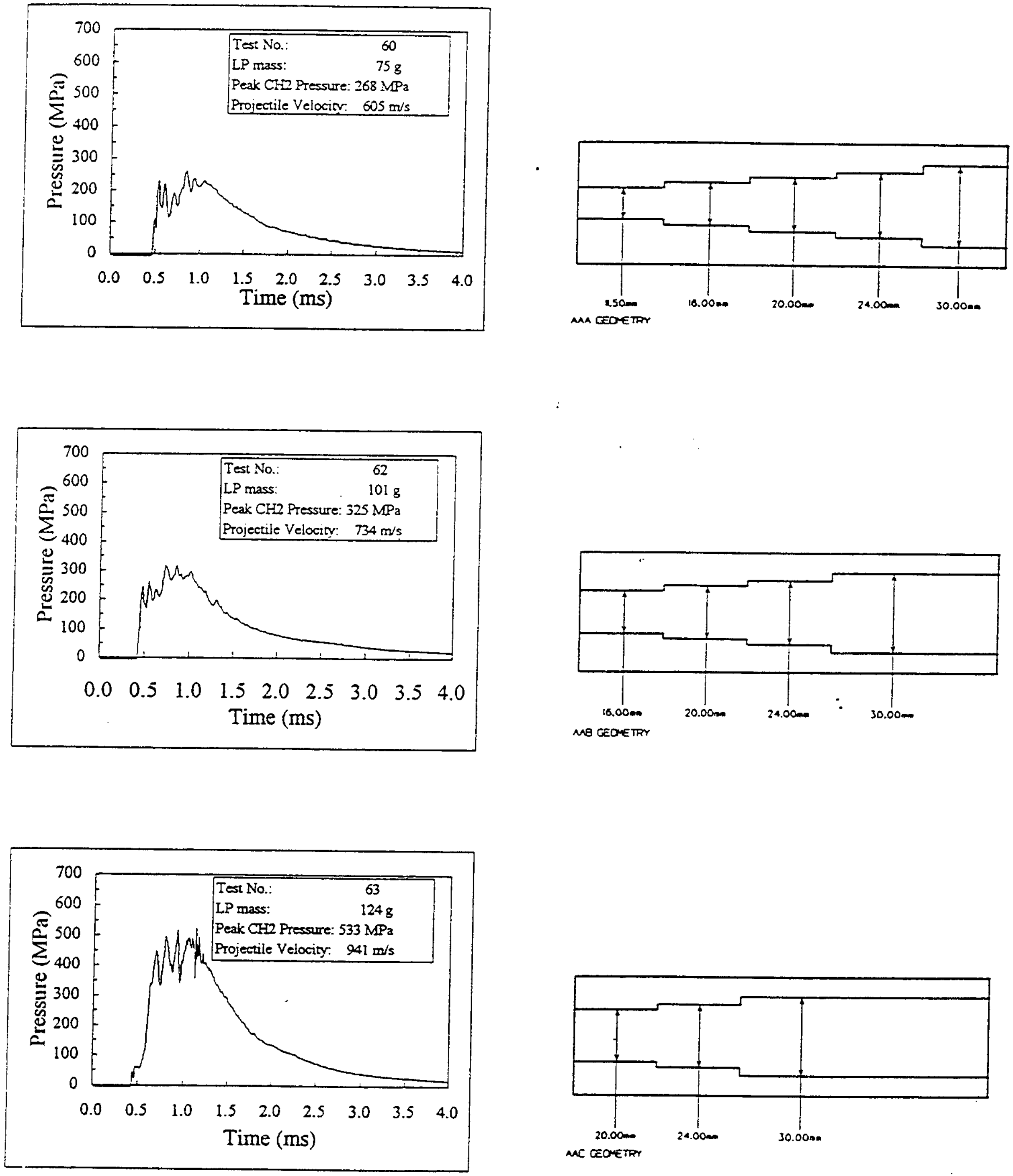

Figure 35. Effects of increasing first-stage diameters on the generated chamber pressures in the 30-mm gun.

was shorter. The difference from tests 63 to 64 indicated that the step lengths after the first section may be important in controlling and sustaining the combustion in the chamber, but confirmation with further test results are recommended.

4.1.6.2 First-Stage Length Changes. Along with investigating the effects of changes in the first-stage diameter, three tests were completed in which the first-stage lengths were increased. The lengths were increased from 30.5 mm in test 153, to 35.6 mm in test 160, and to 40.7 mm in test 156. These tests used modifications to the mostly AAB-1 geometry (2.27 mm of Delrin in first stage) with a 16-mm first-stage diameter, a 20-mm second-stage diameter, a 24-mm third-stage diameter, and a 28-mm fourth-stage diameter. As the lengths were increased in the first stage, they were removed from the fourth-stage length. These changes affected the pressure traces by decreasing the magnitude and duration of the pressures within the chamber (Figure 36). This suggests that the longer first stage controlled the growth of initial combustion following ignition by constraining the LP burn surface for a longer period within the small-diameter first stage.

4.1.7 Velocity Scaling. During this effort, the forward sections of the chamber were varied in an attempt to investigate the effects on the chamber pressures and projectile velocities. Findings from the multichamber tests (section 4.2.1) suggested that increasing the diameter in the last section of the chamber to a size larger than the barrel-bore diameter and then tapering the chamber down to the bore diameter increased the velocity without significantly increasing the chamber pressure. Therefore, this arrangement was also investigated in the stepped-wall configuration. Three tests were run with increasing diameters in the fourth-stage section of the AAB-1 chamber. The first stage (with a Delrin insert of 1.27-mm thickness) had a 16-mm diameter, the second had a 20-mm diameter, and the third had a 24-mm diameter section. The last-stage diameter in test 153, and in the other reproducibility tests (tests 118, 121, 123, and 127), was increased in test 154 to a diameter of 32 mm and then was tapered with a 5° chambrage to the bore (Figure 11, AAB1-B). In test 155, the fourth-stage diameter of 37.7 mm was tapered with a 12° chambrage to the bore diameter (Figure 11, AAB1-C).

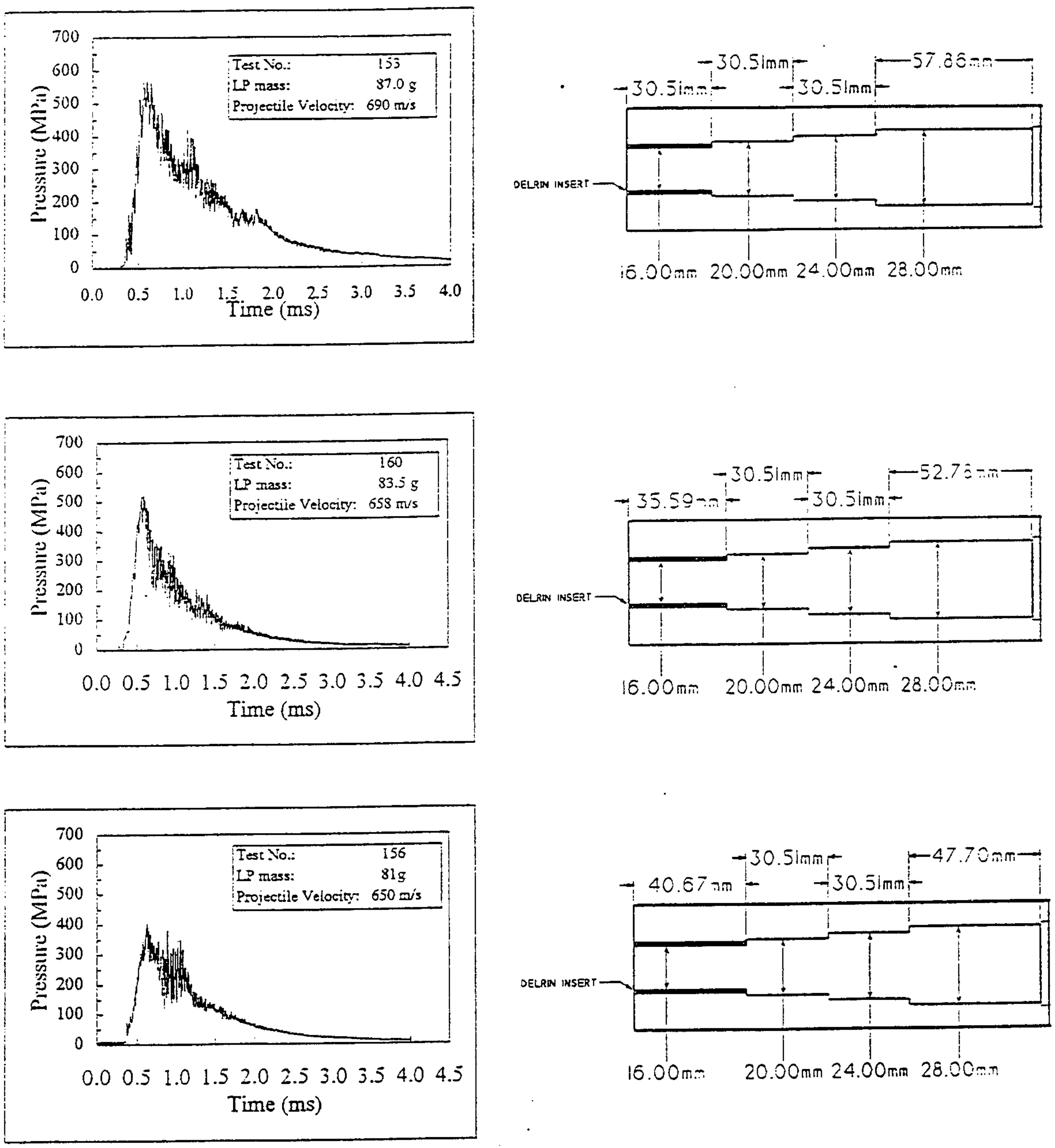

Figure 36. Effects of an increasing first-stage length on the pressures generated in a 30-mm gun.

Together with the straight fourth-stage chamber configuration, Figure 37 shows the two diameter increases to the stepped-wall chamber configuration and the resultant P-t curves for each change. In general, the overall peak chamber pressures did not increase, but were longer in duration. The resultant projectile velocities increased from 692 m/s with a fourth-stage diameter of 28 mm, to 990 m/s with a 37.7-mm fourth-stage diameter (Figure 37). This finding was encouraging because the ballistic performance of the 30-mm gun fixture was increased without significantly increasing the internal chamber pressures by just modifying the chamber configuration.

4.2 Multichamber Configuration. A series of multichamber combustion tests with bulk-loaded LP XM46 were completed using plastic multichamber inserts. The chamber inserts were initially fabricated from acrylic, and later were made from Delrin because the acrylic was brittle and fractured on combustion while the Delrin could be deformed significantly without breaking. It was important that the material used for inserts be plastic in order to damp possible pressure-wave pulses that might be encountered during exploratory test runs; these pulses could be detrimental to the structural integrity of the gun test fixture. The inserts in these cases consisted of the following basic parts: (1) an input section to control the basic pressure level to be expected during test firings, (2) the transition region to continue combustion from the input section to the multichambers, (3) the multichamber region where much of the LP combustion was expected to occur under geometrically controlled burning conditions, and (4) a transition section where the output of the multichamber LP combustion was brought back together in a single chamber-chambrage region. The last of these sections, of course, directed the remaining LP and combustion gas into the barrel. The original geometry of the multichamber concept, as discussed in the setup section of this report, consisted of a single, cylindrical, first-stage section followed by a second section containing three cylindrical tubes, and a third section containing three cylindrical tubes. This configuration was designated as the 1-3-3 geometry.

In this testing, the attributes of the original concept (1-3-3 configuration) were varied to investigate the coupling of the front and rear sections of the chamber. Using a design similar to the 1-3-3, the number of tubes used was increased to four and six while keeping the combined cross-sectional areas of the tube sections constant. Also, the number of tubes in the last-stage section was

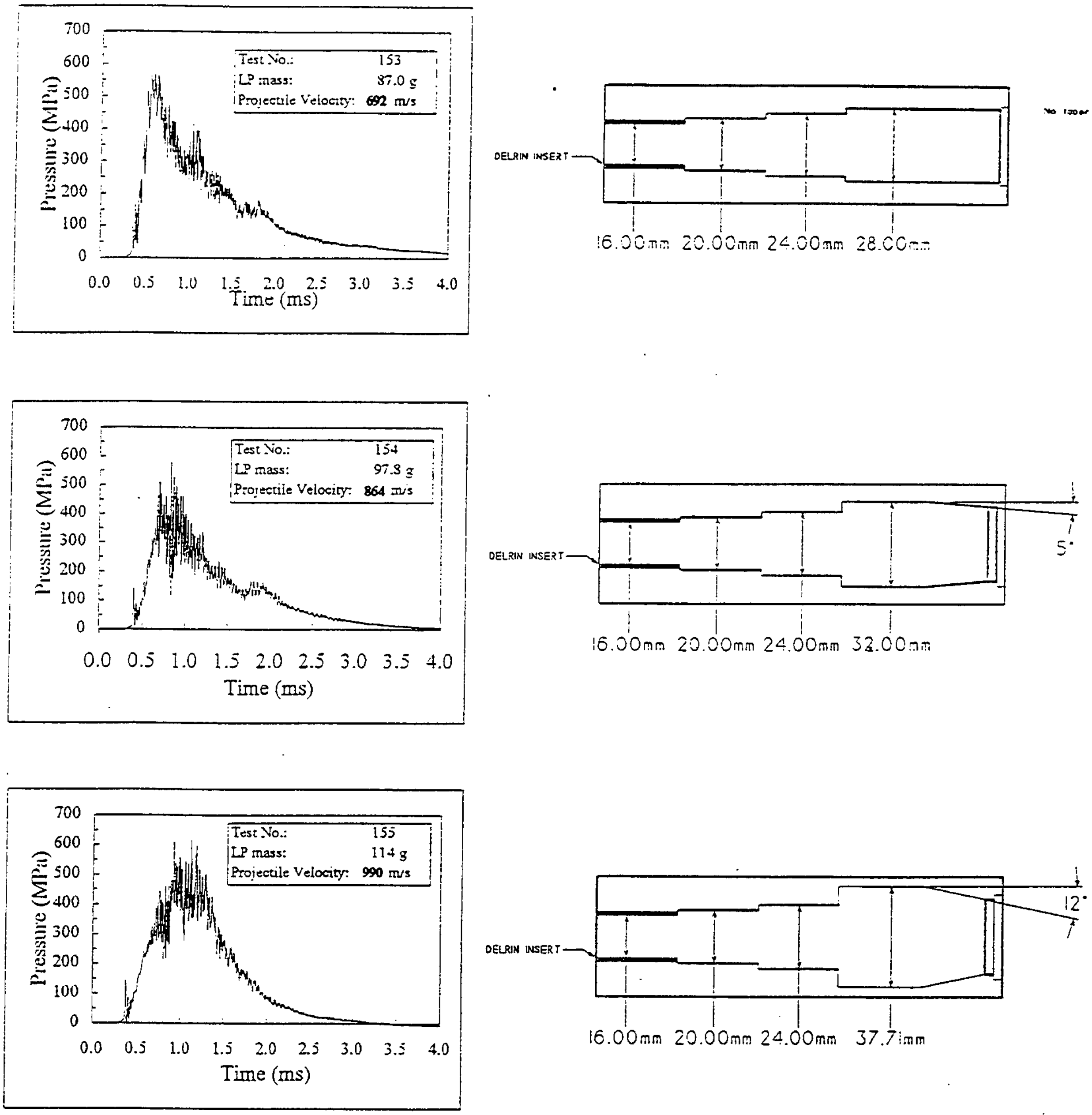

Figure 37. Increased ballistic performance without pressure from an increasing fourth-stage diameter.

increased from three to nine tubes (Figure 13, 1-3-9 chamber configuration). An extension of the multichamber concept, the 1-1-19 configuration, incorporated attributes of the stepped-wall chamber and the multichamber configurations.

4.2.1 Front Coupling. The effect of changing the chamber design in the front section of the multichamber configuration was investigated first. The "front section" refers to the areas after the first stage of the multichamber that usually affect the secondary pressures in the combustion results.

Since difficulties were expected in controlling an increased rate of combustion in the transition region between the third-stage chamber section and the single 30-mm bore of the barrel, a smooth transition geometry was included in the multichamber assembly by means of an inserted component. In Figure 12, this was referred to as the transition ring. This shape was included to reduce the number of sharp corners contained in the geometry that could have allowed turbulence or cavitation in the LP to develop as the LP passed. It is believed that turbulence and/or cavitation in this area can cause an unwanted increase in combustion to occur in or near the breech end of the barrel.

4.2.1.1 Tapering. The initial test (test 134) in the 30-mm multichamber phase of testing was conducted using the 1-3-3 insert chamber geometry. This geometry consisted of a 11.5-mm first-stage diameter, three 13.5-mm diameter second-stage tubes, and three 16.7-mm diameter third-stage tubes. The equivalent diameters of the combined tube areas in each stage were 11.5 mm, 23 mm, and 29 mm, respectively. When this design was used as a chamber insert, it produced a P-t trace with a large, secondary pressure spike. Because of this undesirable "double-humped" curve, it was determined that the transition region at the front of the chamber alone was not enough to alleviate fluid-dynamic effects (such as turbulence, cavitation, or droplet formation) and subsequent secondary ignition within the barrel. As a result, the area of plastic between the three third-stage chambers was tapered to reduce the square edges at the ends of the tubes. This transition tapering proved to be an important addition to the design of the multichamber in test 135 because it eliminated the secondary high-pressure hump observed in test 134. The pressures generated in the first-stage section of the chamber for the tests without and with tapering are shown in Figure 38. Since the pressures in the

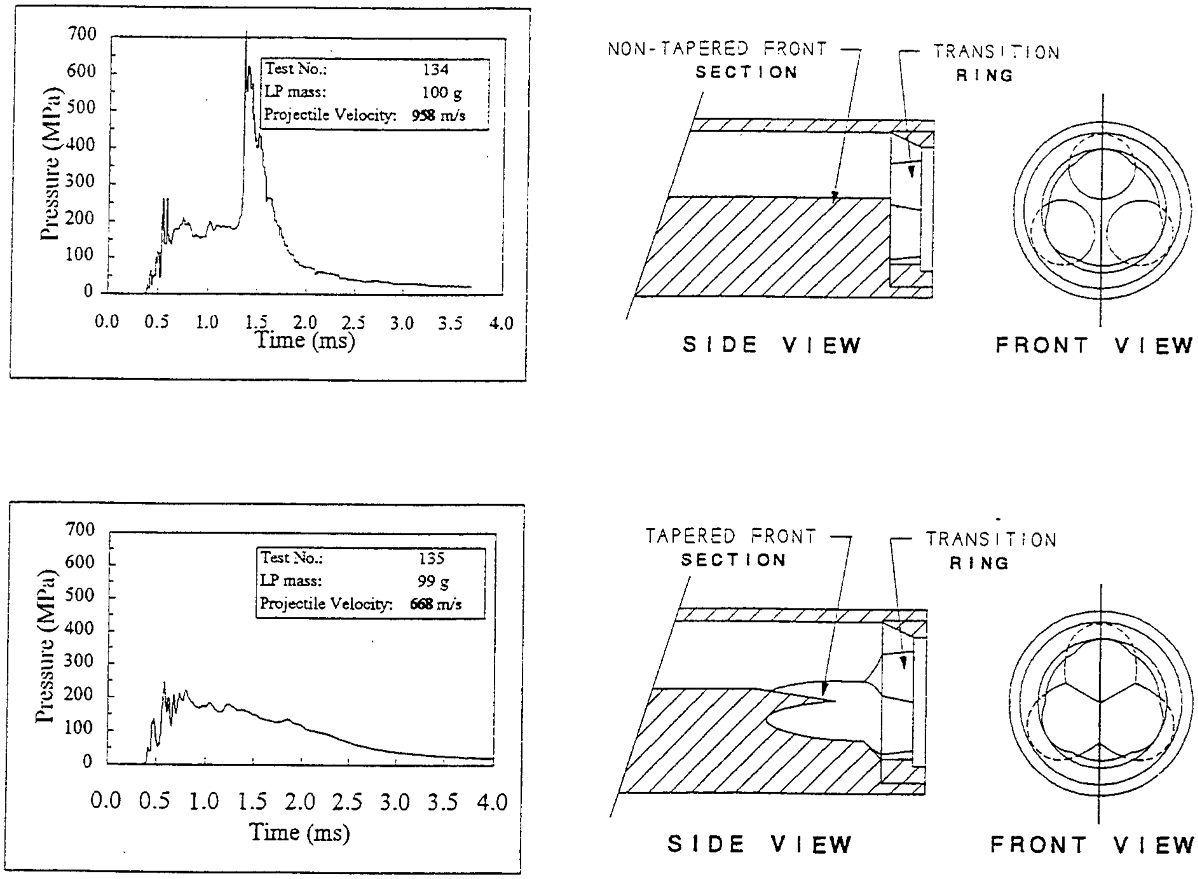

Figure 38. Pressures generated in 30-mm multichamber tests without tapering (test 134) and with tapering (test 135).

beginning part of these curves are very similar, it is evident that changes in the front of the chamber affected the pressures after the initial peak pressure.

4.2.1.2 Second-Stage Diameter. The second-stage diameters were also varied to continue investigation of the effects of changes in the front of the chamber in a 1-3-3 geometry. The three cylindrical tube diameters of the second stage were increased from 13.5 mm each in test 137 to 14.7 mm each in test 138. The result of this increase in diameter (Figure 39) is a secondary combustion pressure spike in the P-t trace (CH2) as compared to test 137 (discounting the early pressure peaks

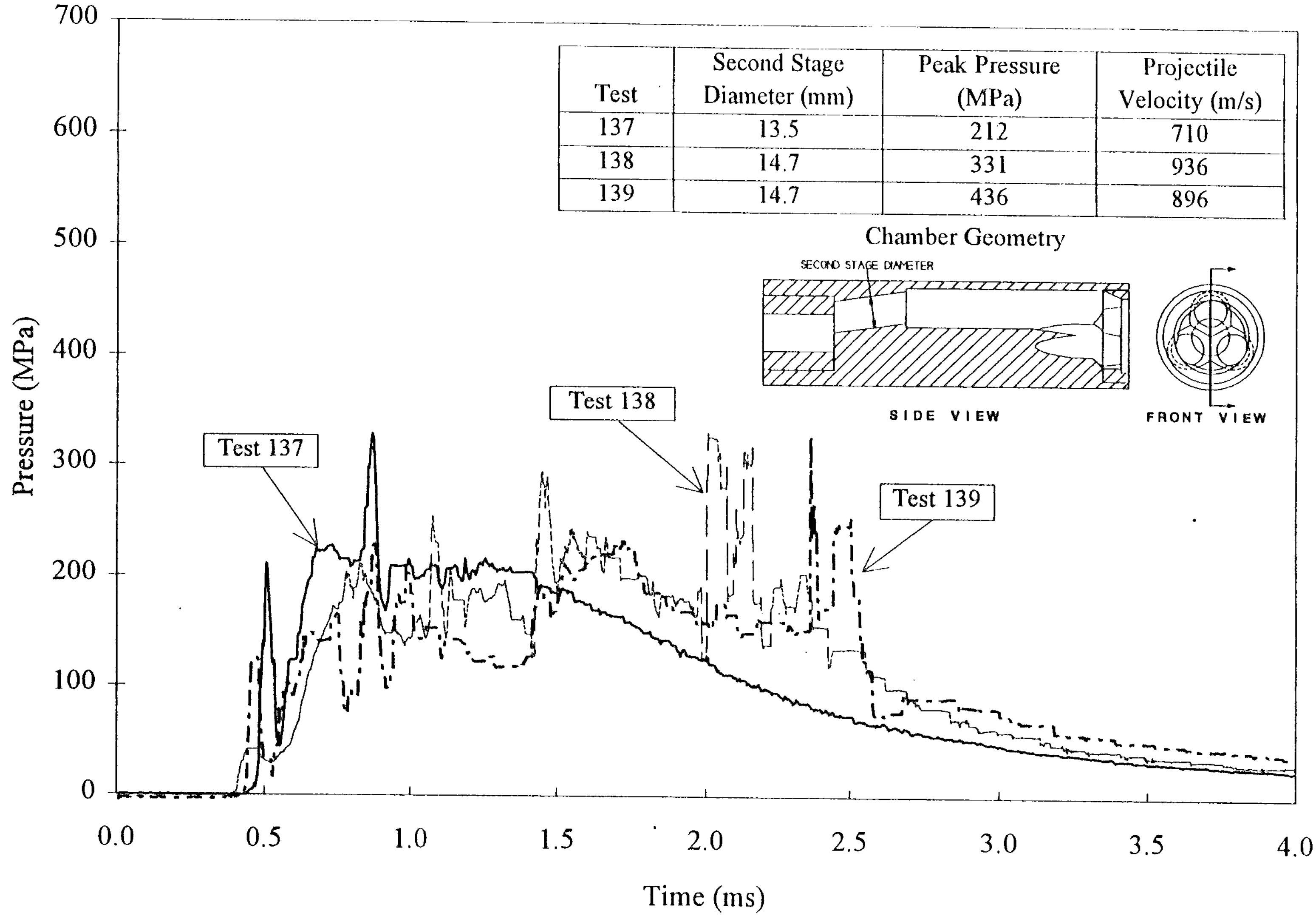

Test	Second Stage Diameter (mm)	Peak Pressure (MPa)	Projectile Velocity (m/s)
137	13.5	212	710
138	14.7	331	936
139	14.7	436	896

Figure 39. Chamber 2 pressures generated in 1-3-3 multichamber tests with an increased second-stage diameter.

in test 37 as a spurious signal). A test under the same conditions (test 139) produced similar results (Figure 39). The origin of the secondary pressure pulses in these tests remains unknown, but appears to be related to an enhanced rate of combustion following passage of the flame front into the third stage tubes—possibly initiated by use of the somewhat larger second-stage tubes than used previously.

4.2.1.3 Third-Stage Diameter. Further investigations involving the combustion pressure changes arising from changing the third-stage tube diameters were conducted for tests 142 and 143. These chambers had a first-stage diameter of 16 mm and a second-stage tube diameter of 13.5 mm. The third-stage tube diameters were increased from 16.7 mm to 17.3 mm. The pressures in the chamber decreased slightly when the diameters were increased from 16.7 mm to 17.3 mm. These results are shown in Figure 40. Again, the exact cause of this slight pressure decrease is unknown. In fact, the increase in third-stage chamber diameter, by analogy with the previous case of a similar increase in the second-stage diameter, might be expected to yield a small pressure increase, rather than the pressure decrease actually observed. Perhaps this small pressure decrease was within the normal uncertainty in the combustion pressure for these nonoptimized chamber configurations.

4.2.2 Number of Tubes. The 1-3-3, 1-4-4, 1-6-6, and 1-3-9 multichamber-type tests include tube diameters at each stage location with equivalent surface areas of a 20-mm diameter first-stage, 24-mm diameter second-stage, and 30-mm diameter third-stage stepped-wall chamber configuration (20 mm/24 mm/30 mm). To create the 1-4-4 configuration, the second-stage tube diameters were decreased from 13.5 mm to 11.7 mm each and the third-stage tube diameters were decreased from 16.7 mm to 14.4 mm. The 1-6-6 configuration was created by decreasing the second-stage tube diameters from 13.5 mm to 9.5 mm and the third-stage tube diameters from 16.7 mm to 11.8 mm as compared to the 1-3-3 configuration. The six tubes could not be centered on the same centerline as the 1-3-3 and 1-4-4 configurations because the wall thickness between the tubes was reduced to zero. Therefore, the centerlines of the six tubes were moved away from the center of the chamber. In doing this, the angle of the second stage and the area between the tubes in the third stage was increased. This area created between the tubes was tapered using the same angle as with the 1-3-3

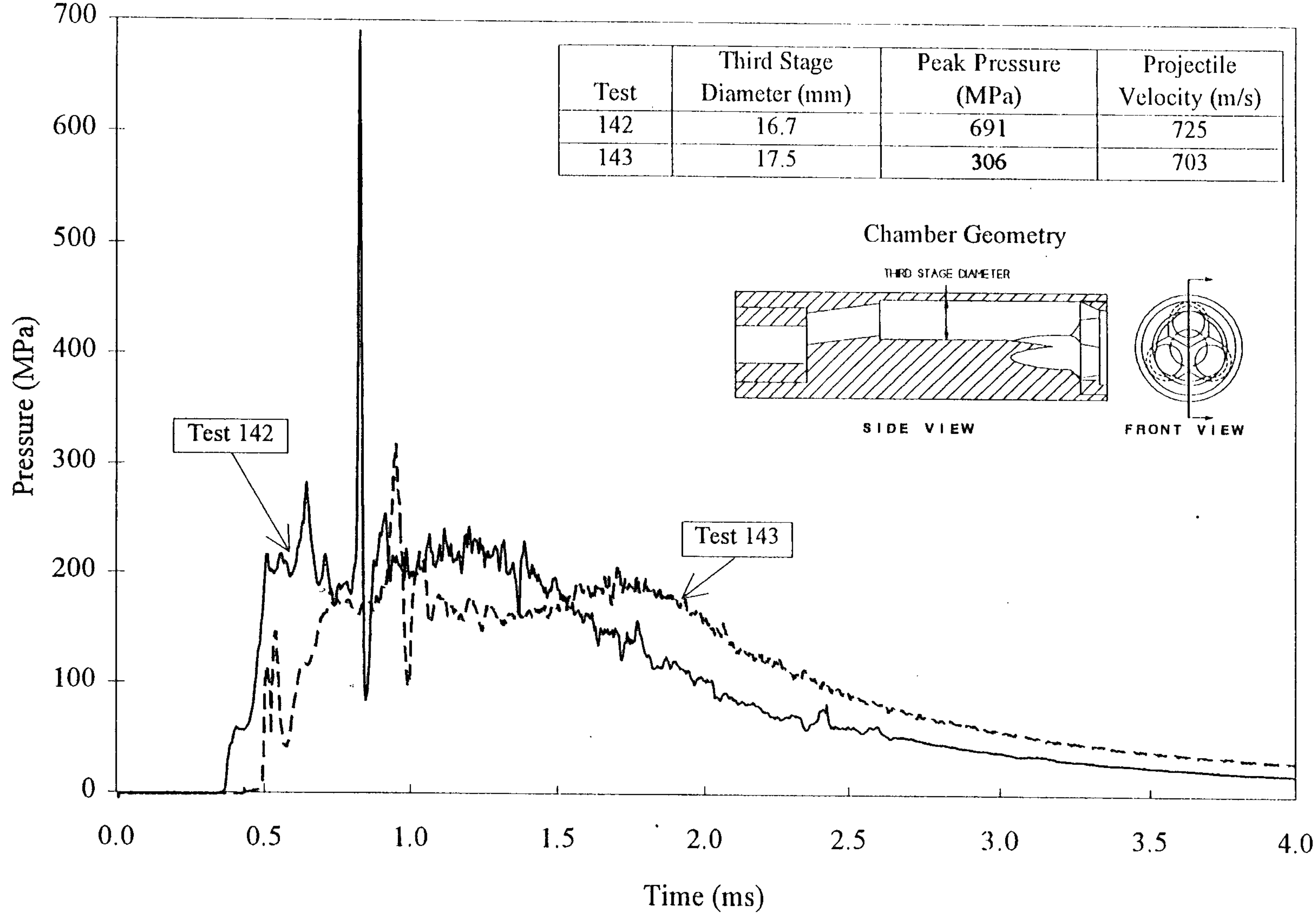

Test	Third Stage Diameter (mm)	Peak Pressure (MPa)	Projectile Velocity (m/s)
142	16.7	691	725
143	17.5	306	703

Figure 40. Chamber 2 pressures generated in 1-3-3 multichamber tests with an increased third-stage diameter.

design, but the depth of the cut was larger. The 1-3-9 multichamber configuration used in test 148 consisted of a single cylindrical first-stage section, three cylindrical second-stage sections, and nine cylindrical third-stage sections. The diameters of these sections were 20 mm, 13.5 mm, and 9.6 mm, respectively, with equivalent section diameters of 20 mm, 24 mm, and 30 mm.

The first three P-t traces shown in Figure 41 are from 30-mm test gun firings using the 1-3-3, 1-4-4, and 1-6-6 multichamber configurations listed in the figure. The P-t traces for the 1-3-3, 1-4-4, and 1-6-6 multichamber tests are very similar, and all three tests tend to show good combustion control. As compared to the pressure traces for the 20-mm/24-mm/30-mm plastic stepped-wall chamber configuration used in test 63 (Figure 42), the multichamber configurations show similar combustion control, but with lower peak pressures (from about 500 MPa to 400 MPa). Also, the muzzle velocities were very similar. All the P-t traces listed in Figures 41 and 42 were recorded in the CH1 position.

The P-t trace for test number 148 (Figure 41) shows that the use of the 1-3-9 chamber configuration exhibited difficulties in its ability to sustain LP combustion. This is observed by the rapid drop in pressure, seen in the P-t trace, at approximately 0.8 ms.

4.2.3 Rear Coupling. Early in this work, it was apparent that the condition of the rear section of the chamber insert was important to the initial ignition and the efficiency of the LP combustion. To investigate this feature further, some of the attributes of the first-stage section of the multichamber were varied. Length and diameter were increased, and the section was stepped in an attempt to control the ignition.

4.2.3.1 Diameter Changes. Tests 135, 137, and 145 were completed to investigate the effect of diameter changes to the first stage of the multichamber (Figure 43). The basic 1-3-3 configuration was utilized with first-stage diameters of 11.5 mm, 16 mm, and 20 mm. The second-section tube diameters were 13.5 mm and the third-section tube diameters were 16.7 mm each. The equivalent section diameters for the second and third stages were 24 mm and 30 mm, respectively. These diameter increases proved to be important in increasing the overall chamber pressures to a reasonable

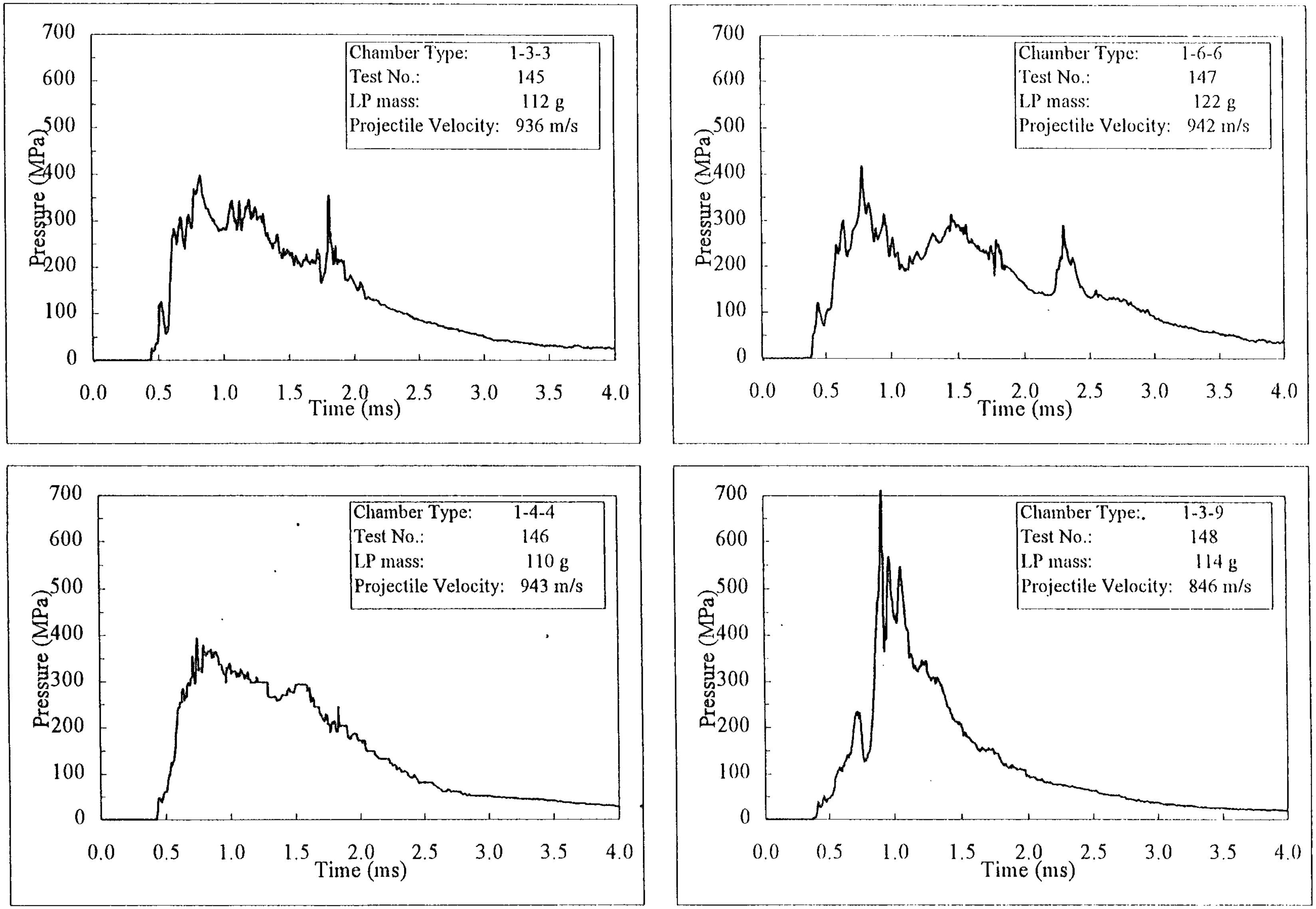

Figure 41. <u>Chamber 1 pressure-time traces for the 1-3-3, 1-4-4, 1-6-6, and 1-3-9 multichamber tests.</u>

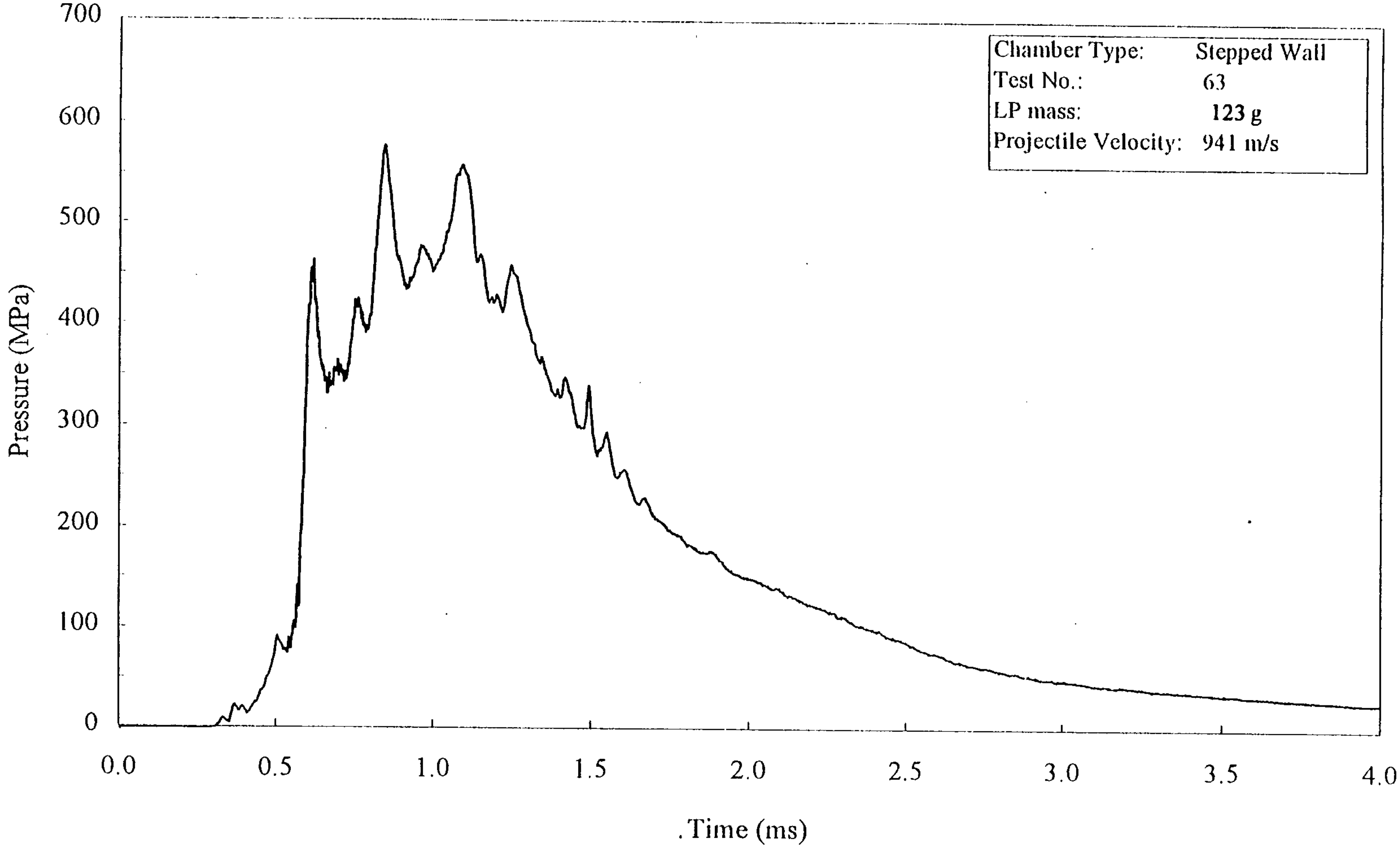

Figure 42. Position 1 chamber pressures generated during the test with the 20/24/30 plastic stepped-wall chamber insert.

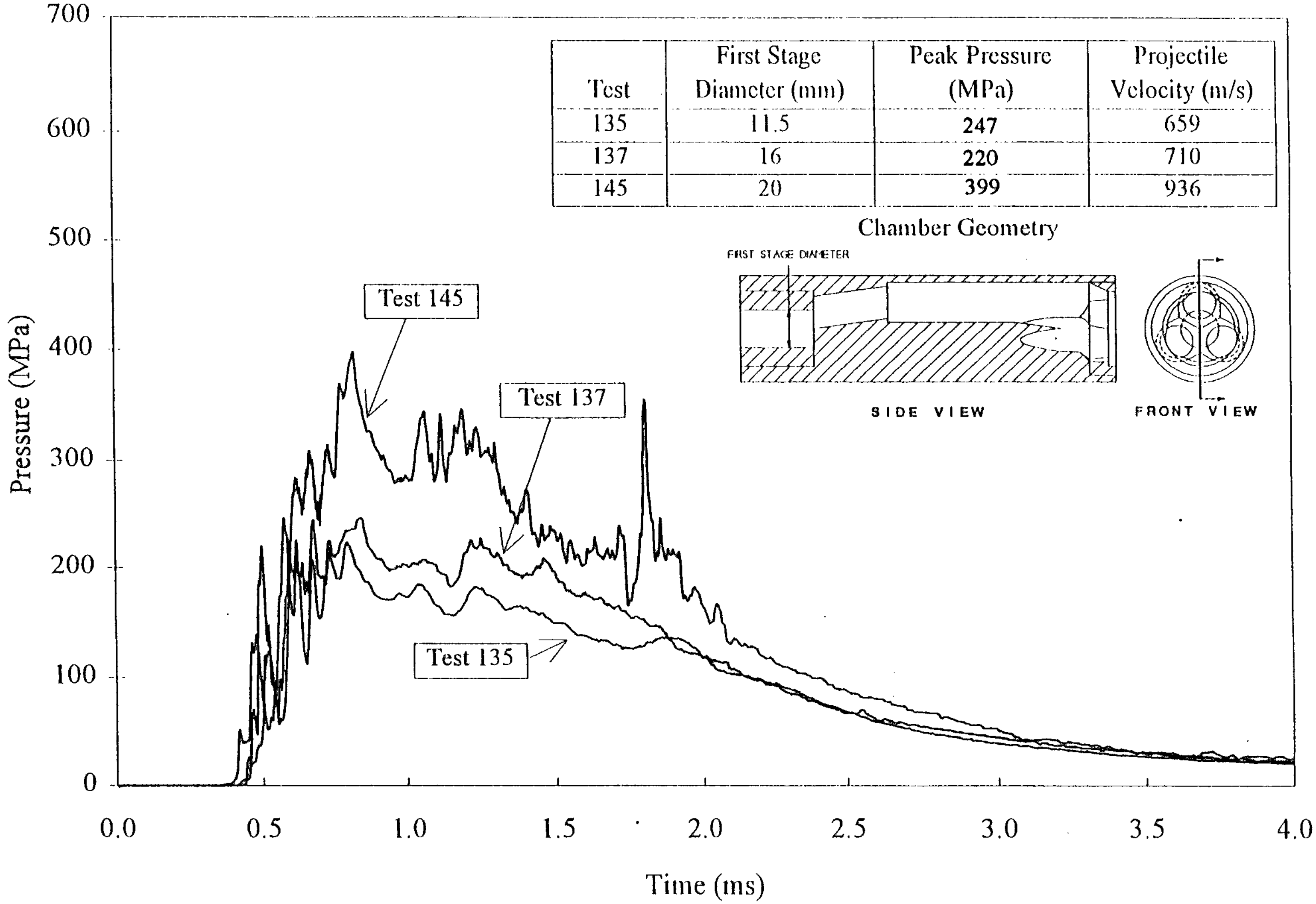

Test	First Stage Diameter (mm)	Peak Pressure (MPa)	Projectile Velocity (m/s)
135	11.5	247	659
137	16	220	710
145	20	399	936

Figure 43. Chamber pressures (position 1) generated when the first-stage diameter of the 1-3-3 multichamber is increased.

operating condition (Figure 43, tests 135, 137, and 145). Reasonable operating pressures were necessary to obtain efficient LP combustion. The increase in the first-stage diameter may have spread the burning and allowed for more ignition of the LP when one tube transitioned into the three tubes.

4.2.3.2 Length Changes. The length of the first-stage section was also varied to investigate its effect on the combustion results. The length was decreased from 30.48 mm in test 135 to 25.4 mm in test 142. Multichamber tests 134–140 and 145–152, inclusive, contained a first-stage section that was 30.48 mm long, while tests 141–146, inclusive, contained a 25.4-mm long first stage. The pressure results of these tests in Figure 44 indicate that the change in the lengths did not significantly affect the pressures generated in the chamber during combustion. The high-pressure spike, which is observed in the chamber pressure position 2, curves for both tests (135 and 142) in Figure 44 and does not appear in any of the other pressure-tap locations during these tests. Since this spike only occurs in the position 2 port, the cause may be attributed to the port itself. Similar pressure spikes in the position 2 location only occurred in most of the 30-mm multichamber test firings.

4.2.4 Extension of Concepts. The 1-3-3 concept performance was extended by combining attributes of the stepped-wall chamber and the multichamber configurations. This concept configuration began using a single first- stage section; this then expanded into a larger second-stage section, and then transitioned into a 19-tubed third-stage section. At the projectile end of the chamber insert, the tubes were feathered with a $10°$ taper to reduce possible cavitation and secondary ignition down the barrel during combustion. The cross-sectional view of each section change and the cut-away side view of this chamber design is shown in Figure 14. In these tests, the projectile was pressed into the forward end of the chamber just as the other multichamber designs.

The 1-1-19 multichamber configuration used in tests 149 to 152 included a single 20-mm diameter first-stage, a 35-mm second-stage, and 19 tubes 5.5 mm in diameter with an additive equivalent diameter of approximately 24 mm. The short second-stage region (from 5 mm to 15.24 mm in length) of this configuration allowed the LP combustion to extend to the farthest of the 19 tubes and, thus, caused early LP initiation to transfer into the 19 tubes. As shown in Figure 45,

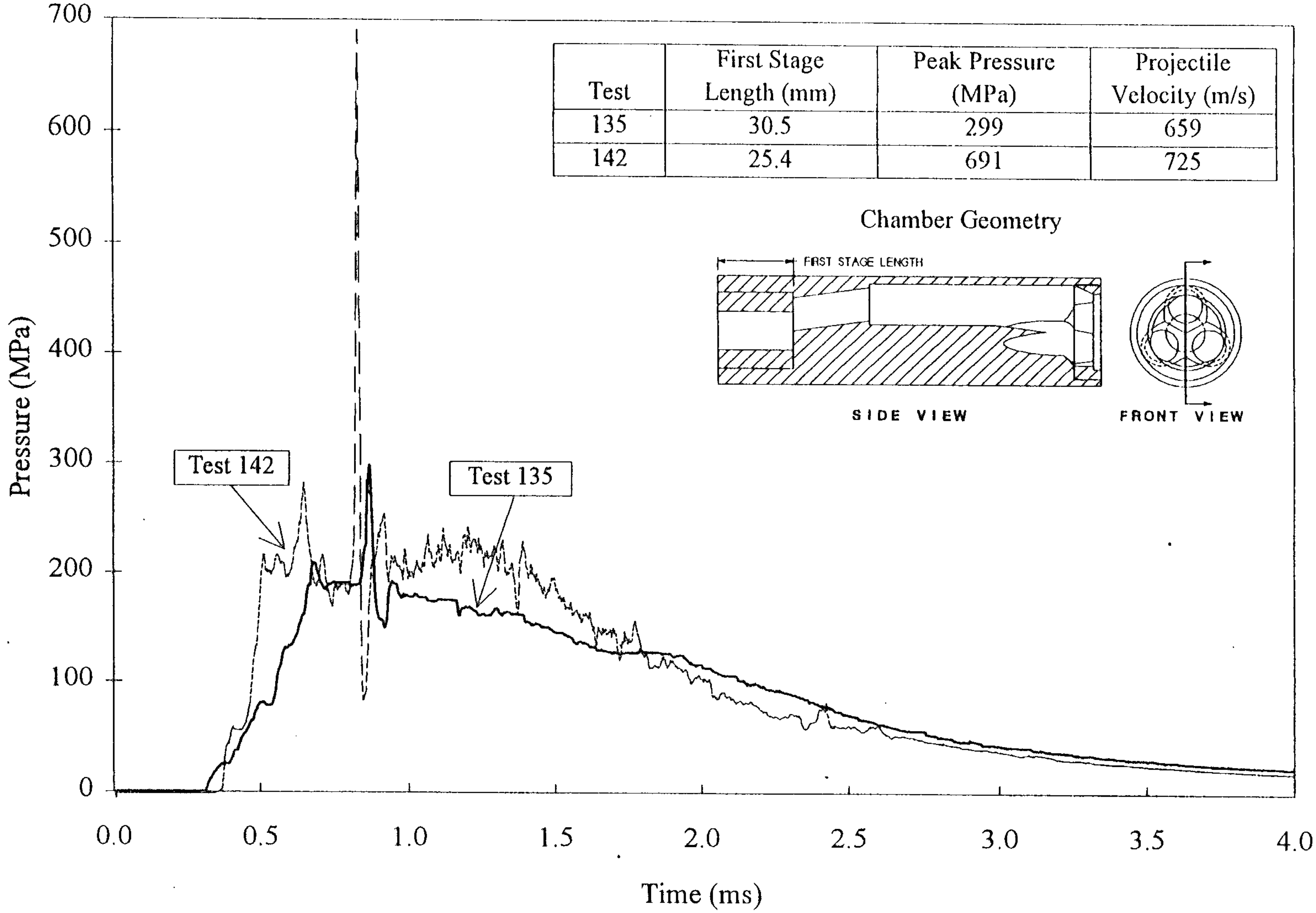

Test	First Stage Length (mm)	Peak Pressure (MPa)	Projectile Velocity (m/s)
135	30.5	299	659
142	25.4	691	725

Figure 44. Effects of changing the first-stage length in the 1-3-3 multichamber configuration (chamber pressure position 2).

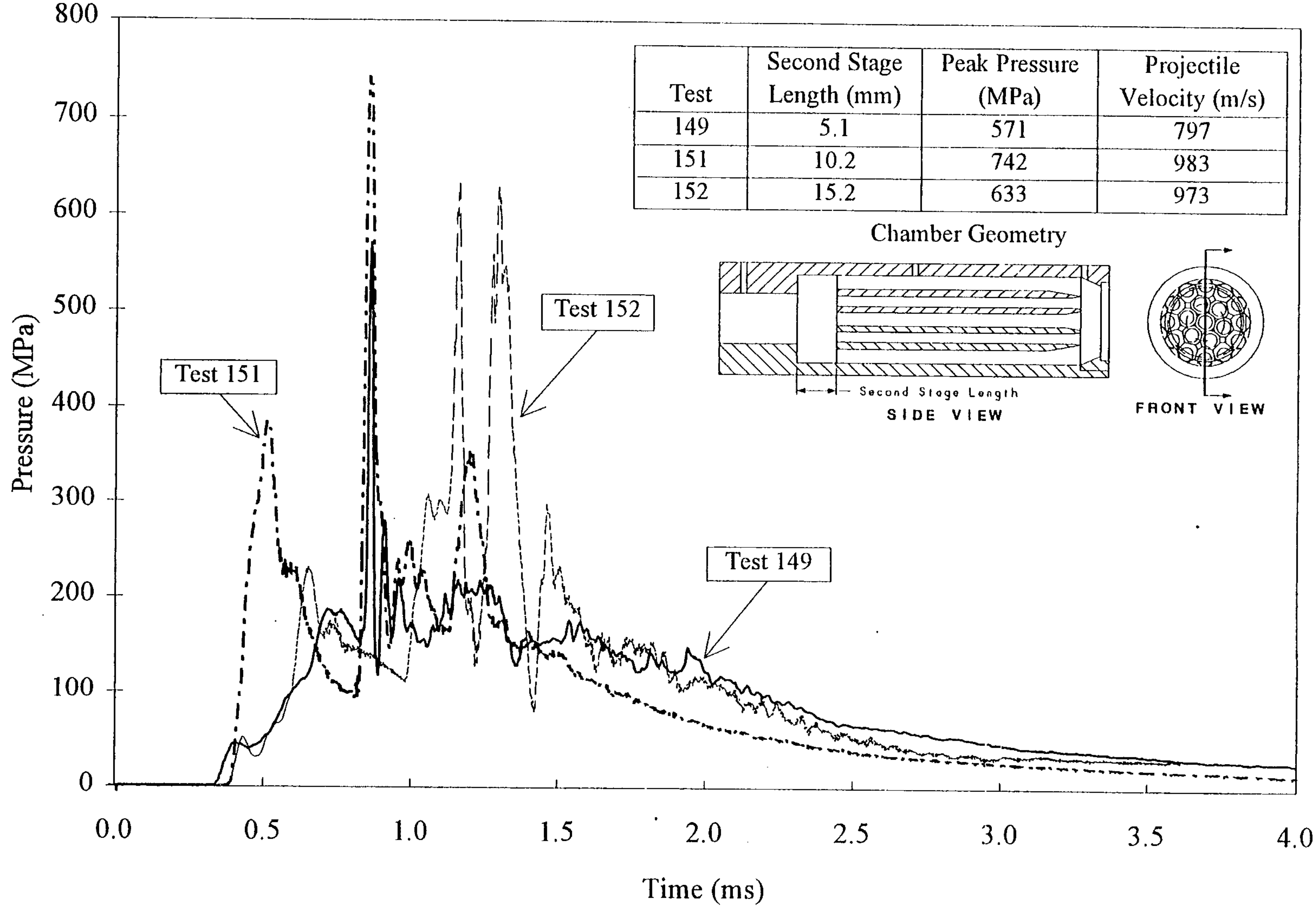

Test	Second Stage Length (mm)	Peak Pressure (MPa)	Projectile Velocity (m/s)
149	5.1	571	797
151	10.2	742	983
152	15.2	633	973

Figure 45. The effects of length changes in the second stage of the 1-1-19 multichamber design (chamber pressure position 2).

the 1-1-19 configuration had a double-humped pressure trace when a 5-mm second-stage was used in the insert design. As the length of the second stage was increased to 10.16 mm in test 151, then to 15.24 mm in test 152, the double-humped pressure curve persisted and increased in magnitude (Figure 45). This 1-1-19 configuration results in many pressure spikes and tends to behave in an unstable manner, but due to the limited amount of testing done with this configuration, it is impossible to make any conclusions about its ability to control combustion.

5. SPURIOUS TEST RESULTS, SOURCES, AND CORRECTIONS

The combustion performance tests in past BLPG systems are replete with alleged spurious and occasional catastrophic high-pressure results that have been attributed to random instabilities and unpredictabilities associated with the dynamic behavior of the LP and gas dynamics during the ballistic cycle. Investigative efforts based on rather extensive testing of bulk-loaded LP test guns at Veritay, including the program reported here, have indicated that ignition-combustion coupling, the use of chamber geometry and boundary constraints, and the reduction/correction of certain configuration details of test guns can all impact the achievement of controlled combustion evolution and behavior in BLPG systems. Particular attention is given in this section to selected configuration details of test guns that were identified as sources of certain, but common, spurious test results.

5.1 <u>Pressure Sealing of Insert Chambers</u>. The 30-mm single-shot modular test gun fixture (Figure 46) was utilized in early firing tests under this program. This modular gun configuration was chosen to facilitate changing the gun chamber geometry without having to rebuild the entire gun or gun chamber for testing each different chamber arrangement. This test gun was originally fitted with a chamber insert consisting of a plastic or steel interior chamber of selected geometry for combustion testing, surrounded by a 17-4 PH steel sleeve, heat-treated to RC 42, that provided added strength and reduced the overall compressibility of the combined insert.

The interior plastic chamber insert was fabricated with an outside diameter that provided a force fit of this insert with the inside of the steel insert sleeve. The outside of this steel sleeve was fabricated undersize by about 0.076 mm (0.003 in) to the inside diameter of the chamber bore in the

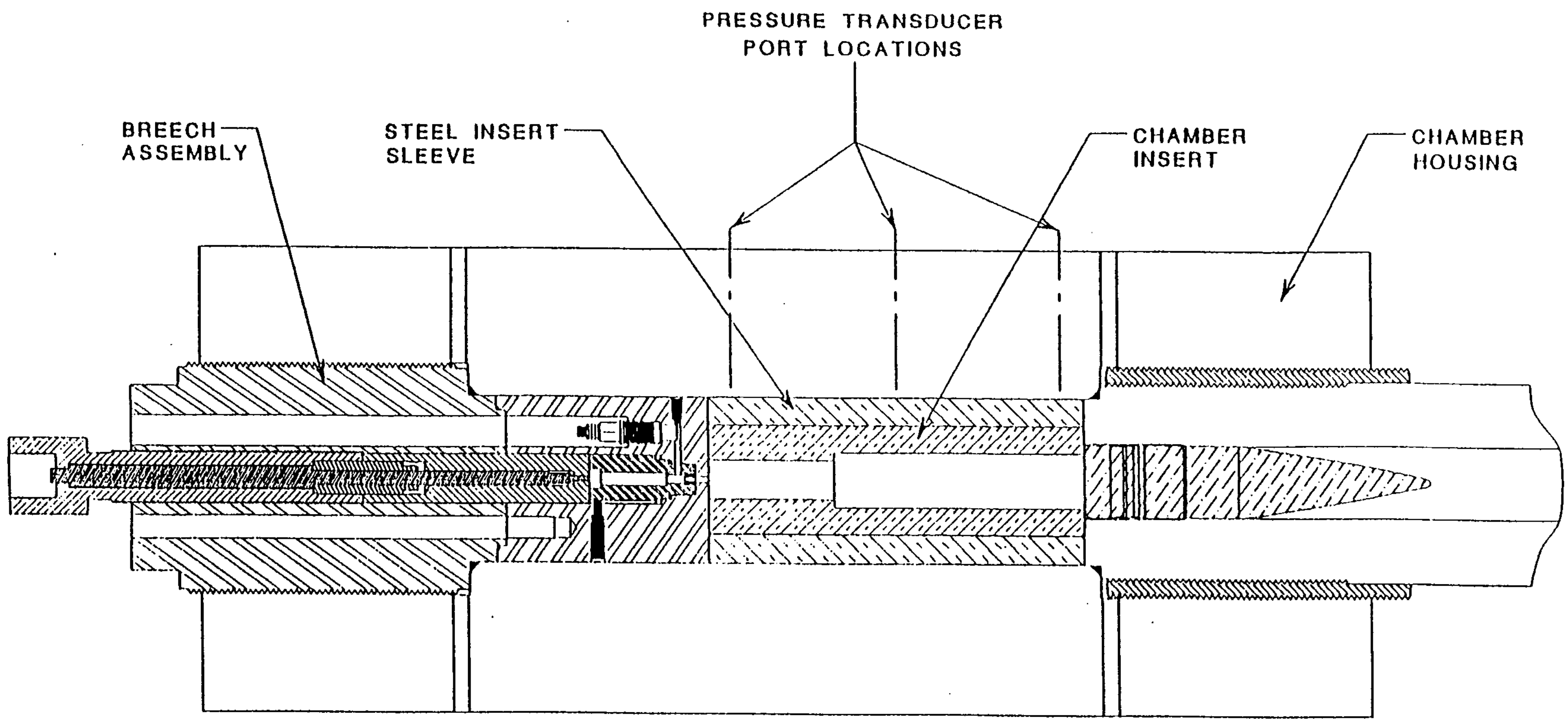

Figure 46. 30-mm single-shot gun fixture used in early tests.

17-4 PH steel chamber housing. This provided clearance for assembly of the overall insert/sleeve chamber unit since it was filled with LP outside the test gun before insertion into the gun. The sleeve-to-chamber clearance region and the transducer ports were coated or filled with silicone grease to fill void spaces between the chamber insert and housing after assembly.

This arrangement did not provide a reliable pressure-tight seal either between the sleeve and chamber housing, or at the ends of the chamber insert (because of longitudinal expansion of the overall chamber housing relative to that of the insert). Further, gas and/or LP leakage around the ends of the chamber insert could sometimes pass radially along the ends of the chamber insert and then along the cylindrical steel-to-steel interface and cause spurious pressure pulses to register on pressure transducers.

A later 30-mm gun test fixture (Figure 17) used a one-piece, heat-treated 17-4 PH steel chamber insert. The ends of the chamber insert were machined perpendicular to the tube axis to provide tight fits against surfaces of similar perpendicularity (at the breech end a plug with pyrotechnic igniter and at the forward end of the base of the barrel). A Viton o-ring at each end of the chamber insert was trapped in corresponding grooves in the mating steel parts and each formed an effective high-pressure seal to contain liquid LP and LP combustion gas during test firings. The pressure transducers were mounted and sealed directly in the steel insert sleeve so that leakage of interface gas or LP was avoided.

Later, these same high-pressure end seals were used in the steel insert sleeve of the early test gun fixture of Figure 46. This arrangement significantly improved the realism of measured P-t traces obtained during a few test firings conducted in the modified early type test gun fixture.

5.2 Reducing Spurious Pressure Pulses. A variety of spurious pressure pulses have been observed in experimental P-t traces associated with a range of test gun chamber configurations and initial test conditions in this project. By using more than one pressure transducer in the gun chamber, it was sometimes possible to identify the nature and/or general region from which selected pulses, especially isolated pulses, arose.

Two general types of regular pulses observed tended to be associated with radial and longitudinal pressure waves moving within the interior medium of the gun chamber, while the latter medium was experiencing a comparatively slow-changing, high, average pressure. In addition, isolated, single pressure pulses of rather short duration were sometimes observed within P-t traces. Each such pulse appeared to arise near the location of the projectile at front of the chamber. This type of pulse may be caused by localized adiabatic ignition of LP in the vicinity of the projectile.

Adiabatic ignition can arise by rapid compression and associated heating of trapped air (and perhaps LP vapor) to very high temperatures in small regions near the base of the projectile. Since the LP itself is the pressure-transfer medium in immediate contact with the trapped air, the necessary conditions of high temperature and pressure for LP ignition can readily by satisfied.

The most likely region where sufficient air could have been trapped near the base of the standard 30-mm GAU-8 projectiles fired under this program was the gap region between the projectile base and barrel and behind the projectile rotating band. This gap region is shown in the unmodified projectile portion of Figure 47.

To eliminate trapped air in this gap region, the group of modifications to the projectile base area considered is shown together in the modified projectile base portion of Figure 47. This modified base region eliminated the airgap by using a plastic sleeve around the base of the projectile aft of the rotating band. To preclude interfering with the rotating band integrity and attachment to the projectile, a small gap was left between the band and the sleeve. The projectile base was machined to a smaller diameter to enable a plastic (Delrin) sleeve of a workable thickness to be force fit over this new diameter. This plastic sleeve was held in place by a steel washer-type plate, slightly smaller in diameter (for clearance) than the lands in the rifled barrel, and this washer was attached to the projectile base by an on-axis bolt (not shown).

In addition, Figure 47 also shows a plastic disk and a plastic hemispherical cap attached to the base of the projectile. These, taken individually or together, were candidates for buffering pressure pulses, which typically arose near the base of the projectile during these test firings.

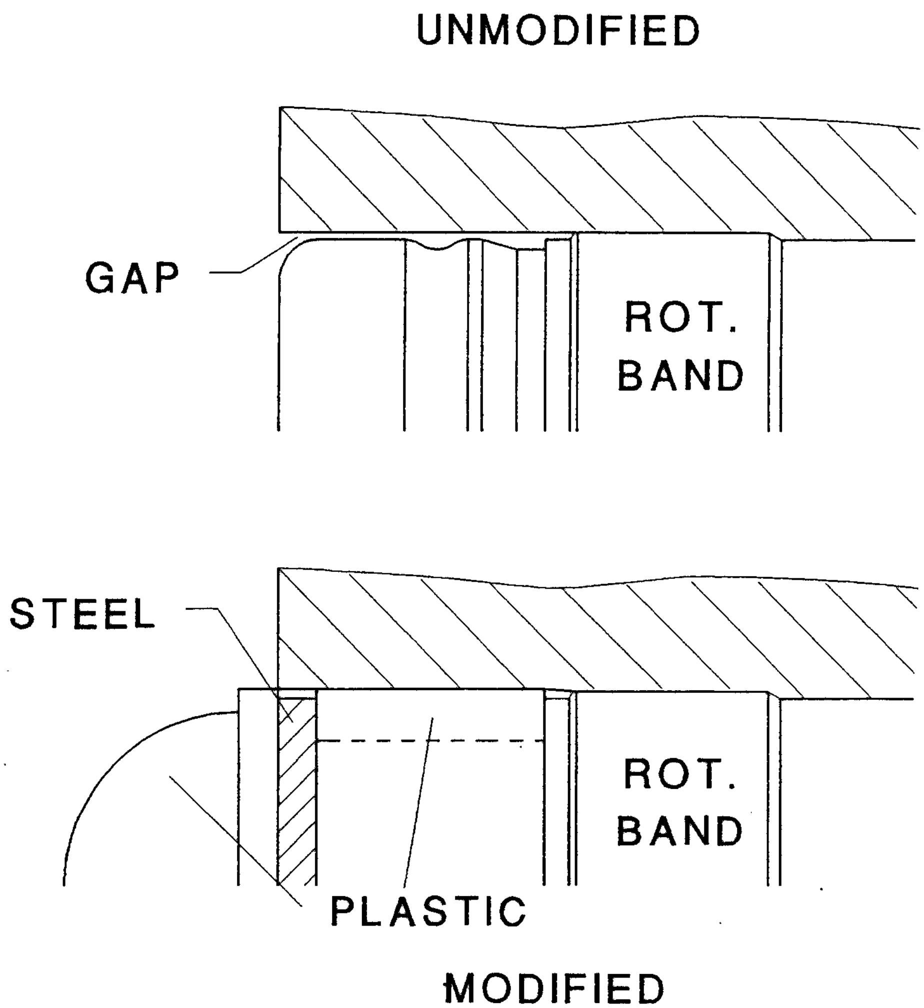

Figure 47. Base of unmodified 30-mm projectile and modified configuration to reduce spurious high-pressure pulses arising from this region.

The first 30-mm gun test using a wave deflector attached to the base of the projectile was test 117. Prior to test 117, the 30-mm gun firings contained pressure pulses that originated near the base of the projectile. This was determined by examining the P-t data, which showed the pulses occurring in the CH3, CH4, and CH5 locations at an earlier time than the CH1 and CH2 locations.

The sequence of projectile gap and base modifications actually fired in tests are shown in Figure 5, together with the standard 30-mm GAU-8 projectile that was the prototype. The results of these tests are not shown in detail in this section, but can readily be summarized.

Each projectile that was fitted with steel (plate or hemisphere) at the base did not give sufficient pulse attenuation to merit further consideration. These included the first, fifth, sixth, and seventh modifications.

The second modification emphasized filling the airgap about the remachined projectile base, as noted previously. This particular base modification failed because the Delrin base structure failed mechanically under the high chamber pressure. The Delrin sleeve part apparently became stuck in or near the rear end of the barrel; the Delrin hemispherical base sheared from the sleeve and followed the projectile down the barrel. The remaining stuck tube of Delrin apparently forced the moving LP into a smaller diameter and then rapidly into a larger diameter. This sudden flow change appeared to cause either cavitation or significant droplet formation of the LP, and in turn, caused a high-pressure combustion pulse to form just inside the barrel. The addition of a steel washer to hold the Delrin sleeve to the projectile base (Figure 5, 3rd modification) in subsequent tests bypassed the low shear strength of the Delrin and alleviated secondary ignition arising in the airgap region using this modified standard projectile.

The fourth modification (Figure 5), which used a flat Delrin base as a pulse buffer, did show some effectiveness, but did not work as well in this role as the hemispherical base used in the third-modification case.

In effect, the Delrin plate or hemisphere, together with the sleeve fastened to the projectile base, tended to eliminate the airgap and secondary ignition and to damp or deflect pressure pulses in the chamber during combustion evolution. These features significantly reduced the magnitude and the occurrence of spurious pressure pulses—usually to tolerable levels.

6. CONCLUSIONS

This experimental program investigated the use of mechanical concepts as a primary means of achieving interior ballistic process control in medium-caliber BLPGs. The overall results of this program indicate that the stepped-wall chamber approach is a useful technique toward achieving such control in medium-caliber BLPGs. In particular, the magnitude of the peak pressure has been shown to be controlled by the diameter and length of the first-stage section (closest to the igniter) of the stepped-wall chamber geometry in combination with the size of the igniter. The peak chamber pressure is relatively independent of the mass of the projectile, and the igniter must be tailored to the system to prevent chamber overpressures as a result of over or under ignition.

The findings to date have also shown that the multichamber concept for such process control can be useful, but further exploration of its effectiveness needs to be completed using steel chambers to confirm its utility for potential BLPG applications. In addition, the combining of a stepped-wall chamber geometry with a three, four, or more subchamber may have the potential for scaling BLPGs to sizes larger than medium-caliber, while maintaining control of the interior ballistic process by an extension of the mechanical concepts explored under this program.

This effort has demonstrated that plastic, stepped-wall chamber inserts can be used effectively to explore combustion phenomena in a BLPG system, and many of the findings can be effectively transitioned into a corresponding, mostly steel chamber geometry. However, the phenomena leading to combustion control must be demonstrated in an all-steel chamber.

This study has confirmed that LP ignition and early combustion stability in a mostly steel, stepped-wall chamber can be achieved by proper selection of the booster load for an appropriately sized first- section chamber element of the overall chamber.

A useful degree of reproducible combustion and interior ballistic behavior has been achieved in BLPG test fixtures using steel-wall chambers with a first-stage section that contains a thin-walled (~1 mm) plastic liner, even though the test gun system was not optimized. The peak-pressure values for one such reproducibility set of firings indicated unbiased standard deviations in peak pressures of 5.3% and in muzzle velocities of 1.2%.

Changing the 99-g "standard" mass of a 20-mm target practice bullet from an M55-A2 round over the range of charge-to-projectile mass ratios from 0.1 to 0.6 did not greatly influence the corresponding peak chamber pressures. The duration of chamber pressures near the peak values increased significantly as the projectile masses increased.

A range of 30-mm projectile muzzle velocities was achieved by properly selecting corresponding stepped-wall chamber geometries and propellant charge-to-projectile mass ratios without significantly altering peak chamber pressures.

It was observed that the efficacy of LP XM46 ignition in the 30-mm test gun appeared to be influenced by the radiative interaction nature of the chamber wall in the region of earliest growth in the ignition kernel.

INTENTIONALLY LEFT BLANK.

7. REFERENCES

1. Morrison, W. F., J. D. Knapton, and M. J. Bulman. "Liquid Propellant Guns." Gun Propulsion Technology, edited by L. Stiefel, vol. 109, Progress in Astronautics and Aeronautics, AIAA, Washington, DC, pp. 413–471, 1988.

2. Comer, R. H., R. H. Shearer, and R. N. Jones. "Interior Ballistics of Liquid Propellant Guns." BRL-TR-1205, U.S. Army Ballistic Research Laboratory, Aberdeen Proving Ground, MD, May 1963.

3. Knapton, J. D., J. DeSpirito, T. E. Rosenberger, I. C. Stobie, R. L. Talley, and J. A. Owczarczak. "Correlation of Igniter Output to Early Combustion Chamber Pressure Rise in Bulk Loaded Liquid Propellant Guns." Proceedings of the 32nd JANNAF Combustion Subcommittee Meeting, Update: CPIA Publication 631, vol. I, October 1995.

4. Elmore, L. C. "Final Technical Report for Phase I Effort on a High Performance Medium Caliber Liquid Propellant Anti-Armor Gun System." Pulsepower Systems Inc., Report TRID4, NWC Contract N00123-73-C-1982, December 1974.

5. Sterbutzel, G., and E. B. Fisher. "Investigation of Ignition/Combustion Phenomena in a 30-mm Liquid Monopropellant Gun." Final Report, April 1975 - October 1976, CALSPAN Report KB-6002-X1, NWC Contract N00123-75-C-1520, December 1976.

6. Talley, R. L., and A. Bracuti. "Diagnostics of Ignition-Combustion Coupling in a Liquid-Propellant Gun." Contractor Report: Veritay Technology A10-02-90, U.S. Army Armament Research, Development and Engineering Center, Picatinny Arsenal, NJ, August 1990.

7. Talley, R. L. "Diagnostics of Combustion Evolution in a Bulk-Loaded LP Gun." Proceedings of the 27th Combustion Subcommittee Meeting, Update: CPIA Publication 557, vol I, pp. 461–471, November 1990.

8. Talley, R. L., J. A. Owczarczak, and A. Bracuti. "Ballistic Testing of Liquid Propellant in a Bulk-Loaded Gun with Combustion Control Features." Veritay Report C90-001, U.S. Army Armament Research, Development, and Engineering Center, Picatinny Arsenal, NJ, September 1991.

9. Talley, R. L., J. A. Owczarczak, and A. Bracuti. "Ballistic Testing of Liquid Propellant in a Bulk-Loaded Gun with Combustion Control Features: II." Veritay Report D07-001, U.S. Army Armament Research, Development, and Engineering Center, Picatinny Arsenal, NJ, November 1992.

10. Owczarczak, J. A., and R. L. Talley. "Interior and Exterior Testing of Bulk-Loaded Propellant in a 40-mm Gun." Veritay Report D32-001, U.S. Army Armament Research, Development, and Engineering Center, Picatinny Arsenal, NJ, August 1994.

11. Talley, R. L., J. A. Owczarczak, and M. Geise. "Interior and Exterior Ballistic Testing of Bulk-Loaded Liquid Propellant in a 40-mm Gun." Veritay Report D48-95-001, U.S. Army Armament Research, Development, and Engineering Center, Picatinny Arsenal, NJ, September 1995.

12. Talley, R. L., and J. A. Owczarczak. "Investigation of Bulk-Loaded Liquid Propellant Gun Concepts." ARL-CR-127, U.S. Army Research Laboratory, Aberdeen Proving Ground, MD, April 1994 (Contract No. DAAA15-92-C-0018).

13. Talley, R. L. "Interior Ballistic Process Control Using Mechanical Concepts in Medium Caliber Bulk Loaded LP Guns." Proceedings of the 31st JANNAF Combustion Subcommittee Meeting, Update: CPIA Publication 620, vol. I, pp. 303–312, October 1994.

14. Talley, R. L. "Exploration of Mechanical Concepts to Achieve Interior Ballistic Process Control in Bulk-Loaded Liquid Propellant Guns." Proceedings of the 32nd JANNAF Combustion Subcommittee Meeting, Update: CPIA Publication 631, vol. I, October 1995.

15. Puckett, L. C. "Combustion Sub-Channels for Bulk Loaded Liquid." U.S. Patent 4,936,188, June 26, 1990.

16. Rosenberger, T. E., I. C. Stobie, and J. D. Knapton. "Test Results From a 37-mm Segmented-Chamber Bulk-Loaded Liquid Propellant Gun." ARL-TR-871, U.S. Army Research Laboratory, Aberdeen Proving Ground, MD, September 1995.

17. Rosenberger, T. E., I. C. Stobie, and J. D. Knapton. "Test Results From a 30-mm Segmented-Chamber Bulk Loaded Liquid Propellant Gun." Proceedings of the 32nd JANNAF Combustion Subcommittee Meeting, Update: CPIA Publication 631, vol. I, October 1995.

18. Talley, R. L., and J. A. Owczarczak. "Ignition of High-Energy Density Charges—Liquid Propellant." Veritay Final Report, Contract No. DAAA21-93-C-0061, Picatinny Arsenal, NJ, June 1995.

19. Hercules Inc. "Physical and Chemical Data of Hercules Canister Powders." (Data Sheet), Hercules Plaza, Wilmington, DE, 1992.

APPENDIX:

RESULTS OF THE 20-mm AND 30-mm TEST FIRINGS

INTENTIONALLY LEFT BLANK.

TEST #	TEST DATE	FIXTURE NUMBER	CHAMBER TYPE	LP VOLUME (cc)	LP MASS (g)	LP TEMP. (C)	BOOSTER TYPE	BOOSTER MASS (g)	BOOST. HOUSING CAPACITY (cc)	LOAD DENSITY (g/cc)	ORIFICE DIAMETER (mm)	PROJECTILE TYPE	PROJECTILE MASS
1	6/29/93	C90-001	I, PLASTIC	29.5	42.243	22	UNIQUE	0.335	0.69	0.486	1.32	M55A2TP	98.9
2	6/30/93	C90-001	I, PLASTIC	29.14	40.8	20	UNIQUE	0.389	0.69	0.564	1.32	M55A2TP	97.8
3	6/30/93	C90-001	I, PLASTIC	28.67	41	21	UNIQUE	0.42	0.69	0.609	1.32	M55A2TP	99
4	7/1/93	C90-001	I, PLASTIC	28.04	40.1	20	UNIQUE	0.335	0.69	0.486	1.51	M55A2TP	99
5	7/20/93	C90-001	I, PLASTIC	28.88	41.3	25	UNIQUE	0.335	0.69	0.486	1.51	M55A2TP	98.5
6	7/21/93	C90-001	I, PLASTIC	29.1	41.6	23	UNIQUE	0.39	0.69	0.565	1.51	M55A2TP	98.7
7	7/21/93	C90-001	I, PLASTIC	28.7	41	24	UNIQUE	0.418	0.69	0.606	1.51	M55A2TP	99
8	7/22/93	C90-001	I, PLASTIC	28.04	40.1	24	UNIQUE	0.335	0.69	0.486	1.7	M55A2TP	98.9
9	7/27/93	C90-001	H, PLASTIC	26.99	38.6	24	UNIQUE	0.335	0.69	0.486	1.32	M55A2TP	99
10	7/25/93	C90-001	H, PLASTIC	26.72	38.22	24	UNIQUE	0.419	0.69	0.607	1.32	M55A2TP	98.7
11	7/28/93	C90-001	H, PLASTIC	26.92	38.5	25	UNIQUE	0.335	0.69	0.486	1.7	M55A2TP	98.9
12	7/28/93	C90-001	I, PLASTIC	28.77	41.15	24	UNIQUE	0.335	0.69	0.486	1.32	67 GRAM MOD	65.653
13	7/29/93	C90-001	I, PLASTIC	28.81	41.2	24	UNIQUE	0.335	0.69	0.486	1.32	200 GRAM MOD	199.333
14	7/30/93	C90-001	I, PLASTIC	29.88	41.3	24	UNIQUE	0.335	0.69	0.486	1.32	100 GRAM MOD	96.778
15	8/2/93	C90-001	H, PLASTIC	26.71	38.2		UNIQUE	0.335	0.69	0.486	1.32	67 GRAM MOD	65.694
16	8/3/93	C90-001	H, PLASTIC	26.92	38.5	25	UNIQUE	0.335	0.69	0.486	1.32	200 GRAM MOD	107.879
17	8/4/93	C90-001	H, PLASTIC	26.85	38.4	24	UNIQUE	0.335	0.69	0.486	1.7	M55A2TP	98.570
18	8/5/93	C90-001	H, PLASTIC	27.06	38.7	23	UNIQUE	0.335	0.69	0.486	1.7	M55A2TP	98.945
19	8/5/93	C90-001	H, PLASTIC	27.06	38.7	23	UNIQUE	0.335	0.69	0.486	1.7	M55A2TP	99.028
20	8/18/93	C90-001	H, PLASTIC	26.62	38.07	24	UNIQUE	0.335	0.69	0.486	1.7	M55A2TP	98.668
21	8/19/93	C90-001	H, PLASTIC	26.67	38.135	24	UNIQUE	0.335	0.69	0.486	1.7	M55A2TP	98.766
22	8/19/93	C90-001	H, PLASTIC	26.136	37.375	24	UNIQUE	0.335	0.69	0.486	1.7	M55A2TP	98.758
23	8/23/93	C90-001	I, PLASTIC	28.95	41.4		UNIQUE	0.42	0.69	0.609	1.32	67 GRAM MOD	65.36
24	8/23/93	C90-001	I, PLASTIC	28.84	41.24	24	UNIQUE	0.42	0.69	0.609	1.32	200 GRAM MOD	198.8
25	8/24/93	C90-001	I, PLASTIC	27.797	39.75	24	UNIQUE	0.335	0.69	0.486	1.7	67 GRAM MOD	66.086
26	8/24/93	C90-001	I, PLASTIC	28.02	40.069	24	UNIQUE	0.335	0.69	0.486	1.7	200 GRAM MOD	198.809
27	8/25/93	C90-001	H, PLASTIC	29.371	42	24	UNIQUE	0.335	0.69	0.486	1.7	67 GRAM MOD	65.716
28	8/25/93	C90-001	H, PLASTIC	26.538	37.59	24	UNIQUE	0.335	0.69	0.486	1.7	200 GRAM MOD	199.041
29	8/27/93	C90-001	H, PLASTIC	26.48	37.87	24	UNIQUE	0.42	0.69	0.609	1.32	67 GRAM MOD	66.506
30	8/30/93	C90-001	H, PLASTIC	26.92	38.5		UNIQUE	0.42	0.69	0.609	1.32	200 GRAM MOD	199.183
31	9/14/93	C90-001	I, PLASTIC	28.74	41.1	24	UNIQUE	0.335	0.69	0.486	1.32	M55A2TP	98.5
32	9/15/93	C90-001	I, PLASTIC	28.39	40.6	24	UNIQUE	0.335	0.69	0.486	1.51	M55A2TP	98.3
33	9/15/93	C90-001	H, PLASTIC	26.64	38.1	23	UNIQUE	0.42	0.69	0.609	1.32	200 GRAM MOD	198.4
34	9/28/93	C90-001	H, PLASTIC	26.54	37.95	23	UNIQUE	0.335	0.69	0.486	1.7	250 GRAM MOD	245.3
35	9/28/93	C90-001	H, PLASTIC				UNIQUE	0.335	0.69	0.486	1.7	300 GRAM MOD	294.5
36	9/29/93	C90-001	H, PLASTIC	26.47	38.85	23	UNIQUE	0.335	0.69	0.486	1.7	300 GRAM MOD	297.3
37	9/27/93	C90-001	H, PLASTIC	26.78	38.3	22	UNIQUE	0.335	0.69	0.486	1.7	350 GRAM MOD	342.9
38	9/30/93	C90-001	H, PLASTIC	26.66	38.13	23	UNIQUE	0.335	0.69	0.486	1.7	376 GRAM MOD	370.75
39.1	10/28/93	C90-001	H, PLASTIC	26.42	37.78	21	UNIQUE	0.335	0.69	0.486	1.7	M55A2TP	98.5
39	10/29/93	C90-001	B17-A, PLASTIC	10.01	14.32	22	UNIQUE	0.335	0.574	0.584	1.32	M55A2TP	98.93
40	11/2/93	C90-001	B17-A, PLASTIC	10.01	14.32	22	UNIQUE	0.335	0.574	0.584	1.32	M55A2TP	97.2
41	11/2/93	C90-001	B17-A, STEEL	10.13	14.48	22	UNIQUE	0.3	0.574	0.523	1.32	M55A2TP	98.5
42	11/3/93	C90-001	B17-A, STEEL	10.39	14.86	22	2400	0.3	0.574	0.523	1.32	M55A2TP	99
43	11/3/93	C90-001	B17-A, STEEL	10.21	14.6	22	UNIQUE	0.27	0.574	0.470	1.32	M55A2TP	99.8
44	11/4/93	C90-001	B17-A, STEEL	10.19	14.57	22	UNIQUE	0.24	0.574	0.418	1.32	M55A2TP	99
45	11/5/93	C90-001	B17-B, STEEL	5.3	7.58	23	UNIQUE	0.24	0.574	0.418	1.32	M55A2TP	98.8
46	11/9/93	C90-001	B17-B, STEEL	5.07	7.25	22	UNIQUE	0.24	0.574	0.418	1.32	M55A2TP	98.73
47	11/10/93	C90-001	B17-B, STEEL	5.34	7.64	23	UNIQUE	0.24	0.574	0.418	1.32	M55A2TP	99
48	11/11/93	C90-001	B17-C, STEEL	17.29	24.72	22	UNIQUE	0.24	0.574	0.418	1.32	M55A2TP	98.9
49	11/11/93	C90-001	B17-D, STEEL	11.89	17	22	UNIQUE	0.24	0.574	0.418	1.32	M55A2TP	98.8
50	11/12/93	C90-001	B17-E, STEEL	10.1	14.45	22	UNIQUE	0.24	0.574	0.418	1.32	M55A2TP	98.35
51	11/16/93	C90-001	B17-F, STEEL	16.5	23.6	23	UNIQUE	0.24	0.574	0.418	1.32	M55A2TP	98.05
52	11/19/93	C90-001	B17-G, STEEL	15.07	21.55	23	UNIQUE	0.24	0.574	0.418	1.32	M55A2TP	98.55
53	11/19/93	C90-001	B17-G, STEEL	14.93	21.35	23	UNIQUE	0.24	0.574	0.418	1.32	M55A2TP	98.45
54	11/30/93	C90-001	B17-J, STEEL	14.36	20.53	22	UNIQUE	0.24	0.574	0.418	1.32	M55A2TP	98.81
55	12/1/93	C90-001	B17-K, STEEL	15.5	22.182	23	UNIQUE	0.24	0.574	0.418	1.32	M55A2TP	98.67
56	1/4/94	C90-001	B17-K, STEEL	15.93	22.8	23	UNIQUE	0.15	0.31	0.484	1.32	M55A2TP	98.628
58	1/10/94	C90-001	B17-K, STEEL	15.84	22.65	23	UNIQUE	0.145	0.25	0.580	1.32	M55A2TP	98.71
59	1/11/94	C90-001	B17-K, STEEL	15.67	22.405	23	UNIQUE	0.108	0.25	0.432	1.32	M55A2TP	98.75
61	1/18/94	C90-001	B17-L, STEEL	14.41	22.04	22	UNIQUE	0.145	0.25	0.580	1.32	M55A2TP	98.45

* All tests used XM46 monopropellant, a CCI-400 percussion primer and an axial booster housing

Figure A-1. Initial parameters - 20-mm test firings.

TEST #	BOOSTER PRESSURE (MPa)	CHAMBER PRESSURE 1 (MPa)	CHAMBER PRESSURE 2 (MPa)	CHAMBER PRESSURE 3 (MPa)	CHAMBER PRESSURE 4 (MPa)	BARREL PRESSURE 1 (MPa)	BARREL PRESSURE 2 (MPa)	MUZZLE PRESSURE (MPa)	IGNITION DELAY (ms)	ACTION TIME (ms)	VELOCITY (m/s)
1	354	433	411	672	n/d		114	19	.152	2 466	n/d
2	479	357	359	405	n/d	259	92	16	.260	2 620	n/d
3	370	429	418	494	n/d	294	99	18	248	2 500	929
4	n/d	302	n/d	n/d	n/d	n/d	n/d	n/d	.132	n/d	841
5	330	n/d	n/d	n/d	n/d	274	86	77	n/d	n/d	914
6	364	474	345	531	n/d	309	94	20	n/d	n/d	929
7	538	425	450	602	n/d	335	107	18	n/d	n/d	917
8	n/d	491	n/d	n/d	n/d	n/d	n/d	n/d	n/d	n/d	1037
9	485	682	651	694	n/d	356	99	19	n/d	n/d	1056
10	478	452	324	479	n/d	197	81	15	n/d	n/d	810
11	376	304	305	362	n/d	n/d	111	18	n/d	n/d	885
12	388	478	406	398	n/d	226	89	16	n/d	n/d	1002
13	435	493	428	469	n/d	432	155	23	n/d	n/d	770
14	481	364	349	385	n/d	245	97	15	n/d	n/d	863
15	448	348	468	449	n/d	205	66	16	n/d	n/d	947
16	422	594	575	552	n/d	394	n/d	22	n/d	n/d	761
17	n/d	n/d	n/d	n/d	n/d	263	106	16	n/d	n/d	870 4
18	433	328	325	417	n/d	334	151	19	n/d	n/d	946 1
19	463	336	357	413	n/d	233	109	17	n/d	n/d	870 5
20	486	322	320	438	n/d	242	118	23	n/d	n/d	918 9
21	462	315	540	452	n/d	207	103	18	n/d	n/d	836 6
22	428	3314	370	500	n/d	225	109	20	n/d	n/d	873
23	621	523	366	466	n/d	228	102	16	.427	2 382	989
24	556	548	493	701	n/d	419	161	25	302	2 788	787
25	422	406	397	448	n/d	342	133	22	.433	2 233	1110 4
26	467	498	489	491	n/d	424	170	26	.398	2 913	773 2
27	405	391	316	315	n/d	225	101	16	.447	2 452	988
28	409	435	341	379	n/d	359	163	25	507	3 264	736 9
29	375	383	547	479	n/d	234	104	17	546	2 499	992 8
30	526	525	485	663	n/d	426	168	22	.299	2.858	n/d
31	389	364	355	n/d	n/d	n/d	128	17	.239	2 671	888 5
32	389	452	458	514	n/d	401	107	17	.324	2 3624	917 5
33	536	314	421	303	n/d	290	141	27	.217	3 514	645 87
34	319	497	351	388	n/d	320	151	30	.605	3.748	642 6
35	n/d	n/d	n/d	n/d	n/d	n/d	n/d	n/d	n/d	n/d	633 6
36	520	411	377	543	n/d	394	169	27	.402	3.748	603 5
37	417	453	376	566	n/d	360	178	27	.421	3 905	570 7
38	443	363	479	355	n/d	366	175	29	.554	4.187	553 9
39.1	533	881	888	883	n/d	534	133	18	.396	2.180	1017
39	n/d	453	406	n/d	n/d	137	33	4	.344	3 311	572
40	588	349	272	351	n/d	140	29	4	.377	3 537	544
41	622	882	887	773	n/d	145	38	5	.321	3 045	604
42	571	882	887	881	n/d	168	41	4	.913	3.124	701
43	512	n/d	882	528	n/d	152	30	4	.562	3 233	598
44	486	882	888	884	n/d	199	51	6	.458	2 733	713 9
45	356	882	733	791	n/d	86	21	n/d	.483	n/d	495
46	344	494	387	522	n/d	102	23	n/d	.393	n/d	475
47	405	882	887	882	n/d	86	22	14	.458	n/d	508 9
48	361	598	498	883	n/d	258	53	9	.640	2 083	723 9
49	415	610	604	590	n/d	175	46	8	.489	1 905	595
50	407	600	614	650	n/d	159	388	5	.464	3 311	631
51	407	572	512	512	n/d	196	49	7	.430	1.288	650
52	375	881	600	883	n/d	396	73	10	.633	2 811	827
53	409	471	375	556	n/d	195	48	4	408	n/d	875
54	418	881	604	753	n/d	376	62	21	.430	2 167	816
55	448	799	615	774	n/d	178	43	7	468	3 170	630
56	550	598	545	883	n/d	235	39	9	.349	3 124	604
58	417	611	463	618	n/d	219	76	11	10 12	12.587	698
59	579	878	824	877	n/d	282	88	16	9 667	11.650	819
61	787	871	875	n/d	n/d	234	57	4	17.13	17 42	778 5

n/d=data not acquired because of data acquisition malfunction, setup error, or plugged pressure port a/w=data was not obtained because the event occurred after the 64ms data acquisition window.

Figure A-2. Results - 20-mm stepped-wall test firings.

TEST #	TEST DATE	FIXTURE NUMBER	CHAMBER TYPE	LP VOLUME (cc)	LP MASS (g)	LP TEMP. (C)	BOOSTER TYPE	BOOSTER MASS (g)	BOOST. HOUSING CAPACITY (cc)	LOAD DENSITY (g/cc)	ORIFICE DIAMETER (mm)	PROJECTILE TYPE	PROJECTILE MASS
57	1/6/94	B17-ASSY	AAA 100 pl, AAA	52.2	74.71	23	UNIQUE	0.626	1.1	0.569	2.18	30MM GAU8	377.3
60	1/12/94	B17-ASSY	AAA 100%pl, AAA	52.44	74.985	23	UNIQUE	0.5	1.1	0.455	2.18	30MM GAU8	376.8
62	1/20/94	B17-ASSY	AAB 100%pl, AAB	70.6	100.957	22	UNIQUE	0.5	1.1	0.455	1.32	30MM GAU8	377.6
63	1/25/94	B17-ASSY	AAC 100%pl, AAC	86.4	123.603	23	UNIQUE	0.5	1.1	0.455	1.32	30MM GAU8	377.2
64	1/31/49	B17-ASSY	AAD 100%pl, AAD	90.31	129.143	22	UNIQUE	0.5	1.1	0.455	1.32	30MM GAU8	377.5
65	3/7/94	B17-ASSY	AAB 75%pl/25%st, B17-701p/701s	77.03	103	23	UNIQUE	0.5	1.1	0.455	1.32	30MM GAU8	378.0
66	3/8/94	B17-ASSY	AAB 75%pl/25%st, B17-701p/701s	70.6	101	22	UNIQUE	0.5	1.1	0.455	1.32	30MM GAU8	377.0
67	3/9/94	B17-ASSY	AAB 50%pl/50%st, B17-702p/702s	70.6	101	22	UNIQUE	0.5	1.1	0.455	1.32	30MM GAU8	378.0
68	3/21/94	B17-ASSY	AAB 50%pl/50%st, B17-702p/702s	71.3	102	23	UNIQUE	0.315	1.1	0.286	1.32	30MM GAU8	379.5
69	3/29/94	B17-ASSY	AAB-1 50%pl/50%st, B17-702p/702s1			23	UNIQUE	0.315	1.1	0.286	1.32	30MM GAU8	368.0
70	5/24/94	B17-ASSY	AAA 100%pl, AAA	54	77.5	22.5	HC-33 #82	0.751	1.1	0.683	1.32	30MM GAU8	369.75
71	5/24/94	B17-ASSY	AAA 100%pl, AAA	52	73	23	HC-33 #82	0.912	1.1	0.829	1.32	30MM GAU8	370
72	5/26/94	B17 ASSY	AAB-2 100%pl, AAB-2	70.6	101	23	HC-33 #82	0.905	1.1	0.823	1.32	30MM GAU8	370
73	5/27/94	B17-ASSY	AAB-2 100%pl, AAB-2		101.5		HC-33 #82	0.896	1.1	0.815	1.32	30MM GAU8	377
74	5/31/94	B17-ASSY	AAB-2 100%pl, AAB-2	70.6	101	23	HC-33 #82	0.891	1.1	0.810	1.32	30MM GAU8	376.0
75	6/10/94	B17-ASSY	AAB-2 100%pl, AAB-2	70	100	23	UNIQUE	0.5	1.1	0.455	1.32	30MM GAU8	376
76	6/13/94	B17-ASSY	AAB-2 100%pl, AAB-2	71	101.5	23	UNIQUE	0.5	1.1	0.455	1.32	30MM GAU8	376
77	6/14/94	B17-ASSY	AAD-1 100%pl, AAD-1	89	127	23	UNIQUE	0.5	1.1	0.455	1.32	30MM GAU8	383
78	6/15/94	B17-ASSY	AAD-1 100%pl, AAD-1	91	130	23	UNIQUE	0.5	1.1	0.455	1.32	30MM GAU8	379.5
79	6/30/94	B17-ASSY	AAB-1 50%pl/50%st, B17-702p/702s1	154	107.5	23	UNIQUE	0.5	1.1	0.455	1.32	30MM GAU8	379
80	7/6/94	B17-ASSY	AAB-1 25%pl/75%st, B17-0002-1	64	92	23	UNIQUE	0.5	1.1	0.455	1.32	30mm GAU8	381
81	7/18/94	B17-ASSY	AAB-1 25%pl/75%st, B17-0002-1	65	93	23	UNIQUE	0.5	1.1	0.455	1.32	30mm GAU8	370
82	7/18/94	B17-ASSY	AAB-1 50%pl/50%st, B17-702p/702s1	65.7	94	23	UNIQUE	0.5	1.1	0.455	1.32	30mm GAU8	366
83	7/18/94	B17-ASSY	AAB-1 25%pl/75%st, B17-0002-2	64	92	23	UNIQUE	0.5	1.1	0.455	1.32	30mm GAU8	368
84	7/20/94	B17-ASSY	AAB-1 25%pl/75%st, B17-0002-2	65	93	23	UNIQUE	0.45	1.1	0.409	1.32	30mm GAU8	371
85	7/20/94	B17-ASSY	AAB-1 25%pl/75%st, B17-0002-3	65	93	23	UNIQUE	0.407	1.1	0.370	1.32	30mm GAU8	372
86	7/21/94	B17-ASSY	AAB-1 25%pl/75%st, B17-0002-3	65	92.5	23	UNIQUE	0.405	1.1	0.368	1.32	30mm GAU8	370
87	7/22/94	B17-ASSY	AAB-1 25%pl/75%st, B17-0001-1	65	93	23	UNIQUE	0.394	1.1	0.358	1.32	30mm GAU8	372
88	7/27/94	B17-ASSY	AAB-1 25%pl/75%st, B17-0001-1	67	96	23	UNIQUE	0.349	0.864	0.404	1.32	30mm GAU8	367
89	7/28/94	B17-ASSY	AAB-1 25%pl/75%st, B17-0001-1	65	93.5	23	UNIQUE	0.315	0.764	0.412	1.32	30mm GAU8	368
90	8/3/94	B17-ASSY	AAB-1 25%pl/75%st, B17-0001-2	65	93	23	UNIQUE	0.315	0.691	0.456	1.32	30mm GAU8	368
91	9/2/94	B17-ASSY	AAB-1 25%pl/75%st, B17-0001-2	66.4	95	23	UNIQUE	0.315	0.691	0.456	1.32	30mm GAU8	370
92	9/6/94	B17-ASSY	AAB-1 25%pl/75%st, B17-0001-2	67	98	23	UNIQUE	0.3	0.691	0.434	1.32	30mm GAU8	369
93	9/7/94	B17-ASSY	AAB-1 25%pl/75%st, B17-0001-3	66	95	23	UNIQUE	0.3	0.691	0.434	1.32	30mm GAU8	366.5
94	9/8/94	B17-ASSY	AAB-1 25%pl/75%st, B17-0001-3	65	93	23	UNIQUE	0.285	0.629	0.453	1.32	30mm GAU8	371
95	9/8/94	B17-ASSY	AAB-1 25%pl/75%st, B17-0001-3	66	95	23	UNIQUE	0.285	0.629	0.453	1.32	30mm GAU8	370
96	9/9/94	B17-ASSY	AAB-1 25%pl/75%st, B17-0001-4	66	95	23	UNIQUE	0.285	0.629	0.453	1.32	30mm GAU8	368
97	9/14/94	B17-ASSY	AAB-1 25%pl/75%st, B17-0001-4	67	95.3	23	UNIQUE	0.285	0.629	0.453	1.32	30mm GAU8	368.8
98	9/15/94	B17-ASSY	AAB-1 25%pl/75%st, B17-0001-4	67	98	23	UNIQUE	0.285	0.629	0.453	1.32	30mm GAU8	372
99	9/16/94	B17-ASSY	AAB-1 25%pl/75%st, B17-0001-4	68	94	23	UNIQUE	0.285	0.629	0.453	1.32	30mm GAU8	365
100	9/28/94	B17-ASSY	AAB-1 25%pl/75%st, B17-0001-4	68	95	23	UNIQUE	0.285	0.629	0.453	1.32	30mm GAU8	371
101	9/29/94	B17-ASSY	AAB-1 25%pl/75%st, B17-0001-4	67.1	96	23	UNIQUE	0.288	0.656	0.436	1.32	30mm GAU8	369.1
102	9/30/94	B17-ASSY	AAB-1 25%pl/75%st, B17-0001-4	60.5	86.5	23	UNIQUE	0.285	0.656	0.434	1.32	30mm GAU8	427
103	10/13/94	B17-ASSY	AAB-1 25%pl/75%st, B17-0001-4	66	94	23	UNIQUE	0.285	0.656	0.434	1.32	30mm GAU8	371.5
104	10/18/94	B17-ASSY	AAB-1 25%pl/75%st, B17-0001-4	68	95	23	UNIQUE	0.275	0.656	0.419	1.32	30mm GAU8	370
105	10/19/94	B17-ASSY	AAB-1 25%pl/75%st, B17-0001-5	68	94	23	UNIQUE	0.275	0.656	0.419	1.32	30mm GAU8	372
106	10/20/94	B17-ASSY	AAB-1 25%pl/75%st, B17-0001-5	66	95	23	UNIQUE	0.265	0.656	0.404	1.32	30mm GAU8	371
107	10/21/94	B17-ASSY	AAB-1 25%pl/75%st, B17-0001-5	65	93	23	UNIQUE	0.255	0.656	0.389	1.32	30mm GAU8	370
108	10/31/94	B17-ASSY	AAB-1 25%pl/75%st, B17-0001-5	66	95	23	UNIQUE	0.255	0.562	0.454	1.32	30mm GAU8	370
109	11/4/94	B17-ASSY	AAB-1 25%pl/75%st, B17-0001-6	67	98	23	UNIQUE	0.255	0.562	0.454	1.32	30mm GAU8	370
110	11/9/94	B17-ASSY	AAB-1 25%pl/75%st, B17-0001-6	66	95	23	UNIQUE	0.26	0.562	0.463	1.32	30mm GAU8	369.5
111	11/14/94	B17-ASSY	AAB-1 100%st, B17-0001-1	67	95.8	23	UNIQUE	0.26	0.562	0.463	1.32	30mm GAU8	365
112	11/15/94	B17-ASSY	AAB-1 100%st, B17-0001-1	67	95.1	23	UNIQUE	0.265	0.562	0.472	1.32	30mm GAU8	365.1
113	11/15/94	B17-ASSY	AAB-1 100%st, B17-0001-1	67	95.5	23	UNIQUE	0.25	0.562	0.445	1.32	30mm GAU8	365.5
114	11/16/94	B17-ASSY	AAB-1 100%st, B17-0001-1	67	96	23	UNIQUE	0.25	0.562	0.445	1.32	30mm GAU8	370.4
115	11/16/94	B17-ASSY	AAB-1 100%st, B17-0001-1	67	95.5	23	UNIQUE	0.25	0.562	0.445	1.32	30mm GAU8	369.8

* All tests used XM46 monopropellant, a CCI-400 percussion primer and an axial booster housing

Figure A-3. Initial parameters - 30-mm stepped-wall test firings.

TEST #	BOOSTER PRESSURE (MPa)	CHAMBER PRESSURE 1 (MPa)	CHAMBER PRESSURE 2 (MPa)	CHAMBER PRESSURE 3 (MPa)	CHAMBER PRESSURE 4 (MPa)	BARREL PRESSURE 1 (MPa)	BARREL PRESSURE 2 (MPa)	MUZZLE PRESSURE (MPa)	IGNITION DELAY (ms)	ACTION TIME (ms)	VELOCITY (m/s)
57	482	546	425	762	n/d	221	37	11	468	4 796	597
60	489	409	268	534	n/d	210	26	11	398	4 765	605
62	377	419	325	615	n/d	215	44	6	382	4 061	734
63	515	577	532	647	n/d	568	53	35	547	3 358	941
64	518	616	488	739	n/d	250	52	0	437	3 42	901
65	545	425	405	559	n/d	878	75	28	.468	3 686	871
66	609	330	309	548	n/d	162	27	14	n/d	4 654	617
67	684	456	525	684	n/d	151	43	24	.420	4 264	686
68	491	676	790	n/d	n/d	881	878	13	1 232	2 592	849
69	252	718	810	826	n/d	n/d	n/d	n/d	n/d	n/d	898
70	478	298	240	292	n/d	208	47	14	2 358	6 7000	577
71	479	290	257	500	n/d	239	28	11	1 654	5 998	575
72	528	409	572	660	n/d	327	32	13	1 962	5 434	684
73	n/d	n/d	n/d	n/d	n/d	n/d	n/d	n/d	n/d	n/d	n/d
74	426	638	712	880	n/d	515	62	0	6 012	8 782	893
75	407	259	200	380	n/d	256	31	0	.656	4 716	630
76	404	295	340	15	n/d	290	38	20	686	4 68	642
77	334	366	397	212	n/d	271	69	26	.770	4 342	745
78	402	458	375	211	n/d	511	78	0	1.150	4 310	826
79	466	299	293	69	n/d	408	30	75	.490	4 842	606
80	550	674	667	453	n/d	875	68	26	1.17	3 842	877
81	509	329	360	59	n/d	394	51	0	.568	4 232	690
82	843	435	441	118	n/d	439	92	34	.412	3.732	832
83	629	597	880	231	n/d	436	72	29	.702	3 826	795
84	494	328	322	153	n/d	425	85	153	.296	3 904	758
85	512	878	872	509	n/d	886	55	30	486	3 466	734
86	424	731	869	167	n/d	557	88	363	.468	3.670	854
87	n/d	n/d	n/d	n/d	n/d	n/d	n/d	n/d	n/d	n/d	n/d
88	368	405	406	365	n/d	278	67	0	374	4 287	668
89	327	534	525	505	n/d	399	66	100	.550	3 540	842
90	421	537	451	451	n/d	385	81	29	470	3 576	840
91	506	512	798	436	n/d	361	51	n/d	.694	n/d	827
92	447	483	499	446	n/d	468	n/d	16	.510	4 342	645
93	442	439	638	362	n/d	338	n/d	n/d	452	n/d	644
94	338	461	429	416	n/d	294	73	18	.598	4 372	680
95	387	639	428	428	n/d	289	37	14	.506	4 356	630
96	374	884	624	879	n/d	432	56	26	74	3 592	870
97	371	380	700	362	n/d	371	51	22	.502	4 060	718
98	367	610	453	870	n/d	520	81	35	.560	3 686	827
99	324	606	559	n/d	n/d	434	53	31	.644	3 560	835
100	307	52	19	43	n/d	9	9	n/d	n/d	n/d	n/d
101	481	635	724	881	n/d	418	32	6	644	3 3	865
102	472	449	513	473	n/d	331	57	22	.454	4 248	680
103	503	732	755	781	882	518	49	25	.616	3 404	870
104	472	552	414	375	453	422	103	34	.476	3.700	853
105	372	579	580	546	838	600	66	16	530	3.514	872
106	402	792	654	701	1017	866	51	40	.452	3 342	883
107	345	739	763	756	722	973	90	35	.532	3 560	866
108	369	866	817	539	925	884	73	21	.544	3 634	865
109	367	813	640	863	907	692	86	31	413	3 202	894
110	428	876	881	564	898	854	72	25	320	3 204	916
111	515	745	668	688	887	880	103	16	366	3 138	893
112	535	864	883	471	985	526	79	26	.336	3 318	865
113	440	644	844	805	887	444	78	30	498	3 232	862
114	488	882	882	882	882	882	70	30	48 3	50 05	881
115	a/w	a/w	a/w	a/w	a/w	a/w	a/w	a/w	a/w	a/w	893

n/d=data not acquired because of data acquisition malfunction, setup error, or plugged pressure port a/w=data was not obtained because the event occurred after the 64ms data acquisition window

Figure A-4. Results - 30-mm stepped-wall test firings.

INITIAL PARAMETERS - 30 mm Stepped-wall Test Firings

TEST #	TEST DATE	FIXTURE NUMBER	CHAMBER TYPE	LP VOLUME (cc)	LP MASS (g)	LP TEMP. (C)	BOOSTER TYPE	BOOSTER MASS (g)	BOOST. HOUSING CAPACITY (cc)	LOAD DENSITY (g/cc)	ORIFICE DIAMETER (mm)	PROJECTILE TYPE	PROJECTILE MASS
116	3/1/95	B17-ASSY	AAB-1 25%pl/75%st, B17-0013	68.9	98.5	23	UNIQUE	0.255	0.562	0.454	1.32	30mm MOD1	371
117	3/2/95	B17-ASSY	AAB-1 25%pl/75%st, B17-0013	60.8	87	23	UNIQUE	0.255	0.562	0.454	1.32	30mm MOD1	346.5
118	3/3/95	B17-ASSY	AAB-1 25%pl/75%st, B17-0013	60.8	86	23	UNIQUE	0.255	0.562	0.454	1.32	30mm MOD1	347.5
119	3/6/95	B17-ASSY	AAB-1 25%pl/75%st, B17-0013	60.8	88	23	UNIQUE	0.255	0.562	0.454	1.32	30mm MOD1	348.1
120	3/8/95	B17-ASSY	AAB-1 25%pl/75%st, B17-0013	60.8	87	23	UNIQUE	0.255	0.562	0.454	1.32	30mm MOD2	356
121	3/9/95	B17-ASSY	AAB-1 25%pl/75%st, B17-0013	60.8	86	23	UNIQUE	0.255	0.562	0.454	1.32	30mm MOD2	355
122	3/10/95	B17-ASSY	AAB-1 25%pl/75%st, B17-0013	60.8	86.5	23	UNIQUE	0.255	0.562	0.454	1.32	30mm MOD2	353.4
123	3/15/95	B17-ASSY	AAB-1 25%pl/75%st, B17-0013	60.8	86	23	UNIQUE	0.255	0.562	0.454	1.32	30mm MOD2	355
124	3/16/95	B17-ASSY	AAB-1 25%pl/75%st, B17-0013	60.8	85	23	UNIQUE	0.255	0.562	0.454	1.32	30mm MOD2	353.2
125	3/17/95	B17-ASSY	AAB-1 25%pl/75%st, B17-0013	60.8	88	23	UNIQUE	0.255	0.562	0.454	1.32	30mm MOD2	355
126	3/17/95	B17-ASSY	AAB-1 25%pl/75%st, B17-0013	60.8	89	23	UNIQUE	0.255	0.562	0.454	1.32	30mm MOD2	355
127	3/20/95	B17-ASSY	AAB-1 25%pl/75%st, B17-0013	60.8	88	23	UNIQUE	0.255	0.562	0.454	1.32	30mm MOD2	354.2
128	3/20/95	B17-ASSY	AAB-1 25%pl/75%st, B17-0013	63.0	90	23	UNIQUE	0.255	0.562	0.454	1.32	30mm MOD3	354.9
129	3/21/95	B17-ASSY	AAB-1 25%pl/75%st, B17-0013	63.0	90.5	23	UNIQUE	0.255	0.562	0.454	1.32	30mm MOD3	352.2
130	3/22/95	B17-ASSY	AAB-1 25%pl/75%st, B17-0013	60.8	85	23	UNIQUE	0.255	0.562	0.454	1.32	30mm MOD4	394.3
131	3/28/95	B17-ASSY	AAB-1 25%pl/75%st, B17-0013	60.8	85	23	UNIQUE	0.255	0.562	0.454	1.32	30mm MOD5	401.7
132	3/30/95	B17-ASSY	AAB-1 25%pl/75%st, B17-0013	60.8	85	23	UNIQUE	0.255	0.562	0.454	1.32	30mm MOD2	354
133							NO TEST						

* All tests used XM46 monopropellant, a CCI-400 percussion primer and an axial booster housing

INITIAL PARAMETERS - 30 mm Multi-chamber Test Firings

TEST #	TEST DATE	FIXTURE NUMBER	CHAMBER TYPE	LP VOLUME (cc)	LP MASS (g)	LP TEMP. (C)	BOOSTER TYPE	BOOSTER MASS (g)	BOOST. HOUSING CAPACITY (cc)	LOAD DENSITY (g/cc)	ORIFICE DIAMETER (mm)	PROJECTILE TYPE	PROJECTILE MASS
134	4/4/95	B17-ASSY	Multichamber (1-3-3)	69.9	100	23	Unique	0.335	0.705	0.475	1.3208	30mm MOD2	351.1
135	4/6/95	B17-ASSY	Multichamber (1-3-3)	69.2	99	23	Unique	0.335	0.705	0.475	1.3208	30mm MOD2	350.1
136	4/10/95	B17-ASSY	Multichamber (1-3-3)	78.3	112	23	Unique	0.335	0.705	0.475	1.3208	30mm MOD2	351.3
137	4/13/95	B17-ASSY	Multichamber (1-3-3)	76.9	110	23	Unique	0.335	0.705	0.475	1.3208	30mm MOD2	352.4
138	4/18/95	B17-ASSY	Multichamber (1-3-3)	80.1	114.5	23	Unique	0.335	0.705	0.475	1.3208	30mm MOD2	351.6
139	4/26/95	B17-ASSY	Multichamber (1-3-3)	79.4	113.5	23	Unique	0.335	0.705	0.475	1.3208	30mm MOD2	352.1
140	5/1/95	B17-ASSY	Multichamber (1-3-3)	81.8	117	23	Unique	0.335	0.705	0.475	1.3208	30mm MOD2	352
141							NO TEST						
142	5/8/95	B17-ASSY	Multichamber (1-3-3)	81.1	116	23	Unique	0.335	0.705	0.475	1.3208	30mm MOD2	351.2
143	5/15/95	B17-ASSY	Multichamber (1-3-3)	83.2	119	23	Unique	0.335	0.705	0.475	1.3208	30mm MOD2	351.5
144	5/23/95	B17-ASSY	Multichamber (1-3-3)	76.2	109	23	Unique	0.335	0.705	0.475	1.3208	30mm MOD2	350.8
145	5/30/95	B17-ASSY	Multichamber (1-3-3)	78.3	112	23	Unique	0.335	0.705	0.475	1.3208	30mm MOD2	351
146	6/6/95	B17-ASSY	Multichamber (1-4-4)	77.3	110.5	23	Unique	0.335	0.705	0.475	1.3208	30mm MOD2	351
147	6/28/95	B17-ASSY	Multichamber (1-6-6)	85.3	122	23	Unique	0.335	0.705	0.475	1.3208	30mm MOD2	351.3
148	7/12/95	B17-ASSY	Multichamber (1-3-9)	79.7	114	23	Unique	0.335	0.705	0.475	1.3208	30mm MOD2	350.6
149	7/14/95	B17-ASSY	Multichamber (1-1-19)	65.0	93	23	Unique	0.335	0.705	0.475	1.3208	30mm MOD2	350.2
150	8/7/95	B17-ASSY	Multichamber (1-1-19)	69.2	99	23	Unique	0.335	0.705	0.475	1.3208	30mm MOD2	351
151	8/10/95	B17-ASSY	Multichamber (1-1-19)	69.9	100	23	Unique	0.335	0.705	0.475	1.3208	30mm MOD2	351.8
152	8/15/95	B17-ASSY	Multichamber (1-1-19)	72.7	104	24	Unique	0.335	0.705	0.475	1.3208	30mm MOD2	351.4

* All tests used XM46 monopropellant, a CCI-400 percussion primer and an axial booster housing

INITIAL PARAMETERS - 30 mm Stepped-wall Test Firings

TEST #	TEST DATE	FIXTURE NUMBER	CHAMBER TYPE	LP VOLUME (cc)	LP MASS (g)	LP TEMP. (C)	BOOSTER TYPE	BOOSTER MASS (g)	BOOST. HOUSING CAPACITY (cc)	LOAD DENSITY (g/cc)	ORIFICE DIAMETER (mm)	PROJECTILE TYPE	PROJECTILE MASS
153	8/30/95	B17-ASSY	AAB-1 25%pl/75%st, B17-0013	60.8	87	23	Unique	0.255	0.53	0.477	1.3208	30mm MOD2	354
154	8/31/95	B17-ASSY	AAB-1b 25%pl/75%st, B17-0013	55.9	80	23	Unique	0.255	0.53	0.477	1.3208	30mm MOD2	354
155	9/1/95	B17-ASSY	AAB-1c 25%pl/75%st, B17-0013	79.7	114	23	Unique	0.255	0.53	0.477	1.3208	30mm MOD2	357
156	9/5/95	B17-ASSY	AAB-1g 25%pl/75%st, B17-0013	56.6	81	23	Unique	0.255	0.53	0.477	1.3208	30mm MOD2	352.5
157	9/18/95	B17-ASSY	AAB-1c 25%pl/75%st, B17-0013	78.3	112	20	Unique	0.255	0.53	0.477	1.3208	30mm MOD5	355.5
158	9/22/95	B17-ASSY	AAB-1c 25%pl/75%st, B17-0013	80.4	115	21	Unique	0.255	0.53	0.477	1.3208	30mm MOD5	356
159	9/25/95	B17-ASSY	AAB-1d 25%pl/75%st, B17-0013	81.8	117	23	Unique	0.255	0.53	0.477	1.3208	30mm MOD2	354
160	9/28/95	B17-ASSY	AAB-1f 25%pl/75%st, B17-0013	58.4	83.5	23	Unique	0.255	0.53	0.477	1.3208	30mm MOD2	351.5
161	10/3/95	B17-ASSY	AAB-1 25%pl/75%st, B17-0013	61.5	88	23	Unique	0.255	0.53	0.477	1.3208	30mm MOD2	352
162	10/9/95	B17-ASSY	AAB-1 25%pl/75%st, B17-0013	63.6	91	23	Unique	0.255	0.53	0.477	1.3208	30mm MOD2	355
163	10/10/95	B17-ASSY	AAB-1 25%pl/75%st, B17-0013	63.6	91	23	Unique	0.255	0.53	0.477	1.3208	30mm MOD2	353

* All tests used XM46 monopropellant, a CCI-400 percussion primer and an axial booster housing

Figure A-5. Initial parameters - 30-mm stepped-wall test firings.

RESULTS - 30 mm Stepped-wall Test Firings

TEST v #	BOOSTER PRESSURE (MPa)	STAND. CHAMBER PRESSURE 1 (MPa)	STAND. CHAMBER PRESSURE 2 (MPa)	FLUSH CHAMBER PRESSURE 2 (MPa)	CHAMBER PRESSURE 3 (MPa)	CHAMBER PRESSURE 5 (MPa)	BARREL PRESSURE 1 (MPa)	BARREL PRESSURE 2 (MPa)	MUZZLE RESSURE (MPa	IGNITION DELAY (ms)	ACTION TIME (ms)	VELOCITY (m/s)
116	153	587	881	618	n/d	890	643	50	19	512	3 608	857
117	371	584	542	620	95.7(plugged)	n/d	47	36	16	222	4 014	708
118	388	460	463	546	8 8(plugged)	n/d	433	41	16	214	4 108	690
119	384	456	459	593	132(plugged)	n/d	882	99	24	236	3 466	884
120	498	510	513	638	1 65(plugged)	666	348	56	17	202	3 888	727
121	418	433	809	527	n/d	765	364	91	15	212	3 998	706
122	681	543	827	668	n/d	550	415	120	25	222	3 358	871
123	411	561	473	562	n/d	559	440	10	28	212	4 06	685
124	428	714	855	857	n/d	883	659	133	78	212	3 248	892
125	n/d	525	593	630	n/d	593	411	90	121	226	3 748	790
126	n/d	474	490	579	n/d	435	455	91	26	200	3 780	791
127	610	403	431	544	n/d	508	451	102	13	236	4 060	686
128	443	594	630	679	n/d	476	480	133	33	186	3.372	864
129	430	875	651	616	n/d	826	545	110	22	226	3 436	867
130	398	560	747	682	n/d	n/d	519	46	22	214	3 498	769
131	476	469	528	705	n/d	661	418	74	15	170	4 154	673
132	450	a/w	a/w	a/w	n/d	a/w	a/w	a/w	a/w	a/w	a/w	773
133	N O T E S T											

n/d=data not acquired because of data acquisition malfunction, setup error, or plugged pressure port. a/w=data was not obtained because the event occurred after the 64ms data acquisition window

RESULTS - 30 mm Multi-chamber Test Firings

TEST #	BOOSTER PRESSURE (MPa)	CHAMBER PRESSURE 1 (MPa)	CHAMBER PRESSURE 2 (MPa)	CHAMBER PRESSURE 3 (MPa)	CHAMBER PRESSURE 5 (MPa)	CHAMBER PRESSURE D (MPa)	BARREL PRESSURE 1 (MPa)	BARREL PRESSURE 2 (MPa)	MUZZLE RESSURE (MPa	IGNITION DELAY (ms)	ACTION TIME (ms)	VELOCITY (m/s)
134	371	79	590	376	887	762	884	101	45	0 676	3 300	938
135	491	247	299	86	220	214	176	75	12	0 382	4 576	659
136	300	540	309	n/d	275	538	245	62	17	0 384	3 938	733
137	530	220	212	72	226	152	226	66	80	0.426	4 216	710
138	457	294	331	218	596	479	681	85	34	0 374	2 203	936
139	530	358	436	116	364	428	415	82	38	0 404	4 054	896
140	451	518	531	880	734	608	845	82	30	0 424	3 904	805
141	N O T E S T											
142	319	280	691	158	249	290	306	68	32	0 324	4 028	725
143	575	203	306	235	202	206	239	59	22	0 430	4 436	703
144	570	358	302	159	268	284	373	96	n/d	n/d	n/d	900
145	418	399	677	407	348	377	474	101	31	0.412	3 498	936
146	148	394	507	451	321	427	412	110	29	0 404	3 436	943
147	651	419	468	291	284	318	286	93	49	0 366	3 622	942
148	527	769	487	633	573	627	576	79	24	0 374	3 592	848
149	491	372	571	n/d	340	309	320	121	22	0 262	3 872	797
150	501	521	409	561	498	344	450	175	51	0.334	3 404	925
151	880	653	742	884	819	593	666	120	24	0.304	2 998	983
152	408	648	633	845	886	799	881	126	112	0 726	3 622	973

n/d=data not acquired because of data acquisition malfunction, setup error, or plugged pressure port. a/w=data was not obtained because the event occurred after the 64ms data acquisition window

RESULTS - 30 mm Stepped-wall Test Firings

TEST #	BOOSTER PRESSURE (MPa)	STAND. CHAMBER PRESSURE 1 (MPa)	STAND. CHAMBER PRESSURE 2 (MPa)	FLUSH CHAMBER PRESSURE 2 (MPa)	CHAMBER PRESSURE 3 (MPa)	CHAMBER PRESSURE 5 (MPa)	BARREL PRESSURE 1 (MPa)	BARREL PRESSURE 2 (MPa)	MUZZLE RESSURE (MPa	IGNITION DELAY (ms)	ACTION TIME (ms)	VELOCITY (m/s)
153	401	428	568	461	n/d	369	876	49	15	0 344	4 154	690
154	352	409	421	595	n/d	556	385	65	33	0 424	3 716	860
155	297	323	442	521	n/d	885	667	76	33	0 460	3 342	983
156	389	420	399	411	n/d	435	242	33	11	0 412	4 356	847
157	209	405	669	652	n/d	760	571	n/d	39	0 302	3 202	1009
158	355	348	400	371	n/d	395	877	n/d	177	0 456	2 030	1009
159	437	395	537	461	n/d	412	876	n/d	31	0 232	3 112	1001
160	326	505	518	509	n/d	417	279	87	16	0 284	4 200	854
161	464	395	480	577	n/d	524	243	68	14	0 272	4 154	865
162	496	588	590	580	424	424	197	82	32	0 152	3 704	789
163	415	620	530	541	407	407	243	78	18	0 168	4 076	698

n/d=data not acquired because of data acquisition malfunction, setup error, or plugged pressure port. a/w=data was not obtained because the event occurred after the 64ms data acquisition window

Figure A-6. Results - 30-mm stepped-wall test firings.

NO. OF COPIES	ORGANIZATION
2	DEFENSE TECHNICAL INFORMATION CENTER DTIC DDA 8725 JOHN J KINGMAN RD STE 0944 FT BELVOIR VA 22060-6218
1	HQDA DAMO FDQ DENNIS SCHMIDT 400 ARMY PENTAGON WASHINGTON DC 20310-0460
1	CECOM SP & TRRSTRL COMMCTN DIV AMSEL RD ST MC M H SOICHER FT MONMOUTH NJ 07703-5203
1	PRIN DPTY FOR TCHNLGY HQ US ARMY MATCOM AMCDCG T M FISETTE 5001 EISENHOWER AVE ALEXANDRIA VA 22333-0001
1	PRIN DPTY FOR ACQUSTN HQS US ARMY MATCOM AMCDCG A D ADAMS 5001 EISENHOWER AVE ALEXANDRIA VA 22333-0001
1	DPTY CG FOR RDE HQS US ARMY MATCOM AMCRD BG BEAUCHAMP 5001 EISENHOWER AVE ALEXANDRIA VA 22333-0001
1	DPTY ASSIST SCY FOR R&T SARD TT T KILLION THE PENTAGON WASHINGTON DC 20310-0103
1	OSD OUSD(A&T)/ODDDR&E(R) J LUPO THE PENTAGON WASHINGTON DC 20301-7100

NO. OF COPIES	ORGANIZATION
1	INST FOR ADVNCD TCHNLGY THE UNIV OF TEXAS AT AUSTIN PO BOX 202797 AUSTIN TX 78720-2797
1	DUSD SPACE 1E765 J G MCNEFF 3900 DEFENSE PENTAGON WASHINGTON DC 20301-3900
1	USAASA MOAS AI W PARRON 9325 GUNSTON RD STE N319 FT BELVOIR VA 22060-5582
1	CECOM PM GPS COL S YOUNG FT MONMOUTH NJ 07703
1	GPS JOINT PROG OFC DIR COL J CLAY 2435 VELA WAY STE 1613 LOS ANGELES AFB CA 90245-5500
1	ELECTRONIC SYS DIV DIR CECOM RDEC J NIEMELA FT MONMOUTH NJ 07703
3	DARPA L STOTTS J PENNELLA B KASPAR 3701 N FAIRFAX DR ARLINGTON VA 22203-1714
1	SPCL ASST TO WING CMNDR 50SW/CCX CAPT P H BERNSTEIN 300 O'MALLEY AVE STE 20 FALCON AFB CO 80912-3020
1	USAF SMC/CED DMA/JPO M ISON 2435 VELA WAY STE 1613 LOS ANGELES AFB CA 90245-5500

NO. OF COPIES	ORGANIZATION
1	US MILITARY ACADEMY MATH SCI CTR OF EXCELLENCE DEPT OF MATHEMATICAL SCI MDN A MAJ DON ENGEN THAYER HALL WEST POINT NY 10996-1786
1	DIRECTOR US ARMY RESEARCH LAB AMSRL CS AL TP 2800 POWDER MILL RD ADELPHI MD 20783-1145
1	DIRECTOR US ARMY RESEARCH LAB AMSRL CS AL TA 2800 POWDER MILL RD ADELPHI MD 20783-1145
3	DIRECTOR US ARMY RESEARCH LAB AMSRL CI LL 2800 POWDER MILL RD ADELPHI MD 20783-1145
	<u>ABERDEEN PROVING GROUND</u>
3	DIR USARL AMSRL CI LP (305)

NO. OF COPIES	ORGANIZATION
1	DIRECTOR BENET LABORATORIES W KITCHENS USA WATERVLIET ARSENAL WATERVLIET NY 12189
1	DIRECTOR BENET LABS APPLIED MATH AND MECH BR B PFLEGL WATERVLIET NY 12189
1	COMMANDER USA ARDEC AMSTA FSA T M SALSBURY PICATINNY ARSENAL NJ 07806-5000
1	COMMANDER USA ARDEC AMSTA FSE T GORA PICATINNY ARSENAL NJ 07806-5000
3	COMMANDER USA ARDEC AMSTA AR AEE B D DOWNS A BRACUTI D CHIU PICATINNY ARSENAL NJ 07806-5000
4	COMMANDER USA ARDEC AMSTA AR FSS DA B MACHAK J IRIZARRY R KOPMANN C PERAZZO PICATINNY ARSENAL NJ 07806-5000
2	COMMANDER HQ AMCCOM AMSMC LSL B KELEBER AMSMC SAS WF G SCHELENKER ROCK ISLAND IL 61299-6000

NO. OF COPIES	ORGANIZATION
1	COMMANDER USA RESEARCH OFFICE TECH LIB PO BOX 12211 RESEARCH TRIANGLE PARK NC 27709-2211
1	PRESIDENT USA ARTILLERY BOARD FORT SILL OK 73503
1	COMMANDANT USA CMD & GEN STAFF COLL FORT LEAVENWORTH KS 66027-5200
1	COMMANDANT USA SPECIAL WARFARE SCHOOL REV & TNG LIT DIV FORT BRAGG NC 28307
1	COMMANDER RADFORD ARMY AMMUN PLANT SMCRA QA HI LIBRARY RADFORD VA 24141
1	COMMANDANT USA FLD ART SCHL STSF TSM CN FORT SILL OK 73503-5600
1	US ARMY EUROPEAN RESEARCH OFC R REICHENBACH PSC 802 BOX 15 APO AE 09499-1500
1	NAVAL RESEARCH LAB TECHNICAL LIBRARY WASHINGTON DC 20375
3	COMMANDER NSWC 610 C SMITH 6110J K RICE 6110C S PETERS INDIAN HEAD MD 20640-5035
2	COMMANDER CODE G33 T DORAN J COPLEY DAHLGEN VA 22448-5000

NO. OF COPIES	ORGANIZATION
1	NC STATE UNIV J G GILLIGAN BOX 7909 1110 BURLINGTON ENG LABS RALEIGH NC 27695-7909
3	INST FOR ADV STUDIES DR H FAIR DR T KIEHNE DR I MCNAB 4030 2 W BAKER LN AUSTIN TX 78759-5329
3	FMC CORPORATION B GODDELL DR D COOK J DYVIK 4800 E RIVER RD MINNEAPOLIS MN 55343
1	ALLIANT TECHSYSTEMS INC J KENNEDY MN38 3300 10400 YELLOW CIRCLE DR MINNETONKA MN 55343
1	PAUL GOUGH ASSOCIATES INC P S GOUGH 1048 SOUTH ST PORTSMOUTH NH 03801-5423
1	ELI FREEDMAN & ASSOC E FREEDMAN 2411 DIANA RD BALTIMORE MD 21209
10	VERITAY TECHNOLOGY INC 4845 MILLERSPORT HWY PO BOX 305 EAST AMHERST NY 14051-0305
1	STATE UNIV OF NY DEPT OF ELECT ENGRG DR W J SARGEANT BONNER HALL RM 312 BUFFALO NY 14260

NO. OF COPIES	ORGANIZATION
1	USA RESEARCH OFFICE ENGINEERING SCI DIV DR D MANN 4300 S MIAMI BLVD RESEARCH TRIANGLE PARK NC 27709
1	ARMY HIGH PERFORM CMPTG RESEARCH CENTER UNIV OF MINNESOTA DR T TEZDUYAR 1100 WASHINGTON AVE S STE 101 MINNEAPOLIS MN 55415
1	ELMORE ASSOC 125 BEAR GULCH DRIVE PORTOLA VALLEY CA 94028
4	GEN DYNAMICS DEFNS SYS G KEELER B FEATHEROFF I MAGOON T KURIATA 100 PLASTICS AVE PITTFIELD MA 01201-3698
2	OLIN CHEMICALS L WILKSTRON G ROTHGERY 350 KNOTTER DRIVE PHESHIRE CT 06410
2	PRINCETON COMBUSTION RESEARCH LAB INC N MESSINA M TARCZYNSKI 4275 US HIGHWAY ONE NORTH MONMOUTH JUNCTION NJ 08852
3	CRAFT TECH INC S DASH A HOSANGADI N SINHA COMBUSTION RESEARCH & FLOW TECH INC 174 N MAIN STR BLDG 3 PO BOX 1150 DUBLIN PA 18917

NO. OF COPIES	ORGANIZATION
1	THE PENNA STATE UNIV DEPT OF MECHANICAL ENGRG K K KUO 140 RESEARCH BLDG EAST UNIVERSITY PARK PA 16802
1	THE PENNA STATE UNIV DEPT OF MECHANICAL ENGRG S T THYNELL 309 REBER BLDG UNIVERSITY PARK PA 16802
	ABERDEEN PROVING GROUND
49	DIR USARL AMSRL WM P A HORST W CIEPICLA M SMITH E SCHMIDT AMSRL WM PA T COFFEE G WREN A BIRK J DESPIRITO (10 CPS) J KNAPTON C LEVERITT T MINOR W OBERLE P TRAN K WHITE L-M CHANG J COLBURN P CONROY G KELLER D KOOKER T ROSENBERGER M NUSCA S RAY G KATULKA G REEVES I STOBIE R ANDERSON A BRANDT M DEL GUERCIO S HOWARD A JOHNSON M RIDGLEY C RUTH A WILLIAMS

NO. OF COPIES	ORGANIZATION
	AMSRL WM PB P PLOSTINS AMSRL WM PC B FORCH R BEYER A JUHASZ M MCQUAID AMSRL WM PC B BURNS AMSRL WM T W MORRISON

NO. OF COPIES	ORGANIZATION
2	RARDE DR C WOODLEY MR STEVE GILBERT GS2 DIVISION BUILDING R31 FORT HALSTEAD SEVENOAKS KENT TN14 7BP ENGLAND
1	WEAPONS SYSTEM DIVISION DR ANNA WILDEGGER-GAISSMAIER PO BOX 1500 SALISBURY SOUTH AUSTRALIA 5108

REPORT DOCUMENTATION PAGE

Form Approved
OMB No. 0704-0188

1. AGENCY USE ONLY *(Leave blank)*	2. REPORT DATE	3. REPORT TYPE AND DATES COVERED
	September 1997	Final, Jun 93 - Nov 95

4. TITLE AND SUBTITLE

Investigation of Bulk-Loaded Liquid Propellant Gun Concepts

5. FUNDING NUMBERS

C: DAAA15-93-C-0031

6. AUTHOR(S)

Robert L. Talley, John Owczarczak, and Matthew Geise

7. PERFORMING ORGANIZATION NAME(S) AND ADDRESS(ES)

Veritay Technology, Inc.
4845 Millersport Highway
P.O. Box 305
East Amherst, NY 14051-0305

8. PERFORMING ORGANIZATION REPORT NUMBER

ARL-CR-335

9. SPONSORING/MONITORING AGENCY NAMES(S) AND ADDRESS(ES)

U.S. Army Research Laboratory
ATTN: AMSRL-WM-PA
Aberdeen Proving Ground, MD 21005-5066

10.SPONSORING/MONITORING AGENCY REPORT NUMBER

11. SUPPLEMENTARY NOTES

The point of contact for this report is James DeSpirito, U.S. Army Research Laboratory, ATTN: AMSRL-WM-PA, Aberdeen Proving Ground, MD 21005-5066

12a. DISTRIBUTION/AVAILABILITY STATEMENT

Approved for public release; distribution is unlimited.

12b. DISTRIBUTION CODE

13. ABSTRACT ***(Maximum 200 words)***

The approach of using chamber geometry (in the forms of stepped-wall and multichambers) in conjunction with using a repeatable igniter was investigated as a means for controlling the interior ballistic variability in 20-mm and 30-mm bulk-loaded liquid propellant guns (BLPGs). Full-scale, gun firing tests were conducted using the liquid monopropellant XM46 to experimentally develop a database for assessing the utility of these mechanical control concepts.

The 30-mm gun test data indicate that a useful degree of control of both the pressure-time trace shape and the projectile muzzle velocity may be achieved by using either a stepped-wall or a multichamber geometry, and that a useful degree of ballistic repeatability can often be achieved, even in a nonoptimized test gun.

The 30-mm gun test data also indicate that the igniter needs to be tailored to the size and geometry of the input stage of the main liquid propellent chamber to achieve near-optimal ballistic repeatability.

14. SUBJECT TERMS

bulk-loaded liquid propellant gun, liquid propellants, interior ballistics, combustion control

15. NUMBER OF PAGES

120

16. PRICE CODE

17. SECURITY CLASSIFICATION OF REPORT	18. SECURITY CLASSIFICATION OF THIS PAGE	19. SECURITY CLASSIFICATION OF ABSTRACT	20. LIMITATION OF ABSTRACT
UNCLASSIFIED	UNCLASSIFIED	UNCLASSIFIED	UL

NSN 7540-01-280-5500

Standard Form 298 (Rev. 2-89)
Prescribed by ANSI Std. 239-18 298-102

INTENTIONALLY LEFT BLANK.

USER EVALUATION SHEET/CHANGE OF ADDRESS

This Laboratory undertakes a continuing effort to improve the quality of the reports it publishes. Your comments/answers to the items/questions below will aid us in our efforts.

1. ARL Report Number/Author ARL-CR-335 (Talley [POC: DeSpirito]) ______ Date of Report September 1997 ______

2. Date Report Received ____________________

3. Does this report satisfy a need? (Comment on purpose, related project, or other area of interest for which the report will be used.) ____________________

4. Specifically, how is the report being used? (Information source, design data, procedure, source of ideas, etc.) ____________________

5. Has the information in this report led to any quantitative savings as far as man-hours or dollars saved, operating costs avoided, or efficiencies achieved, etc? If so, please elaborate. ____________________

6. General Comments. What do you think should be changed to improve future reports? (Indicate changes to organization, technical content, format, etc.) ____________________

CURRENT ADDRESS

Organization

Name	E-mail Name

Street or P.O. Box No.

City, State, Zip Code

7. If indicating a Change of Address or Address Correction, please provide the Current or Correct address above and the Old or Incorrect address below.

OLD ADDRESS

Organization

Name

Street or P.O. Box No.

City, State, Zip Code

(Remove this sheet, fold as indicated, tape closed, and mail.)

(DO NOT STAPLE)